



PUCP



TECHNISCHE UNIVERSITÄT
ILMENAU

Implementation of a triboelectrical workstation for the investigation of the influence of electrical current on the tribological properties of thin films

Thesis submitted for the degree of master in mechatronics

Presented by:

Edson Igor Yupanqui Aliaga

Supervising Professor at TU Ilmenau:

AOR Dr.-Ing. Tom Ströhla

Supervising professor at PUCP:

Dr. Francisco Rumiche

Practical Advisor:

Dr.-Ing. Rolf Grieseler

Ilmenau-Germany/ Lima Perú

March 2016

Acknowledgement

I would like to thank Dipl.-Ing. Mike Stubenrauch and Mr. Wolfgang Kempf from the Faculty of Mechanical Engineering FG biomechatronics for their advice and support with the tribological station and facilitating the different tools and devices for developing the present work.

I would like to thank to my supervising professors Dr. Ströhla and Dr. Rumiche from the TU Ilmenau and PUCP respectively for their support in the project.

I would like to thank also to my practical advisor Dr.-Ing. Rolf Grieseler for all his support during the development of the project.

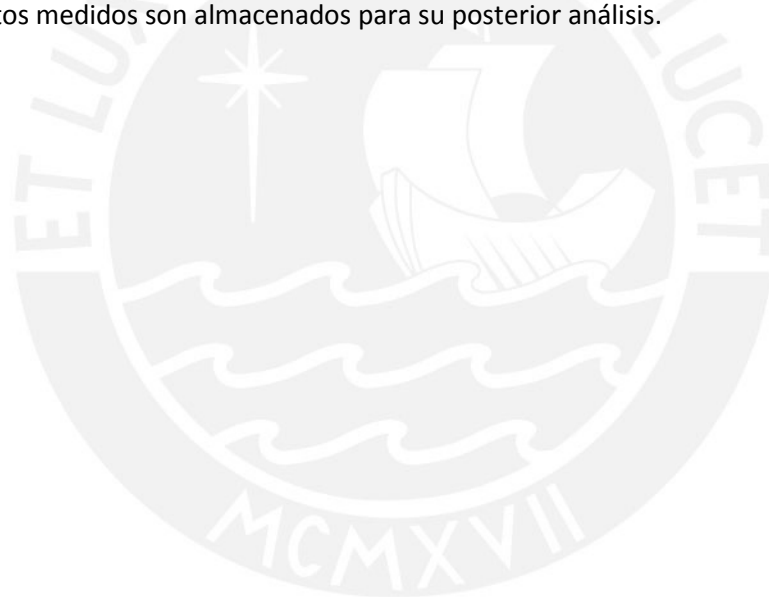
I would like to thank to my family in Peru, their best wishes and moral support keep me working hard.

Finally I would like to thank the Fondecyt CONCYTEC for finance my studies for these two years. Without their help this would not have been possible.



Resumen

Con el fin de hacer que las máquinas, circuitos electrónicos o contactos eléctricos para diversas aplicaciones, funcionen correctamente; es necesario conocer sus características. La mayoría de las máquinas desarrolladas o dispositivos electrónicos están formados por varios componentes que están interconectados. Cuando estos componentes interactúan entre sí o con el medio ambiente, están sometidos a estrés, fricción y desgaste. Por lo tanto, se requiere predecir el comportamiento de estos materiales cuando están sometidos a fricción y desgaste para así tener una interpretación adecuada de lo que ocurre en estos puntos de contacto. La presente tesis se centra en la caracterización de materiales por medio de un sistema tribológico basado en un "punto plano-contacto", donde una bola estacionaria hace de punto y el material de muestra se hace oscilar debajo. Con este sistema es posible determinar el valor de la fuerza tangencial y la fuerza normal, y a partir de estos dos, se puede calcular el coeficiente de fricción. Además, apoyamos el análisis de materiales mediante una caracterización eléctrica en paralelo durante el experimento. Para este propósito, una corriente se inyecta en la muestra. Luego, la caída de tensión y la corriente son medidas y con estos datos, la resistencia eléctrica se puede determinar. El sistema de medición está controlado por un ordenador central que usa LabVIEW y los datos medidos son almacenados para su posterior análisis.



Abstract

In order to make machines, electronic circuits or electrical contacts for various applications, it is necessary to know their characteristics and to characterize them precisely. Most of the developed machines or electronic devices are composed of various components that are interconnected. When these components interact with each other or with the environment, it comes to stress, friction and wear. Therefore, prediction of the behavior of these materials in emerging friction and wear is required for an adequate interpretation of these contact points. The thesis presented here focuses on the characterization of materials by means of a tribological system, based on a "point-plane-contact" where the point is realized on a stationary ball and the material sample is oscillating below. With this system it is possible to determine the value of tangential force and normal force, and to calculate from these two the coefficient of friction. In addition, we support the material analysis by a parallel electrical characterization during rubs. For this purpose, a current is injected into the sample and the voltage drop and the current measured. From this, the electrical resistance during the experiments determine. The whole measurement setup is controlled by a central computer via LabVIEW® and the recorded measurement data is stored for later analysis.



Kurzfassung

Um Maschinen, elektronische Schaltkreise oder elektrische Kontakte für verschiedene Anwendungen ordnungsgemäß zu gestalten, ist es erforderlich deren Eigenschaften zu kennen bzw. genau zu charakterisieren. Die meisten der entwickelten Maschinen oder elektronische Geräte sind aus verschiedenen Komponenten zusammengesetzt, die miteinander verbunden sind. Wenn diese Komponenten in Wechselwirkung untereinander oder mit der Umgebung treten, so kommt es zu Belastung, Reibung und Verschleiß. Daher ist für eine ausreichende Auslegung dieser Kontaktstellen eine Vorhersage zum Verhalten dieser Materialien bei auftretender Reibung und Verschleiß erforderlich. Die hier vorgelegte Masterarbeit konzentriert sich auf die Materialcharakterisierung mittels eines tribologischen Systems, basierend auf einer „Punkt-Ebene-Berührung“ wobei der Punkt über eine ortsfeste Kugel realisiert ist und die Materialprobe oszillierend darunter bewegt wird. Mit diesem System ist es möglich, den Wert von Tangentialkraft und Normalkraft zu ermitteln, und aus diesen beiden den Reibungskoeffizienten zu berechnen. Zusätzlich wird die Materialanalyse durch eine parallele elektrische Charakterisierung während der Reibversuche unterstützt. Dazu wird ein Strom in die Probe injiziert und der Spannungsabfall sowie der Strom gemessen. Daraus lässt sich der elektrische Widerstand während der Experimente bestimmen. Der gesamte Messaufbau wird von einem zentralen Rechner per LabVIEW® gesteuert und die Messdaten aufgenommen und für spätere Analysen gespeichert.

Content

1 Introduction	1
2 State of the art	3
2.1 Four point probe measurement	3
2.2 Tribology	4
2.2.1 Friction	4
2.2.1.1 Laws of friction	5
2.2.1.2 Real contact area	6
2.2.1.3 Interfacial bonds	6
2.2.1.4 Sliding friction	7
2.2.2 Wear	8
2.2.2.1 Wear mechanisms	8
2.2.2.2 Wear modes	8
2.2.2.3 Sliding wear test methods	9
2.2.3 Lubrication	11
2.2.3.1 Lubrication regimes and the Stribeck curve	11
3 Electronic interconnections	13
3.1 Materials for electronic connections	14
3.2 Contact materials	14
3.3 Coating techniques for electrical contacts	16
3.3.1 Surface segregation	16
3.3.2 Ion implantation	17
3.3.3 Electroplating	17
3.3.4 Electroless plating	17
3.3.5 Cladding	18
3.3.6 Chemical deposition	18
3.3.7 Plating by swabbing	18
3.3.8 Physical vapor deposition technology	18
3.3.9 Electro-Spark Deposition (ESD)	18
4 Experimental procedure and software	19
4.1 Connection setup	19
4.2 BASALT-MUST Precision Tester	21
4.2.1 Basalt MUST working principle	22

4.2.2 Measurement module Basalt MUST 2D-FM 1N -----	22
4.2.2.1 Operational principle of the force transducer -----	23
4.2.2.2 Operational principle of the fiber optic sensors (FOS) -----	23
4.2.3 Motion module Basalt MUST LMS20 -----	24
4.3 LabVIEW program structure -----	26
4.3.1 Keithley virtual instrument modules -----	26
4.3.2 Basalt MUST VI modules -----	30
4.4 Program description -----	33
4.4.1 Tribological program -----	33
4.4.1.1 Connect event -----	34
4.4.1.2 Start Streaming event -----	35
4.4.1.3 Homing LMS20 event -----	35
4.4.1.4 Timeout event -----	36
4.4.1.4.1 Calibration Tab -----	36
4.4.1.4.2 Measurement Tab -----	41
4.4.1.5 Go To PosXYZ event -----	45
4.4.1.6 LMS20 Goto pos event -----	46
4.4.1.7 Start Test event -----	48
4.4.1.8 Calculate event -----	49
4.4.1.9 Start_calib event -----	50
4.4.1.10 Sel. as peak event -----	50
4.4.1.11 Tarring Fn and Tarring Ft events -----	51
4.4.1.12 Save configurations event -----	51
4.4.1.13 Load configuration event -----	52
4.4.1.14 Z-Positioning event -----	52
4.4.2 Electrical program -----	54
4.4.2.1 Timeout event -----	55
4.4.2.2 Start Electrical event -----	56
4.4.2.3 Create File event -----	57
4.4.2.4 Start Recording Electrical event -----	58
5 Calibration -----	59
5.1 FOS calibration -----	59
5.2 Determination of the spring constant -----	63
6 Measurement tab and error handling -----	70
6.1 Measurement tab -----	70
6.2 Error handling -----	73

6.2.1 Errors in the program-----	76
7 Experiments -----	78
8 Conclusions and future work -----	86
8.1 Conclusions -----	86
8.2 Future work -----	88
9 Figures-----	89
10 Tables-----	95
11 References-----	97



1 Introduction

Tribology is the science and technology which studies the interaction of surfaces in relative motion or static. Although the terminology is new, the science and the knowledge of the field is not [1]. Tribology includes the study of lubricants, lubrication, friction, wear and bearings.

Even though humans have an intuitive idea about wear and friction throughout the history; in recent times, the study of friction and wear of the machines has become important for the industry as the aim is to improve the lifespan of the machines. One possibility to do this is by reducing friction [1]. In the automotive industry, one aim is to improve the fuel efficiency of cars. It is known that the losses due to friction inside the engine of a car represents approximately 15% of fuel consumption [1]. Therefore, one focus of the industry to save fuel lies on the reduction of the friction in the engine. Another possibility to increase the lifespan of machinery is by reducing the wear between the contact surfaces [2], [3], [4]. There are different types of wear that machines can experience such as abrasion, adhesion, corrosion, fretting, etc. [2], [3].

In the industry, there are many different types of systems that realize tribological tests. Many of these testers use the pin on disc, ball on disc, block on ring, pin on flat or can perform more than one of these test methods. These devices measure the frictional force and calculate the friction coefficient. Some of these systems can perform the tribological test and include electrical parameters with a two wire system.

For the present thesis, the aim is to implement a tribological system that is including the measurement of electrical parameters such as voltage and current during the testing of the tribological properties. These electrical parameters are included using a variation of the four point probe measurement. At the market there are tribometers that include electrical parameters but none of them utilizes four point probe measurement yet.

In order to achieve this, a tribometer system is used. A current source and the respective measurement instruments for the voltage and current are connected to this tribometer. This specific tribometer uses the ball on disc setup on a reciprocating module to perform the tribological test (Figure 1).

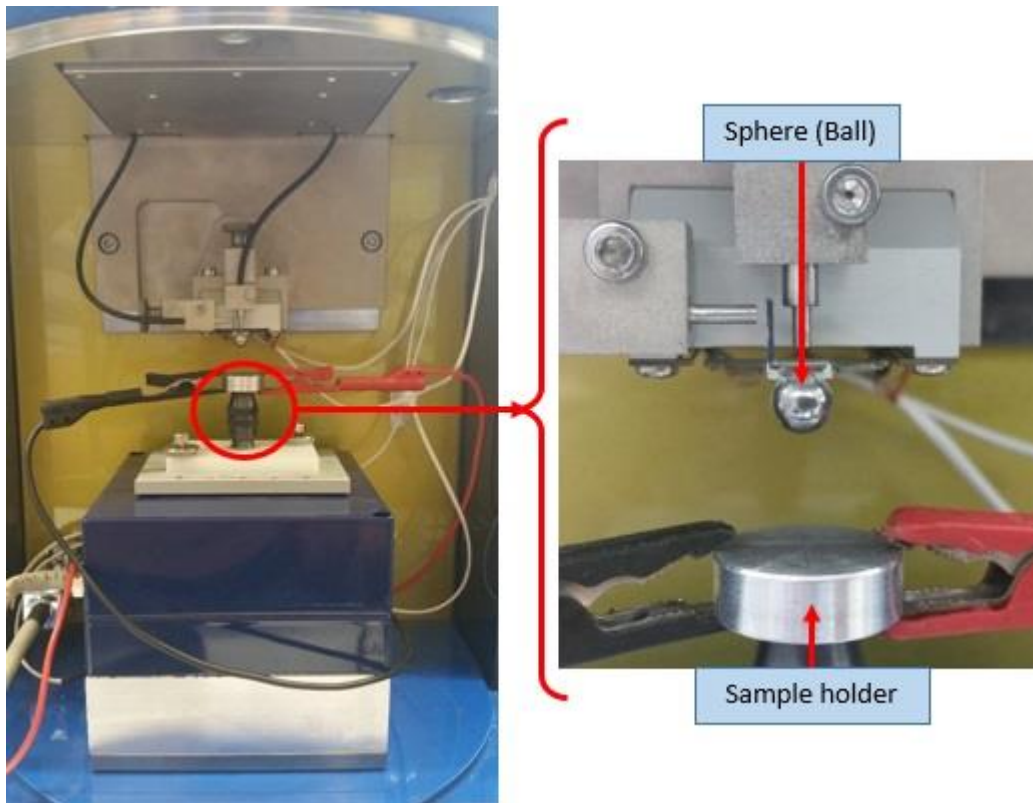


Figure 1: Basalt MUST LMS20 Ball on disk tribometer with reciprocating motion. The black and red clamps connected to the sample holder are used for injecting the current into the system.

The tribometer, has its own integrated software developed in Linux. When using an external computer, the connection with the machine is done using Ethernet. It also has special blocks designed for LabVIEW interface.

The current generator and the measuring devices have also a LabVIEW interface developed. Therefore, for controlling the whole system, LabVIEW will be used.

2 State of the art

2.1 Four point probe measurement

This method is used to calculate the resistivity of materials. It uses four tips to do the measurements. Two of them are used to inject the current, and the other two are used to measure voltage.

The four point probe measurement is widely used in device designing and manufacturing for measuring resistance and finally the resistivity of semiconductors and other materials [5]. This method uses a linear array of four thin tips equally spaced which are in contact with the surface of the sample. In this method, is common to use the exterior tips (1 and 4) shown in Figure 2 for injecting the current and the inner tips (2 and 3) for measuring the voltage in the surface of the sample [6].

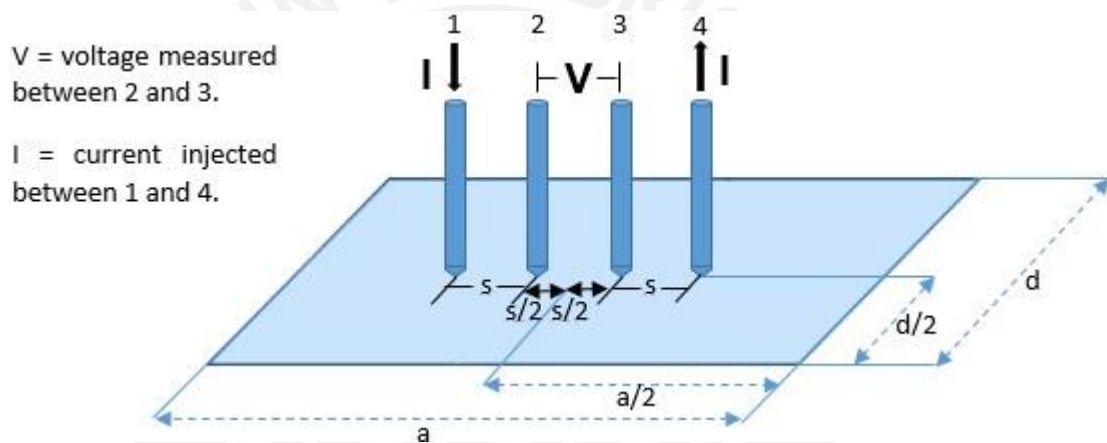


Figure 2: Four point probe measurement [7]

Although the four point probe measurement is used to calculate resistivity, for the present thesis, it will not be possible to set the four tips of the method due to the equipment that is used. In this particular case, the method that will be applied will be the four wire sensing that is used to determine resistance when there is a high current been injected and a low voltage been measured. Both methods operate using a similar principle.

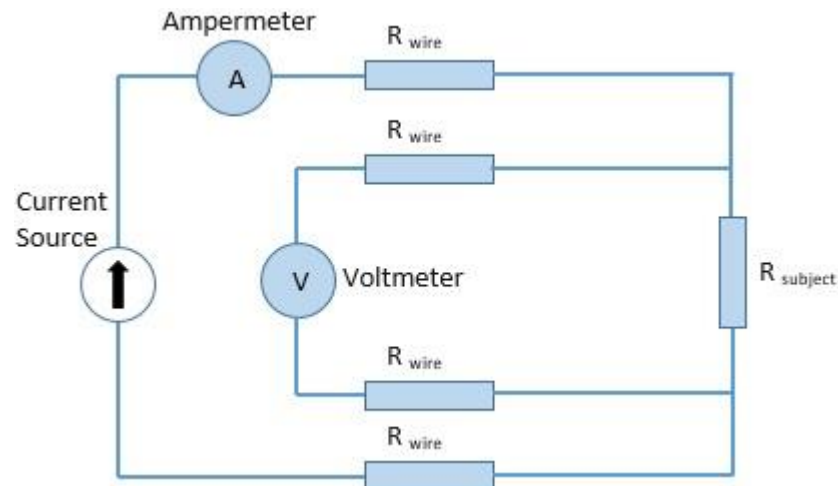


Figure 3: four wire sensing

From Figure 3, the resistant $R_{subject}$ is calculated as follows:

$$R_{subject} = \frac{Volts}{Ampere}$$

Equation 1

2.2 Tribology

Tribology is the science and technology of interacting surfaces in relative motion. It studies the interaction of friction, wear and lubrication[8].

2.2.1 Friction

Friction is defined as the resistance to the movement or the tendency for displacement that a solid body experiences when it moves or is about to be moved over another body in contact with it [2]. This resistance to the movement depends on the characteristics of the surfaces. From the definition given, there are considered two cases of bodies in relative motion: rolling and sliding. In both cases as illustrated in Figure 4, a tangential force F is applied to the upper body in order to move it over the surface of the static body [2].

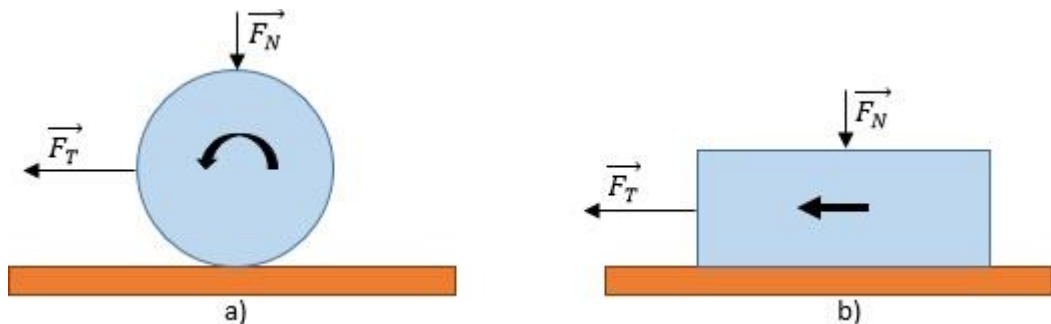


Figure 4: Frictional force \vec{F}_T used to cause motion by (a) rolling and (b) sliding

From the Figure 4, the ratio between this tangential force \vec{F}_T and the normal force \vec{F}_N is known as the coefficient of friction, which is denoted by the symbol μ and is calculated as follows:

$$\mu = \frac{\vec{F}_T}{\vec{F}_N}$$

Equation 2

As stated before, friction appears when two bodies are in contact. When a tangential force is applied in order to generate the relative motion, this force increases from zero to a finite value and generates some microdisplacements δ but the body does not move [4]. The tangential force will increase until it reaches a certain value, called static friction force F_s . The intermediate values of the tangential force are termed as partial static friction force [4].

Once the body starts to move, the resistance to the motion reduces too but it never disappears completely and remains constant. This friction force is termed as the kinetic friction force F_k [4].

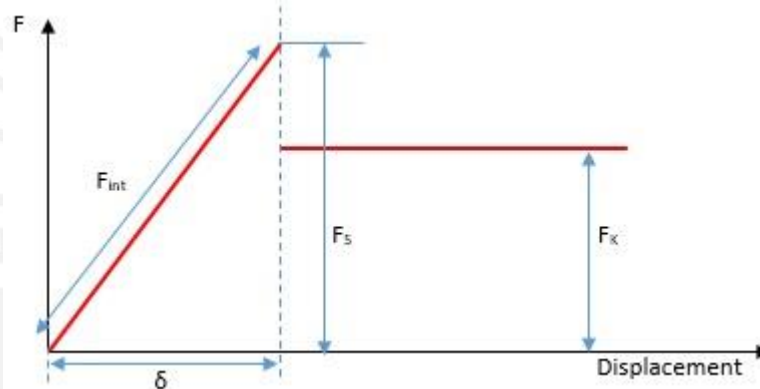


Figure 5: Microdisplacements δ , F_s maximum static friction, F_{int} intermediate static friction and F_k kinetic friction [4].

2.2.1.1 Laws of friction

The laws of friction are of varying reliability, but except in some cases, they provide useful summaries of empirical observations. The first law states that the friction force is proportional to the normal load as shown in the Equation 2 [2]. This means that if the load of the body increases by a factor of n , the tangential force must increase by the factor n too (Figure 6).

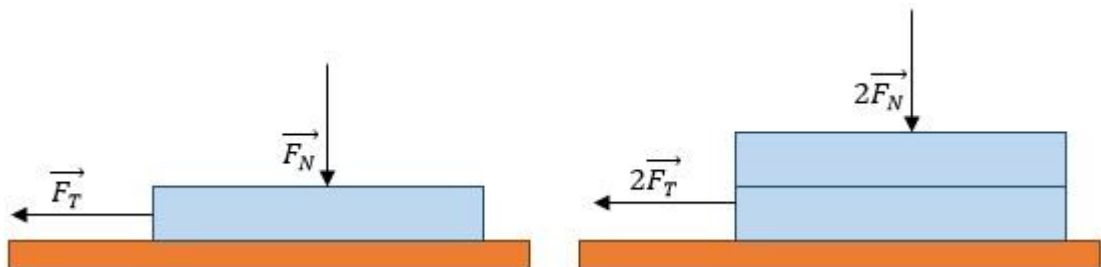


Figure 6: First law of friction

This law is valid for many materials under lubricated or unlubricated sliding conditions. Although most metals and other materials obey this rule, polymers often do not because polymers tend to reduce their friction coefficient when the normal force increases [2].

The second law states “the friction force is independent of the apparent area of contact” [2] (see Figure 7). This means that the contact between two bodies, happens in individual spots rather than in their whole area. This is due to the roughness of both surfaces and therefore, they are unable to contact over their entire nominal surface [2], [4]. This nominal surface is called the apparent area of contact while the area of all the spots in contact is called the real area of contact. The area of this spots is very small compared to nominal area, so the real area is smaller than the area that cover both bodies [4].

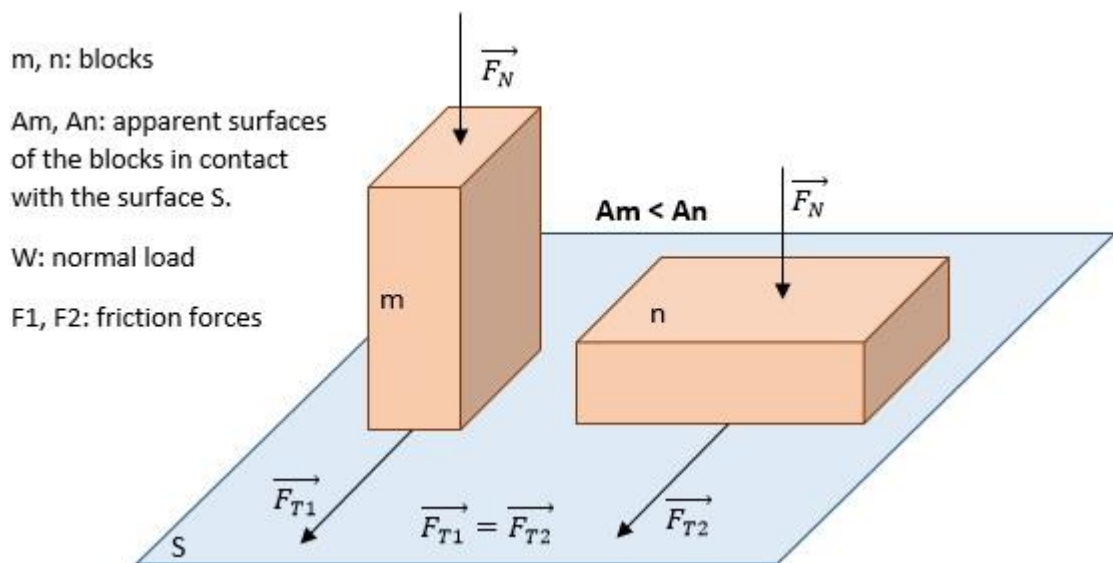


Figure 7: Second law of friction

The third law states “the friction force is independent of the sliding velocity” [2]. The frictional force needed to start sliding is higher than the friction necessary to maintain it, and hence, the coefficient of static friction (μ_s) is higher than the coefficient of dynamic friction (μ_d) [2]. But once sliding is established, the coefficient of dynamic friction is independent of the sliding velocity over a wide range [2]. This is true only if the material does not change during the sliding (e.g. wear).

2.2.1.2 Real contact area

When two surfaces come closer to each other, their asperities with maximum height come into contact. As the load increases, new asperities come into contact forming individual spots [4]. The total area of these spots is called the real contact area. This area depends on both mechanical behavior of the spots of the surface layers such as elastic and plastic deformation and the roughness [4]. When the real contact area is built up, some parts of the surface asperities elastically deform while others go plastic. So in general case, the deformation is elastoplastic [4].

2.2.1.3 Interfacial bonds

If two clean surfaces are in contact, the interatomic attraction forces are the same as in the bulk [4]. Several types of interatomic bonds can be identified.

Ionic bonding occurs between anions and cations held together by electrostatic forces. Ionic solids have high strength [4].

The covalent bonding between neutral atoms is generated by overlap of their electron fields that results in very strong bonding forces in crystalline solids like diamond [4].

The van der Waals bonding may occur between any atom or molecule due to dipole-dipole interaction. This bond is responsible for the adsorption of environmental species by a solid surface [4].

The metallic bonding can be found in all metals and is caused by free electrons freely moving in ionic lattice. The bonding is generated between the contact surfaces only when the surface films are absent (e.g. when sliding in high vacuum) [4].

Each individual atom in the bulk of a material interacts with its nearest neighbors through these forces. A specific amount of energy associated with the interaction is referred to as the cohesive energy that plays an important part in tribology [4]. An atom on the free surface is under different conditions because its number of neighbors has been reduced and as a result there is no bonding outside the solid. For this reason, the surfaces exhibits an excess of energy known as the surface energy. This energy controls the capacity of surfaces to form adhesive junctions [4].

2.2.1.4 Sliding friction

A simple way to understand friction is that a force is caused by two sources: an adhesion force developed at the real contact area between the surfaces and a deformation force needed to plough the asperities of the harder surface through the softer. At the end, the resulting frictional force F is the sum of the two contribution terms friction due to the adhesion F_{adh} and friction due to deformation F_{def} [2].

$$F = F_{adh} + F_{def}$$

Equation 3

Adhesion refers to an atomic bonding process that occurs between contacting points on opposing surfaces. Although this statement seem to be implausible, the adhesion between two metals is possible when both surfaces are clean this means free of oxides, other surface films and gases under very low levels of pressure [2].

Mechanical deformation due to friction is another source that increases the frictional force. This occurs when the asperities of two sliding surfaces come into contact. This deformation is accompanied by dissipation of mechanical energy.

2.2.2 Wear

Wear is the damage to a solid surface, which involves progressive loss of material, due to relative motion between that surface and the contacting surface. This includes degradation by the displacement of material at the surface as well as removal of material. The wear process common in machines in which one surface slides or rolls against the other with or without the presence of lubricants, and the more specialized types of wear which occur when the surface is abraded by hard particles moving across it. Furthermore, erosion by solid particles or liquid drops striking it or by the collapse of cavitation bubbles in a liquid can occur [3].

Wear is not a material property but a system response. The wear rate of a material can vary from 10^{-10} to 10^{-3} mm³/Nm depending on contact conditions such as the counterpart material, contact pressure, sliding velocity contact shape, suspension stiffness, environment and the lubricant [3].

2.2.2.1 Wear mechanisms

Mechanical wear describes wear governed mainly by the processes of deformation and fracturing. The deformation process has a substantial role in the overall wear of ductile materials and the fracturing process has a major role in the wear of brittle materials. Chemical wear describes wear governed mainly by the growth rate of chemical reaction films. This growth is accelerated mechanically by friction. Thermal wear describes wear governed mainly by local melting due to frictional heating. Diffusive wear is also included in the term “thermal wear”, since it becomes noticeable only at high temperatures. The wear of brittle materials caused by fractures following thermal shocks may also be included in thermal wear [3].

2.2.2.2 Wear modes

In order to understand wear better, in the following, the “abrasive”, “adhesive”, “fatigue”, “corrosive” and “fretting” wear will be described and a brief schematic in Figure 8 will be shown [3].

Abrasive wear is attributed to hard particles or protuberances forced against and moving along a solid surface cutting or plowing it [3]. This is one of the most common forms of wear and a major form of damage to machinery especially in mining and agriculture industries [3], [4].

Adhesive wear results from the shear of the friction junctions. The basic mechanism of this type of wear is adhesion. This wear process evolves in exactly the same way as adhesion friction. A very distinguishable feature of this form of wear is that transfer of materials from one surface to another occurs due to localized bonding between the contacting solid surfaces [3], [4].

Fatigue wear, is the damage due to the high stress that a material experiences. This damage includes the formation of cracks on the surface [3], [4].

Corrosive wear occurs due to the formation of corrosion products at the friction surfaces that exert significant effect on the wear behavior. Corrosive wear depends on many factors such as chemical composition and micro structures of the contact surfaces, rigidity and porosity of contact surfaces, pressure or absence of surface cracks and grain boundaries, etc. [3], [4].

Fretting wear occurs due to the oscillation between two surfaces that are not intended to move [4]. Two general types of fretting wear have been identified. Fretting fatigue is caused by cyclic loading. This leads to wear and the formation of cracks on the surface of the materials. The other possibility is fretting corrosion. This fretting occurs when chemical interaction is predominant.

This leads to the formation of oxides. This oxide particles act as an abrasive material at the surfaces [2], [4]. These two types of fretting occur simultaneously.

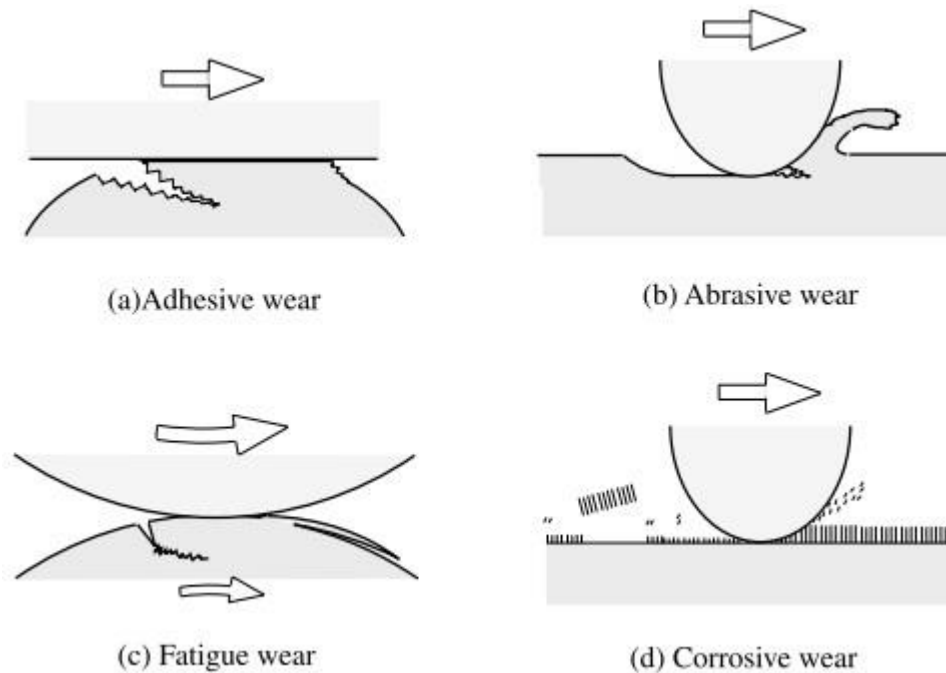


Figure 8: Schematic of representative wear modes [9]

2.2.2.3 Sliding wear test methods

In the following, experimental arrangements are discussed that have been used to study sliding wear. The aim of these tests is to simulate practical applications and provide useful design data on wear rates and coefficient of friction [2].

In Figure 9 the most common geometrical arrangements for wear testing apparatus are shown. The shown methods may be divided in two types: those where the sliding surfaces are symmetrically disposed and the wear rate is expected to be the same; and the more common and used arrangements where the system is asymmetric [2], [10].

The most common setup is a block against a ring (Figure 9b). Further setups are a pin pressed against a disc rim (Figure 9d), pin on rotating disc (Figure 9e), a pin on a translating surface (Figure 9f) or a ball on disc [11].

It is important to notice in these asymmetrical testing that one component of the mating pair, commonly the pin or block, is called the *specimen*. The wear rate of this specimen is measured. The counterpart is called the *counterface*.

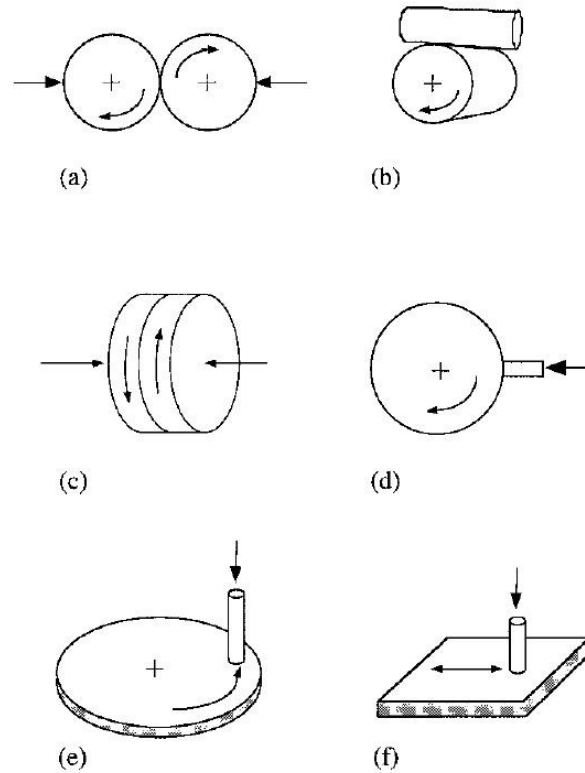


Figure 9: Sliding wear tests [10]

Table 1: Advantages and disadvantages of some wear test configurations [11]

Test	Advantages	Disadvantages
Pin on Disc	After run-in, surface pressure remains constant. Easy to determine wear volume and wear rate. The model closely simulates a linear friction bearing.	Difficult to align pin. If the pin does not stand perfectly vertical on the plate, edge contact results. A very long run-in time is therefore necessary. The front edge of the pin can skim off lubricant. This makes a defined lubrication state impossible.
Ball on Disc	High surface pressures are possible. The ball skims off lubricant less than a pin does. The model is similar to a linear friction bearing and a radial friction bearing.	Very small contact ratio: The contact surface of the ball is small compared to the sliding track on the disk. The contact area is enlarged by wear. Difficult to determine the wear volume of the ball.
Block on Disc	The model is capable of simulating a variety of harsh field conditions, e.g., high temperature, high speed, and high loading pressure.	

2.2.3 Lubrication

The sliding between two solid surfaces of metals, ceramics and polymers is characterized by a high friction coefficient [1], [2]. The higher values of the friction coefficient often causes challenges in engineering applications that leads to intolerable high friction forces and energy losses [1], [2]. For the cases where high friction coefficient is not needed, lubricants are used to reduce both wear and friction [1], [2].

Lubrication is defined as a process that reduces friction and wear by applying a mid-layer of a different material in between the two moving surfaces [4]. This intermediate material is called lubricant. Lubrication also performs other functions such as refrigeration of the rubbing surfaces or protection against corrosion [4].

2.2.3.1 Lubrication regimes and the Stribeck curve

As it was stated before, the lubrication functions by introducing in between the sliding surfaces a layer that reduces the shear strength [1], [2], [12]. There are different types of lubricant layers that are identified from the Stribeck curve and are shown in Table 2.

Table 2: Lubrication regimes [1], [2], [12], [13]

Hydrodynamic lubrication	The fluid film separating the surfaces in relative motion is thick enough for the opposing surfaces to not getting in contact to each other.
Elastohydrodynamic lubrication	For very thin liquid lubricant films and due to high pressures, the fluid film's thickness is not high enough. Therefore, some asperities of the opposing surfaces are in contact and experience deformation.
Boundary lubrication	The asperities of the surfaces in motion are covered with a monolayer of adsorbed lubricant molecules. The appreciable asperity contacts and junctions occur.
Solid lubrication	A solid film with low shear strength separates the surfaces in relative motion.
Self-lubrication	Is characterized by the bearings ability to transfer microscopic amounts of material to the mating surface. This process creates a film that provides lubrication and reduces friction over the length of rail or shaft

The Stribeck curve represents the coefficient of friction as a function of the product of the absolute viscosity (η), and the rotational velocity in revolutions per second (N), divided by the load (\vec{F}_N). this curve has a minimum that allows to identify different lubrication mechanisms (Figure 10) [12].

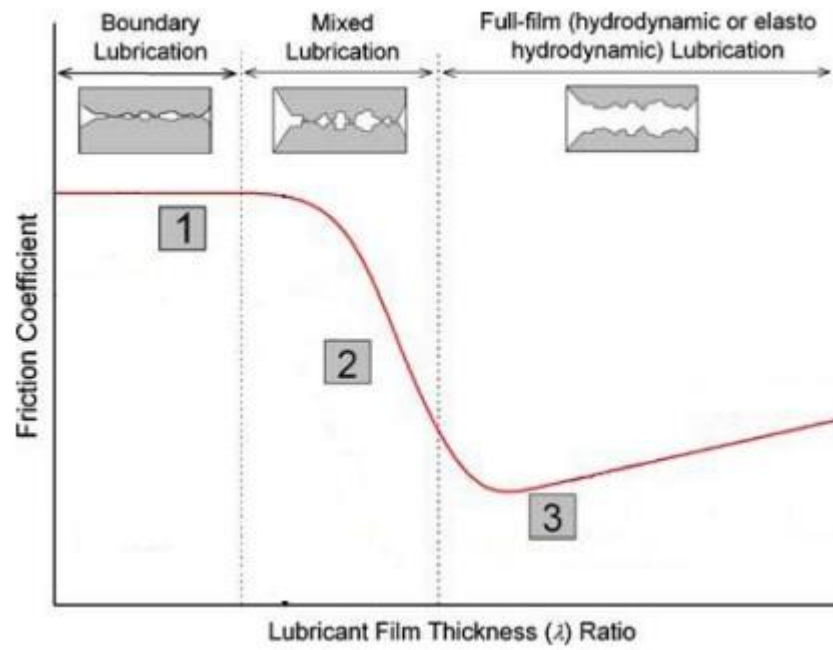
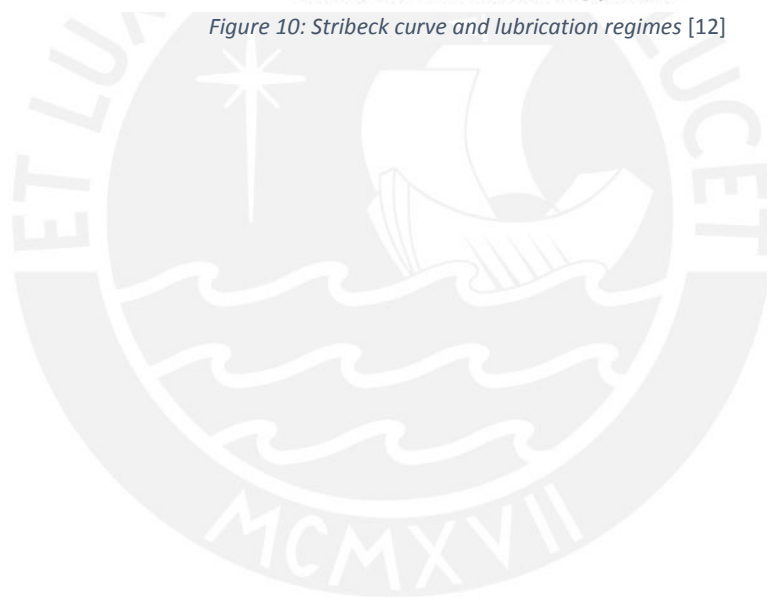


Figure 10: Stribeck curve and lubrication regimes [12]



3 Electronic interconnections

The development of semiconductors and integrated circuits during the past century lead the way of the evolution of the electronic industry. The miniaturization of the components resulted in the development of different manufacturing technologies with the aim of packing more functionalities into a small space. This requires also interconnection reliability, increased device functionality and higher speed circuits [4].

The increased functionality and complexity of microelectronic systems in less space and the need for more reliability, have led to the development of several types of area array packages like dual-in-line packages (DIP), plastic leadless chip carrier (PLCC), ceramic pin grid array (CPGA), ball grid array (BGA) and the most recently, chip scale package (CSP) [4]. The important characteristic of these devices apart from its small size, is the capability to provide environmental protection and reliable electrical performance for use in harsh environments (automotive, military and space applications). All these goals are possible when the connector degradation mechanisms are well defined and various mitigating measures have been identified [4]. Nowadays there is a great variety of types and size of electronic connectors used in different electronic devices applications (see Figure 11) [4].

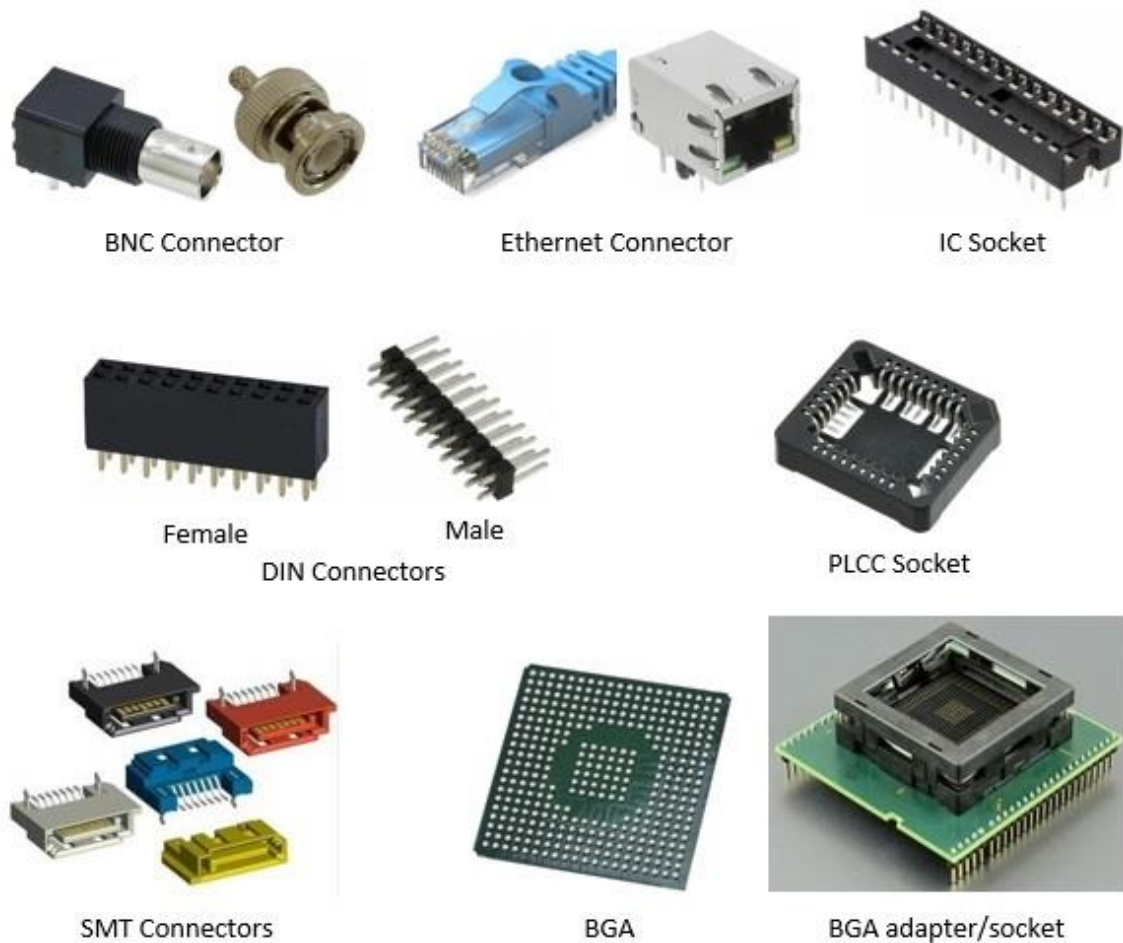


Figure 11: Generic electronic connector designs used in different electronic systems and devices (taken from [14]–[24])

3.1 Materials for electronic connections

Electronic connections are one of the most critical parts for interconnecting systems and essential elements in providing the electronic signal path. Although in the recent past electronic systems have changed radically, the basics of connector technology have remained essentially unchanged [4].

The performance of an electronic connection depends on both: the bulk resistance of the contact and the interface resistance. For an optimal electrical performance, the electrical path should comprise the material with the highest electrical conductivity, largest cross-section, and shortest conductivity path. In the past, the resistance to the adverse effects of environment (corrosion), as well as maintaining a very low contact resistance, were ensured by plating the whole contact with a noble metal such as gold or silver. With the increasing price of gold, the plating is reduced only to the mating area[4]. Also, the thickness of the gold finishes is decreased. This potentially creates porosity problems which can affect the quality of the component [4].

Coating is of a particular importance in electronic connections because it can significantly improve properties of a connection such as mechanical (hardness, toughness and strength), thermal (expansion, conductivity), electrical (resistivity), wear (abrasion and erosion resistance) and chemical (Resistance to oxidation, corrosion, tarnishing) [4].

3.2 Contact materials

In engineering, a solid conductor is a material of high conductivity. The conductivity of these materials is in the order of 10^6 - 10^8 Sm^{-1} at room temperature and these values can increase if the temperature reduces.[4].

Metallic conductors can be classified into two groups according to their applications: technically pure metals such as copper silver and gold which are the most common and widely used, and alloys used as conductors with particular properties such as wear resistance and low friction being the most common bronzes, brasses and some aluminum alloys [4].

For practical applications of these materials, is important to know detailed various properties of the material such as electrical, thermal, chemical, mechanical and tribological characteristics. These properties are important as the conductor material is subjected to different mechanical and thermal stress as well as the environment that surrounds it [4]. From Table 3 to Table 6 are shown some materials used for coatings and their properties.

Materials used for electrical contacts span over a wide range. Those made of copper, aluminum and their alloys are used in high current contacts while noble metals such as gold or silver and their alloys are used in low-current contacts [4].

Table 3: conductor materials used for electrical contacts [4]

Material	Density (g/cm ³)	ρ (10 ⁻⁸ Ω m)	λ (W/m ² C)	H _B	α (°C ⁻¹)	E (10 ⁵ MPa)
Copper	8.9	1.75	380	35	0.004	1.2
Aluminum	2.7	2.9	210	27	0.004	0.72
Silver	10.5	1.65	418	25	0.004	0.75
Platinum	21.4	11.7	70	40	0.0038	1.54
Palladium	12	10.8	70	32	0.0039	5.3
Gold	19.3	2.3	310	20	0.004	0.84
Rhodium	12.4	4.5	88	55	0.0043	3.0
Tungsten	19.3	5.5	190	350	0.005	3.5
Nickel	8.8	8	70	70	0.005	2.1

Table 4: Properties of some Pseudo alloy contact materials [4]

Contact Material	Density (kg/m ³)	Hardness, H _B	Electrical resistivity ($\mu\Omega$ m), not higher than	Thermal Conductivity (W/(m ² C))
Ag-CdO 85/15	9.7	100	0.028	325
Ag-Ni 70/30	9.6	75	0.03	355
Ag-Ni 60/40	9.5	80	0.035	310
Ag-C 97/3	9.3	50	0.026	-
Ag-C 95/5	8.7	40	0.03	420
Ag-Ni-C 68/29/3	8.9	65	0.035	355
Ag-Ni-C 69/29/2	9.5	95	0.035	-
Ag-Wo-Ni 48/50/2	13.5	160	0.041	275
Ag-Wo-Ni 27/70/3	15	210	0.045	230
Cu-C 97/3	7.3	35	0.04	380
Cu-Wo-Ni 48/50/2	12.1	150	0.06	190
Cu-Wo-Ni 27/70/3	13.8	200	0.07	135

Table 5: Compositions and characteristics of Silver-Based contact materials [4]

Material	Oxide (wt %)	Additives	Hardness	Conductivity (m/ Ω mm ²)
Ag/Ni10			H _v 10<60	52-55
Ag/SnO ₂	2	Bi ₂ O ₃ CuO	H _v 1<50	58-59
Ag/SnO ₂	2	Bi ₂ O ₃ CuO	H _v <50	58-59
Ag/SnO ₂	8		H _v 1<55	51-52
Ag/SnO ₂	10		H _v 1<55	48-49
Ag/SnO ₂	12		H _v 1<70	48-49
Ag/ZnO	8	Ag ₂ WO ₄	H _v 3<60	50
Ag/ZnO	12			43

Table 6: Some properties of Silver-Graphite materials [4]

Composition % Ag	Resistivity ($10^{-7} \Omega\text{m}$)	Hardness (10^5 N/m^2)	Density (kg/m^3)	Thermal conductivity ($\text{W/m}^\circ \text{C}$)	Coefficient of Friction
60	10	2.96	3.800	35	0.15
70	3	3.05	4.500	115	0.175
75	1.75	3.10	5.200	210	0.19
80	1	3.13	6.000	345	0.20
90	0.32	3.22	7.000	385	0.23
95	0.2	3.26	8.000	410	0.25

An alternative to metallic electrical contact materials are MAX phases materials. These are a group of ternary compounds with the general formula $M_{n+1}AX_n$ where M refers to an early transition metal, A refers to an element from the group IIIA to VA and X refers either carbon or nitrogen [25], [26]. MAX phases combine some of the properties of metals such as good electrical and thermal conductivity machinability, thermal shock resistance and damage tolerance, with properties of ceramics, such as high elastic moduli, high temperature strength and oxidation and corrosion resistance [25] (see Table 7). Due to this properties, potential fields for these materials are structural materials for high temperatures, tribological protective coatings, electrical contacts in aggressive environments and as sensing materials in sensor technologies [26]. MAX phases are used in this thesis as an example material to proof the operability of the implemented system.

Table 7: Some properties of MAX phases compounds

Compound	Density (g.cm^{-3})	Resistivity ($\mu\Omega\text{.m}$)	CTE ($\times 10^{-6} \text{ K}^{-1}$)	Young module (GPa)
Ti_3SiC_2	4.52	0.227	9.1	322
Ti_2AlN	4.31	0.25	8.8	288
Cr_2AlC	5.21	0.71	13.3	278

3.3 Coating techniques for electrical contacts

The use of protective and wear-resistant coatings for electrical contact applications is increasing nowadays. This trend is due to the many useful functions that the coating of surfaces offers such as corrosion and wear protection, diffusion barriers, conductive circuit elements, fabrication of passive devices on dielectric surfaces among others. Depending on the coating material characteristics, contact operating conditions and intended functions, the thickness of the deposited material onto the contacting surfaces can vary [4].

The act of modifying the surface so that it obtains properties which are different from the bulk properties is called surface engineering. In the following, some techniques used to modify the surface of materials in order to improve the corrosion resistance and/or their tribological properties are shown [4].

3.3.1 Surface segregation

Although this method is widely used in the case of ferrous alloys, thermal treatments are also used to modify the surface of electric contact materials. Segregation is the enrichment of a material constituent at the surface interface of material and provokes an intensive surface

segregation of impurities at the free surface. This segregation may intensify or moderate the tendency of the surface to absorb active species from the environment [4].

The mechanical means of surface modification include cold working by peening, shot blasting, and other machining processes. This process increases the hardness, fatigue and stress corrosion resistance [4].

3.3.2 Ion implantation

This is a process used in the semiconductor device technology, but it is also used as a surface modification technique to improve wear resistance and connectability of electrical contacts.[4].

This process consist of introducing foreign atoms into a solid substrate by bombardment of the solid substrate with energetic ions[4]. This enhances properties such as wear, friction and corrosion resistance [4].

3.3.3 Electroplating

This method is used in the industry of electrical contact manufacturing [4]. Electroplating consists of depositing metals or alloys on the top of an electronically conductive surface [4]. This process is usually done form aqueous electrolytes at room temperature. A unique feature of this process is the possibility to control the deposition rate of the coating and its basic characteristics by changing the current density [4].

The coatings produced by this method possess a higher resistance to electrical erosion and hardness than other coatings of the same composition deposited by other techniques [4]. The advantages of electroplating are high deposition rates, a nonuniform thickness due to ohmic effects, a required conductive surface, a wide variety of metals that can be electroplated, low cost and ease of control [4].

One serious disadvantages of electroplating is the presence of high internal stress that can lead to cracking generated in the coatings. Hence, surface preparation prior to the electroplating is required [4]. Another disadvantage of this method is the limited variations in the composition. Due to the instability of metals in different salt solutions, electrolytes for all combinations of metals are not possible [4].

3.3.4 Electroless plating

It is a process whereby any catalytic surface in contact with the plating solution is coated uniformly regardless of the part geometry. Several metals can be plated electroless such as palladium, copper, nickel and silver but the most common are nickel and copper [4].

The nickel electroless plating [27] can be applied with excellent adhesion to many different substrates such as steel, aluminum, copper bronze and brass as well as nonconductors such as ceramics and plastics. These type of coatings have a good wear resistance due to their high hardness and natural lubricity [4].

One of the main uses of electroless nickel in electrical contact applications is to work as coating for aluminum and zinc connectors. This coating provides protection against corrosion, and wear[4].

In the case of copper electroless plating, it is limited for certain applications such as in the semiconductor industry. This property together with the uniformity of the electroless nickel deposit, makes it an ideal wear surface in many sliding wear applications [4].

3.3.5 Cladding

This method involves the combined rolling of several layers at pressures 80-200 MPa. As a result, cold welding occurs at interfaces of different layers. Rolling is often carried out at elevated temperatures to achieve stronger interlayer adhesion [4]. Cladding of common substrate metals such as copper and its alloys, steel and aluminum with precious metals such as gold, silver and platinum is a well-established technique to realize the optimal combination of functional properties. This method permits obtaining a combination of different properties such as thermal and/or electrical conductivity, a high strength, corrosion, wear and heat resistance, light weight and springiness [4].

3.3.6 Chemical deposition

This method involves the reduction of the metal ions present in the solution on the active surface [4]. The hardness of chemical deposited coatings exceeds that of corresponding annealed metals, but it is 30-50% less than that of electroplated coatings. For these reason the wear resistance of these coatings is low [4]. This method is mainly used as the first stage of the metallization of insulating materials, followed by the deposition of an electroplated coating [4].

3.3.7 Plating by swabbing

Although this is not recognized as an acceptable plating method, it is used to provide thin films such as silver on the conductor [4].

3.3.8 Physical vapor deposition technology

This method has been suggested as an alternative method of coating [4]. The sputtering process, used in layer production, is the physical vapor deposition (PVD) technology, which is based on then process resulting from glow discharge. Metal atoms are sputtered from the target by bombardment with inert gas ions (argon) and deposited on the substrate placed in the chamber. The mechanical, electrical and chemical properties of the growing layer be varied by changing deposition parameters, such as residual gas pressure and composition, the sputtering rate, the substrate temperature, and the substrate voltage [4].

Vapor deposition has advantages over electroplating. With this method is possible to create coating structures which are often either difficult or impossible to obtain by electroplating, including multilayers, composites and amorphous alloys of metals and ceramics. It is also an agile manufacturing technique, as the same vapor deposition system can be used to deposit almost any coating material onto any substrate [4].

This technique is used in electronics to deposit contact coatings of precious metal alloys onto microprofile wires and connectors and switching contacts [4]. In order to do the deposition of the material, a vacuum chamber is needed. Therefore, this process is more expensive.

3.3.9 Electro-Spark Deposition (ESD)

ESD is a capacitor discharge, micro-arc welding process that utilizes short duration electrical pulses, discharged at a controlled energy levels to create a metallurgically bonded surface modification [4]. In this process flows very high densities of energy without significant heating of the specimen. Also in spark discharges, the distance between the electrodes and the substrate can be made extremely short in order to eliminate the effect of the environment during the deposition process. This improves surface properties such as wear and corrosion resistance, antisparking surfaces and customized coefficient of friction [4].

4 Experimental procedure and software

4.1 Connection setup

For the present thesis work, two Keithley 2000 multimeters have been used; one multimeter as an amperemeter and the second multimeter as a voltmeter. Furthermore, one Keithley 2400 SourceMeter was used as a current source. For the measurement of the tribological properties, the Basalt MUST tribometer produced by TETRA was applied. The whole system uses two communication protocols to connect all the devices with a computer, all the Keithley devices are connected through the IEEE-488 protocol (GPIB) and connected to the PC via USB converter. The Basalt MUST tribometer is connected to the computer using Ethernet (Figure 12 and Figure 13). The description of the devices is shown in Table 8. The GPIB addresses are chosen randomly and therefore are indicated in the table.

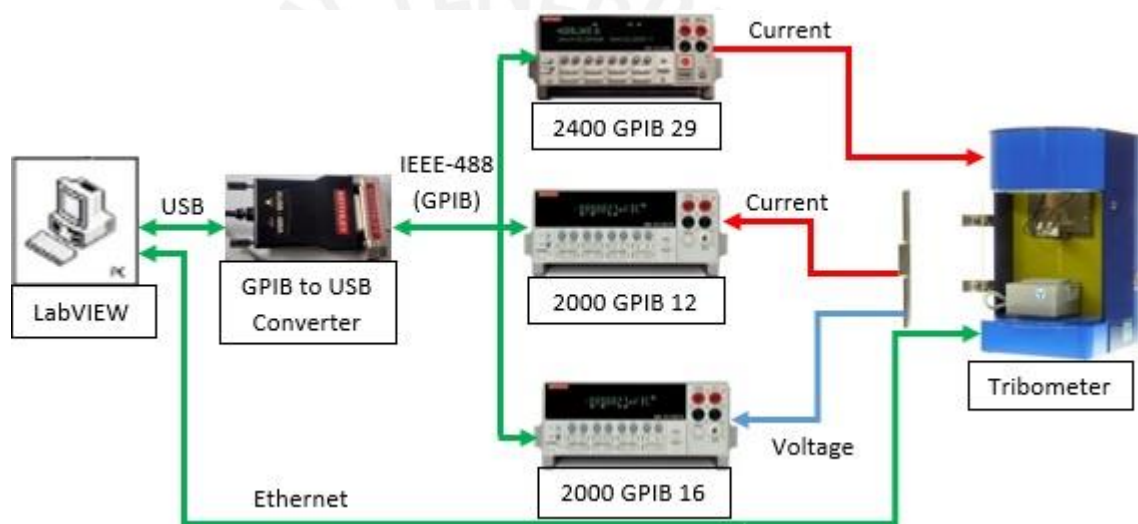


Figure 12: Schematic interconnection diagram. The communication of all the devices with the PC is represented with the green arrows. The voltage measured by the voltmeter is represented by the blue arrow. The current injected by the source to the tribometer is represented by a red arrow as well as the current being measured by the amperemeter

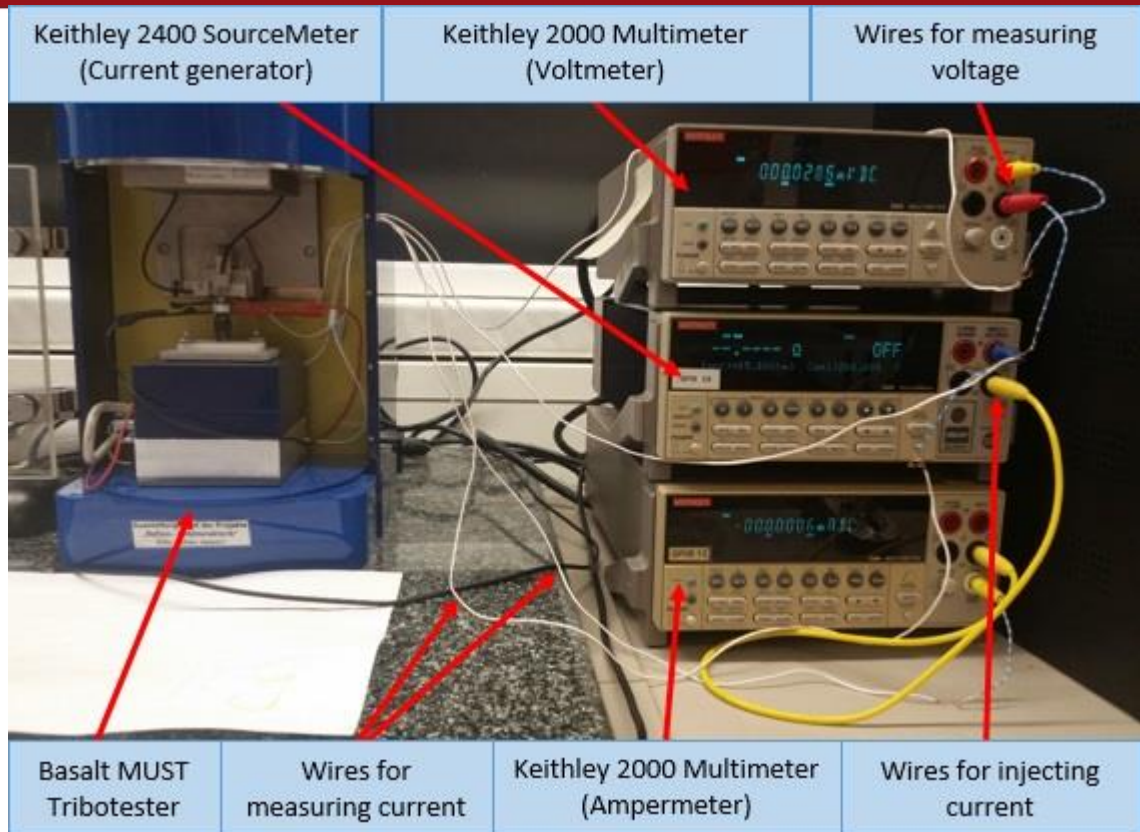


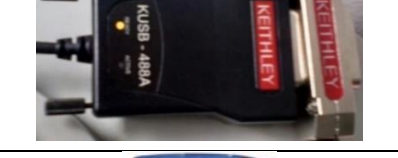



Figure 13: Image of the connection setup indicating all the used devices to measure the electrical as well as the tribological parameters.

Table 8: device description

	<p>Keithley 2400 Source Measure Unit (GPIB 29) This source can provide voltage and current with a resolution of 6 ½ digits.</p>
	<p>Keithley 2000 6 ½ - Digit Multimeter (GPIB 12 and 16) Configured as an ampermeter. GPIB 12 is for the ampermeter and GPIB 16 is for the voltmeter. It is fast up to 2000 readings/second when used 4 ½ digits, accurate, and highly stable.</p>
	<p>Keithley KUSB – 488A IEEE – 488 GPIB Interface It turns any computer with a USB port into a functional GPIB controller. The device is compliant with USB 2.0 and has an IEEE data transfer rate upwards of 1.5 MB/s through the USB port.</p>
	<p>BASALT-MUST Precision Tester Used for characterization of physical properties of surfaces and materials force and movement interactions in the micro range.</p>

4.2 BASALT-MUST Precision Tester

The BASALT-MUST precision tester consists of the BASE UNIT that contains the X-Y positioning unit, the Z-positioning axis as well as the control components, which are powered by an external 12 V DC power supply (Table 9). It is possible to mount on the X-Y positioning unit, the motion module BASALT-MUST LMS20 and the measuring module BASALT-MUST 2D-FM 1N on the Z positioning unit (Figure 14). To protect the sensors and the specimen against airflow and therefore turbulence induced vibrations of the force transducers as well as bigger temperature changes, the test chamber can be closed with a glass door [28].

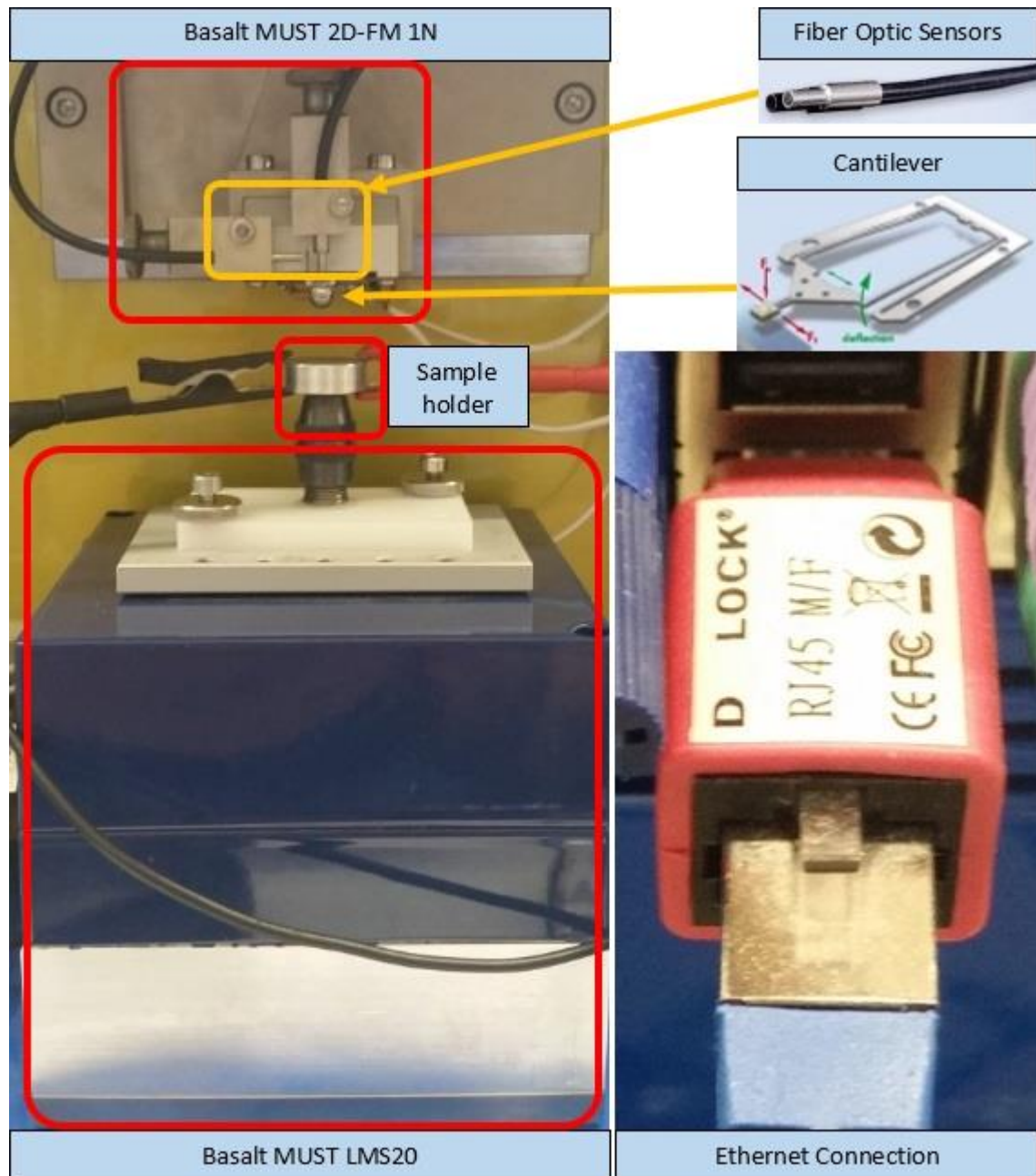


Figure 14: Basalt MUST main parts [28], [29]. On the upper part the square in red shows the Basalt MUST 2D-FM 1N module. The arrows in yellow show the main parts of this module which are the Cantilever and the fiber optic sensors. On the lower part the big red square shows the Basalt MUST LMS20 module and just above it, in a small red square is the sample holder. On the right side of the lower part is shown the Ethernet connector used for the tribometer.

The BASALT-MUST runs normally as a stand-alone-system with an integrated embedded Linux-PC [28]. For customized solutions, an external notebook or desktop PC can be used to control the tester and the experiments. The data transfer can be done via Ethernet [28].

Table 9: BASALT technical parameters [28]

X-Y positioning unit	drive type	stepper motor driven threaded spindle
	positioning range	20 mm x 20 mm
	positioning resolution	1 μm
	positioning accuracy	20 μm
	blocking force	> 30 N
	maximum speed	2 mm/s
Z positioning unit	drive type	stepper motor driven threaded spindle
	positioning range	50 mm
	positioning resolution	1 μm
	positioning accuracy	20 μm
	blocking force	> 30 N
	maximum speed	2 mm/s
Z fine positioning	drive type	piezo stack
	positioning range	40 μm (approx.)
	positioning resolution	0.25 μm
	positioning accuracy	1 μm
	blocking force	> 30 N
	position measurement	Optical incremental encoder with a resolution of 50 nm
Control unit	embedded Linux PC	
Power supply	12 V DC, 8 A	
Housing dimensions	204 mm x 356 mm x 259 mm (W x H x D)	

4.2.1 Basalt MUST working principle

The basic functional components of the BASALT-MUST are a 2D-force transducer and different precision motion modules. Relative motions can therefore be carried out between the micro-tool and the specimen. The two basic tests, linear oscillation or pin on disc are practicable for applications in the field of tribology. During the linear oscillation test the tool at the 2D force transducer is in defined contact with the specimen which is oscillating. The normal force F_N , the tangential force F_T and the displacement d are recorded with respect to the time [28].

4.2.2 Measurement module Basalt MUST 2D-FM 1N

This is the measurement module for both the normal and the tangential force and up to a maximum of approximately 1 N (Table 10). The main elements of this module are the exchangeable cantilever (force transducer) with its two perpendicular mirrors and the contact free measuring fiber optic sensors (FOS) (Figure 15) [28].

When a force is applied to the cantilever, it will bend and its displacement is measured contact less by the fiber optical sensors [28].

Table 10: Technical parameters of the Basalt MUST 2D-FM 1N [28]

Nominal normal force F_n	1 μ N to 1 N
Nominal tangential force F_t	1 μ N to 1 N
Sensor type	Absolute displacement measurement due to contact free working fiber optical sensor
Resolution	1/5000 of the nominal force (resolution is depending on the cantilever's stiffness).

4.2.2.1 Operational principle of the force transducer

The force transducer consists of a cantilever based on a dual double leaf spring, two perpendicular mirrors fixed on the flexible part of the cantilever and a mechanical carrier. At the tip of the cantilever a tool (ball) can be attached (Figure 15) [28].

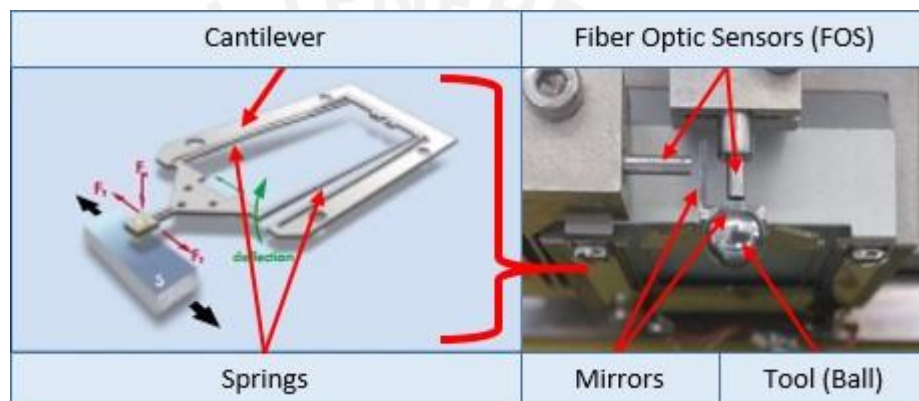


Figure 15: On the left side is shown the cantilever and the bending elements (springs). On the right side is shown the Basalt MUST 2D-FM 1N and the position of the cantilever, the tool, the mirrors and the FOS. [28]

If a force is applied to the cantilever, it will deform and built up an intrinsic force to compensate the applied force [28]. The applied force is proportional to the deflection:

$$F = k * d + F_0 \tag{Equation 4}$$

The constant F_0 can be eliminated by tarring the displacement and so the force F is:

$$F = k * \Delta d \tag{Equation 5}$$

4.2.2.2 Operational principle of the fiber optic sensors (FOS)

The FOS are used to measure the deflection of the force transducers. At the tip of the FOS a glass fiber bundle ends and is glued into a stainless steel tube. The end of the tub and thus the fibers are grinded and polished to achieve the reproducible quality of the tips [28].

About half of the fibers are used to illuminate a mirror. The other half receives the reflected light and guides it to a sensor where the light is converted into an electrical current. After the amplification of the current, it is converted into a voltage and can be digitalized by an A/D converter [28].

The displacement-voltage characteristic curve of the sensor is determined by the optical properties of the fiber bundle and the photometric distance law. A beneficial characteristic of the sensor is that it can be operated in two measuring ranges (Figure 16). The first range (MR1) can be used for measuring short distances with a high precision (50 – 150 μm) due to the great slope of the signal versus the displacement. The second range (MR2) is longer than MR1 by an approximately factor of 10. This means that the slope is almost ten times lower compared to the first range. In this range it is possible to measure longer distances (500 – 1500 μm) but the precision is lower [28].

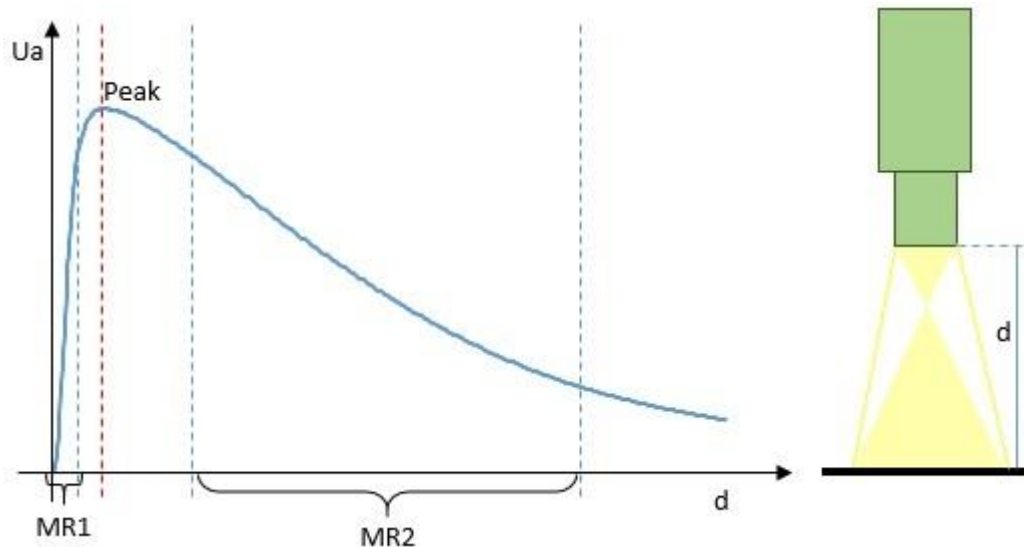


Figure 16: FOS characteristic curve [28]. d is the distance being measured by the sensor. MR1 and MR2 are the measurement ranges 1 and 2 respectively where the curve is considered linear. U_a is the voltage measured where “Peak” is the highest value.

The “Peak” of the signal curve is used to normalize the intensity at every distance between the mirror and the sensor tip.

During the calibration process, these normalized values are stored in a “look-up table” file [28]. The “look-up table” will be discussed in **4.4.1.9 Start_calib event**.

4.2.3 Motion module Basalt MUST LMS20

This module can perform movements of up to 20 mm stroke with a resolution of 0.1 μm and a velocity from 20 $\mu\text{m/s}$ to 20 mm/s. The blocking force is typically 1.5 N (Figure 17). With this module a sample can be moved reversing in x-direction to achieve a linear motion between the tool and the sample to perform various tests. Its working principle is similar to an electronically commutated DC motor with closed loop control [28].

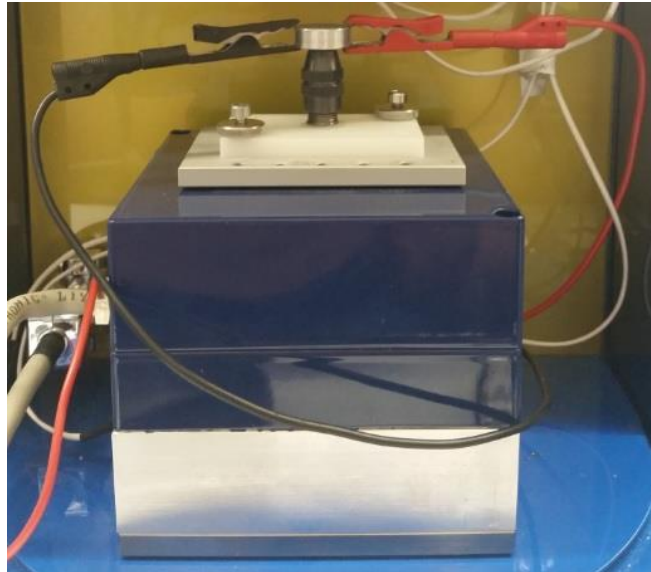


Figure 17: Basalt MUST LMS20

Table 11: Technical parameters of LMS20

Positioning and motion	Drive principle	Electrodynamic actuator
	Positioning range	+/- 10 mm
	Positioning resolution	0.1 μm
	Positioning accuracy	1 μm
	Velocity	Up to 20 mm/s
	Acceleration	5 m/s ²
	Maximum blocking force	Between 1.2 to 1.5 N
Operating temperature	+18 °C to +30 °C	
Dimension	Width: 90 mm, depth: 90 mm, height: 35 mm	
Weight	800 g (approx.)	





4.3 LabVIEW program structure

The developed program interacts with the connected devices described previously. The system injects current to the tribometer and measures voltage, current, tangential force, normal force and the position of the LMS20.

4.3.1 Keithley virtual instrument modules

The virtual instrument (VI) modules for Keithley 2400 SourceMeter used in the present work and a brief description are shown in Table 12.

Table 12: Keithley 2400 series

VI Icon	Module	Description
	Keithley 24XX.lvlb:Initialize.vi	Establishes communications with the instrument and optionally performs an instrument identification query and/or an instrument reset.
	Keithley 24XX.lvlb:Enable Output.vi	Enables the source to the output the assigned voltage or current to the device under test.
	Keithley 24XX.lvlb:Configure Output.vi	Configures whether the output is in terms of current or voltage, the amplitude of the output and compliance settings.
	Keithley 24XX.lvlb:Close.vi	Performs an instrument error query before terminating the software connection to the instrument.

One of the most important blocks of the 2400 is the “Configure Output” block as was stated in Table 12. The most important parameters of this block are shown in Figure 18 and a brief description in Table 13.

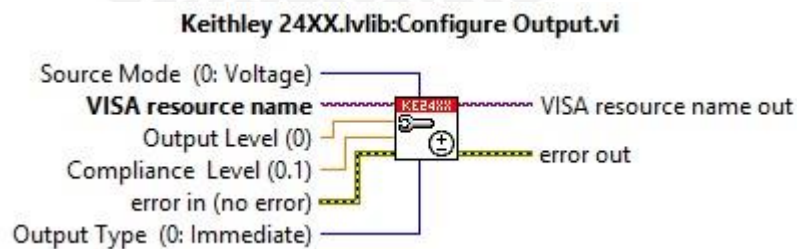







Figure 18: Configure Output library

Table 13: "Configure Output" library description

Parameter	Description	Comment
Source Mode	<p>Selects the voltage or current Source Mode to be configured.</p> <p>Value: 0 : voltage (default) 1 : current</p>	<p>The value "1" was used in order to select the current source mode of the device.</p>
Output Level	<p>The desired output level for the device. The source value unit depends on the Source Mode chosen.</p> <p>Valid range for 2400: -1.05 A to 1.05 A -210 V to 210 V</p>	<p>This is the level of current that is wanted to be generated. This value is set in the graphical user interface (GUI).</p>
Compliance Level	<p>Sets the maximum value for the value not regulated by the Source Mode control. For instance, if the instrument was supplying voltage, the compliance value would be in amps.</p> <p>Valid range for 2400: -1.05 A to 1.05 A -210 V to 210 V</p>	<p>The value used was 200 V to limit the maximum power given by the device.</p>
Output Type	<p>Determines whether the instrument will wait for a trigger to go to the desired output levels.</p> <p>Values: 0 : Immediate (default) 1 : Triggered</p>	<p>Was chosen immediate ("0") so the value entered at the "Output Level" appears soon after the "Start" button of the GUI is pressed.</p>
VISA resource name	<p>A reference to the instrument in use, this reference is created by the Initialize VI.</p>	<p>The GPIB address of the physical device used was 29. This value was already set in the machine but could be changed by the user.</p>

The VI modules for Keithley 2000 Multimeter used in the present work and a brief description are shown in Table 14.

Table 14: Keithley 2000 series

VI Icon	Module	Description
	Keithley 2000.lvlib:Initialize.vi	This VI passes the addressing information in the instrument descriptor to the instrument Open VI and returns the Instrument ID
	Keithley 2000.lvlib:Configure Output.vi	Configures the instrument to measure DC current or DC voltage.
	Keithley 2000.lvlib>Data Read Single.vi	Reads a measurement or calculation from the instrument
	Keithley 2000.lvlib>Data Read Multiple.vi	Reads multiple measurements or calculations from the instrument.
	Keithley 2000.lvlib:Close.vi	Closes the I/O interface with the instrument

One of the most important blocks of the 2000 is the “Data Read Multiple” block. The most important parameters are shown in Figure 19, and a brief description in Table 15.

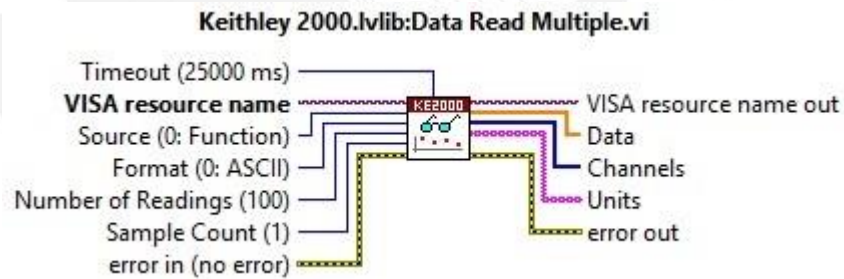


Figure 19: Data Read Multiple library

Table 15: "Data Read Multiple" library description

Parameter	Description	Comment
Timeout	<p>This control sets the amount of time to wait for a measurement. If the measurement is not returned within this amount of time, an error is returned in "error out".</p> <p>Default value. 25000 ms</p>	It was used the default value (25000 ms) because a trigger was not used.
Source	<p>Sets the source measurement to read.</p> <p>Default value: 0 : Function</p>	It was used the default value (0) in order to enhance speed.
Format	<p>Sets the format to request on the instrument.</p> <p>Values: 0 : ASCII 1 : Single precision 2 : Double precision</p>	It was chosen the single precision because it is the fastest format for acquiring data.
Number of Readings	<p>Sets the number of readings to acquire and return on the instrument.</p> <p>Default Value. 100</p> <p>Valid Range 2 - 1024</p>	This value is set by the user in the GUI. The value used in this work was 50 readings/s which is a moderate value for getting electrical parameters.
Sample Count	<p>Sets the number of times the instrument loops around the device action (delay + measurement) phase before waiting for another trigger event in the trigger model.</p> <p>Default Value. 100</p> <p>Valid Range 2 - 1024</p>	It was used the default mode (100) because a trigger was not used.
Visa resource name	<p>Unique reference to an instrument I/O session. It identifies which device to communicate with an all configuration information to perform the I/O</p>	It is the address of the device. In the present work, it was worked with two devices so the address of one is 12 and for the other one is 16.
Data	<p>Returns the measurement values for the selected source.</p>	It is the data obtained.

4.3.2 Basalt MUST VI modules

The most important VI modules for the BASALT MUST use in the present work and a brief description are shown in Table 16.

Table 16: BASALT-MUST Modules

Module	Description
MUSTDrvLW_Connect	Starts the connection with the MUST
MUSTDrvLW_StartStream	Initialize and starts the data stream with the specified time interval
MUSTDrvLW_GetStreamData	Read the data from the ADC channels which contains information of the Fn and Ft sensors in volts.
MUSTDrvLW_BaseUnitMoveAxis	Moves an axis from the base unit to a target position
MUSTDrvLW_BaseUnitGetState	Get the status and position of the base unit
MUSTDrvLW_FOSGetDist	Obtains the distance being measured by the sensor

MUSTDrvLW_Connect:



Figure 20: "Connect" library

Table 17: "Connect" library description

Parameter	Description
pIP_Adr	Sets the IP address of the BASALT MUST

MUSTDrvLW_StartStream:

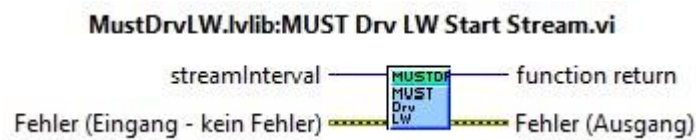


Figure 21: "Start Stream" library

Table 18: "Start Stream" library description

Parameter	Description
StreamInterval	Sets the interval for recording the streaming data in μ s.

MUSTDrvLW_GetStreamData:

MustDrvLW.lvlib:MUST Drv LW Get Stream Data.vi

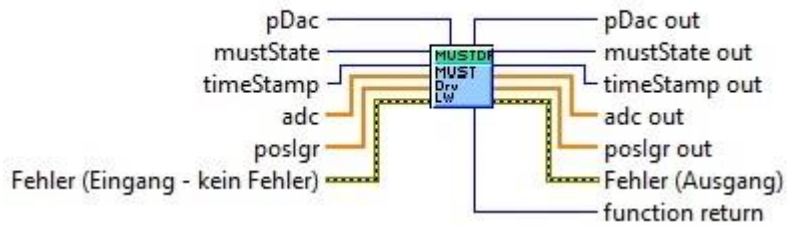


Figure 22: "Get Stream Data" library

Table 19: "Get Stream Data" library description

Parameter	Description
MUSTState	Status of the MUST –tester
TimeStamp	Starting time of the stream mode.
ADC[8]	8 channel ADC (0 – 5 V) Channel 0 – Pos LMP500 (not used) Channel 1 – Voltage Fn sensor in Volt Channel 2 – Voltage Ft sensor in Volts Channel 3 to 7 not used.
PoslGR[2]	2 channel position of the system of length measurement. Channel 0 – Absolute position of LMS20 in mm Channel 1 – Absolute position of the Z axis in mm

MUSTDrvLW_BaseUnitMoveAxis:

MustDrvLW.lvlib:MUST Drv LW Base Unit Move Axis.vi

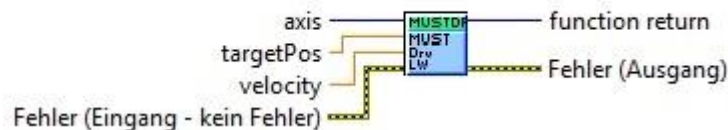


Figure 23: "Base Unit Move Axis" library

Table 20: "Base Unit Move Axis" library description

Parameter	Description
Axis	Choose the axis 0 – x-axis 1 – y-axis 2 – z-axis
TargetPos	Target position in mm
Velocity	Velocity in mm/s

MUSTDrvLW_BaseUnitGetState:

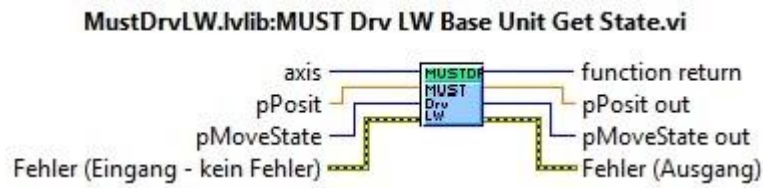


Figure 24: "Base Unit Get State" library

Table 21: "Base Unit Get State" library description

Parameter	Description
Axis	Choose the axis 0 – x-axis 1 – y-axis 2 – z-axis
pPosit	Actual position of the chosen axis in mm
pMoveState	Status of the movement, 0 : no movement 1 : moving

MUSTDrvLW_FOSGetDist:

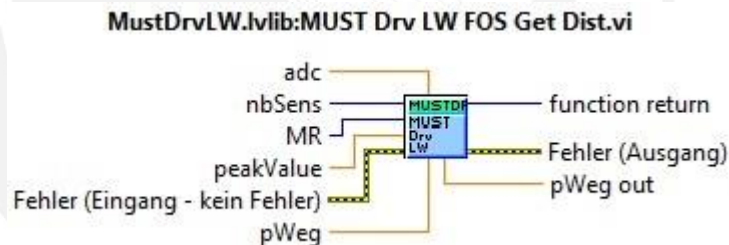


Figure 25: "FOS Get Dist" library

Table 22: "FOS Get Dist" library description.

Parameter	Description
adc	Raw data of the sensor in volts
nbSens	Selects which sensor is read: 0 – Sensor Fn 1 – Sensor Ft
MR	Measurement range (0 or 1) 0 – measurement range 1 1 – measurement range 2
peakValue	The maximum voltage value (peak)
pWeg out	Distance from the table files

4.4 Program description

Two programs were developed using the LabVIEW interface. One program operates the Basalt MUST tribometer and the other program operates the Keithley devices. This interface was chosen because the Basalt tribometer has only LabVIEW VI blocks available and there are also VI sub-routines available for the Keithley devices.

4.4.1 Tribological program

For both programs, all the VIs presented in the previous section have been used. The first developed program named “Tribology”, has an “Event Structure” (Figure 26). In this structure all the events activated by buttons from the graphical user interface are programmed (Figure 27).

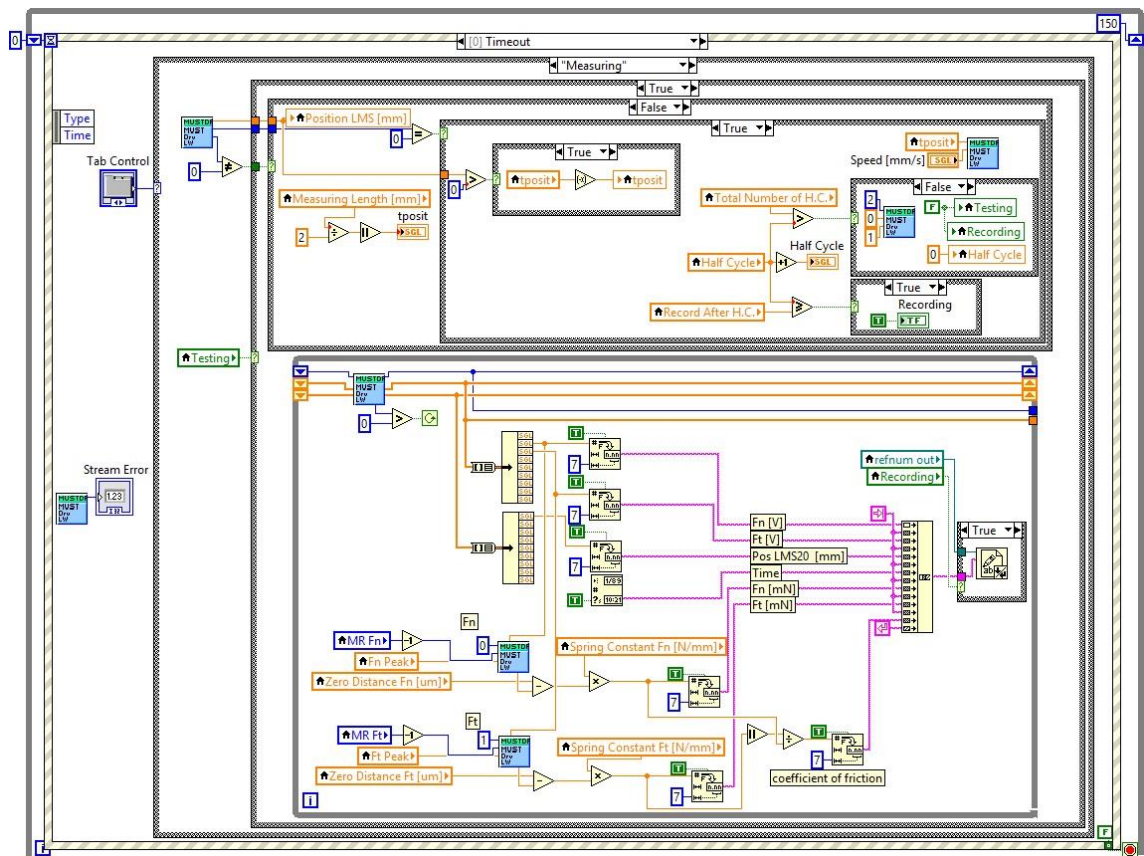


Figure 26: Main loop

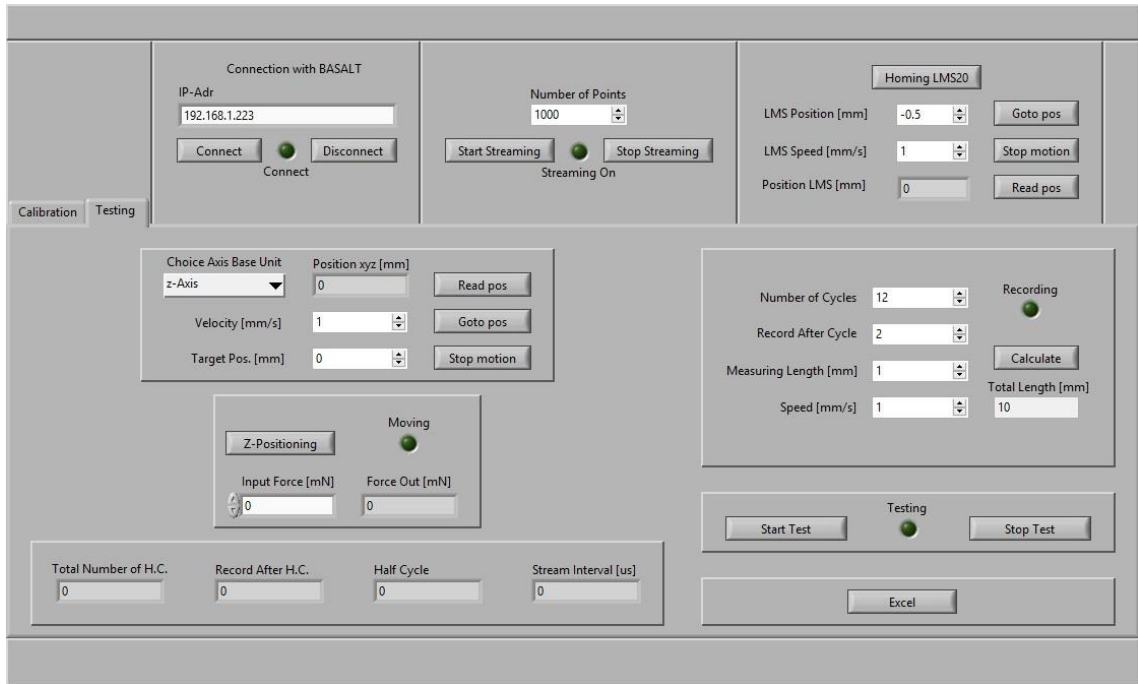


Figure 27: Graphical User Interface

4.4.1.1 Connect event

This is one of the most important events. This event is activated by the button “Connect”. It starts the connection with the Basalt tribometer via Ethernet. The block diagram is shown in Figure 28. In this event, the program gets the IP address of the tribometer with the block “MUST drv LW Connect.vi”. If the IP is correct, it executes the “false case” of the following event case. Here the subsequent blocks start the communication, enables the motors of the tribometer and finally activates the indicator “Connect”. If the “true case” is activated, an error connection message will be returned and no connection with the tribometer will be done.

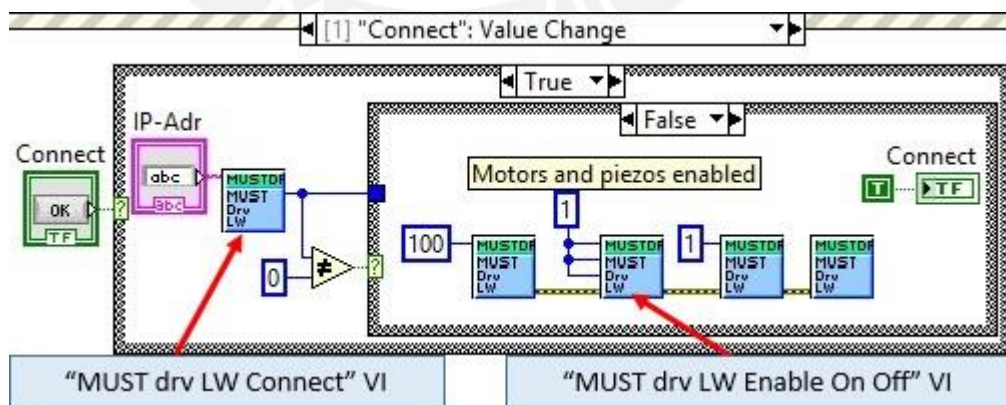


Figure 28: “Connect” event. Starts the communication between the controlling computer and the tribometer

4.4.1.2 Start Streaming event

This event is activated by the “Start Streaming” button. This event labeled as “Start Streaming” activates the streaming mode for the Basalt Must tribometer and thus the “MUST Drv LW Get Stream Data” VI block used in the “Calibration” tab, in the “Testing” tab and in the “Z-Positioning” event can work, otherwise this block will not get any data. The block in charge of starting the streaming mode is the Basalt “MUST Drv LW Start Stream” VI and this block receives as a parameter the “Stream Interval”. This parameter was obtained experimentally and is calculated by dividing one million by the quotient of the division of the variable “Number of Points” entered by the user by two (See Figure 29). Once the streaming mode is started, the indicator “Streaming On” is activated.

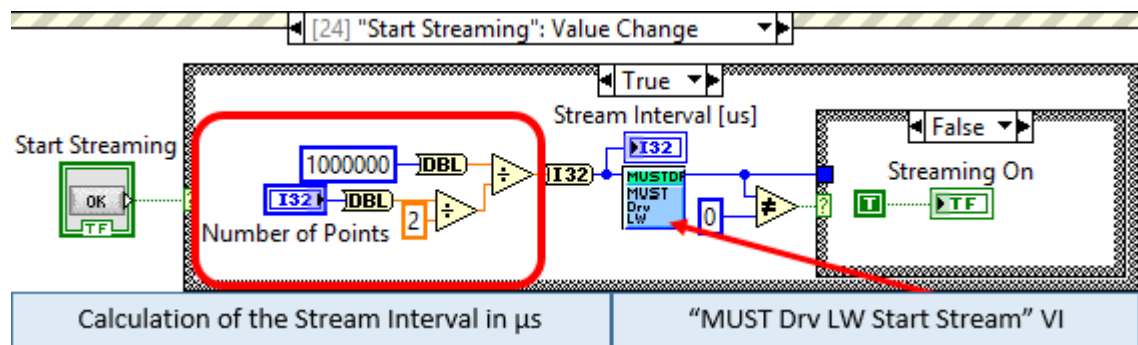


Figure 29: “Start Streaming” event. Starts the streaming mode of the tribometer.

4.4.1.3 Homing LMS20 event

This event is activated by the button “Homing LMS20”. This event performs the reference movement of the LMS20 module and puts the module on to the center of the X and Y axis. This action is done using the block “MUST Drv LW LMS20 Homing” and has no input parameters. If the “function return” output is different from zero, then the “True case” of the case event is executed and an error message is returned (Figure 30).

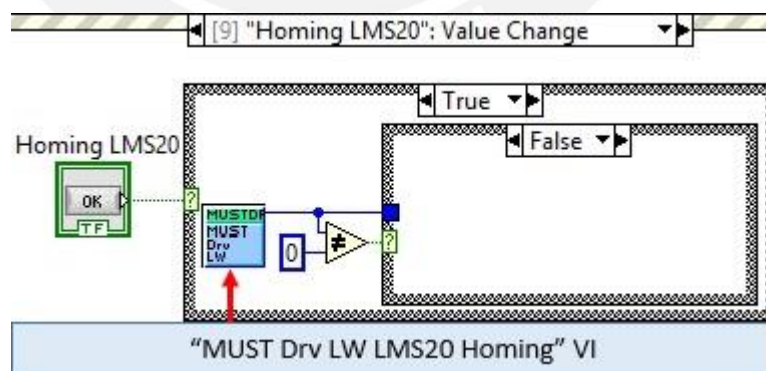


Figure 30: “Homing LMS20” event. Puts the LMS20 module to the center of the X and Y axis.

4.4.1.4 Timeout event

For the present work, the “Event Structure” executes an event activated by a button, and once the event is executed, it returns to the zero event called “Timeout”. In this zero event, which is executed by default, the main part of the program is written.

In the “Timeout” event, there is one case structure controlled by a “TabControl”. The tab control has two options to choose for. The first tab is called “Calibration” and is executed by default and other one is the “Measuring” tab (Figure 31). In the first tab, the user can do the calibration of the tribometer. The calibration process will be discussed in the **5 Calibration**.

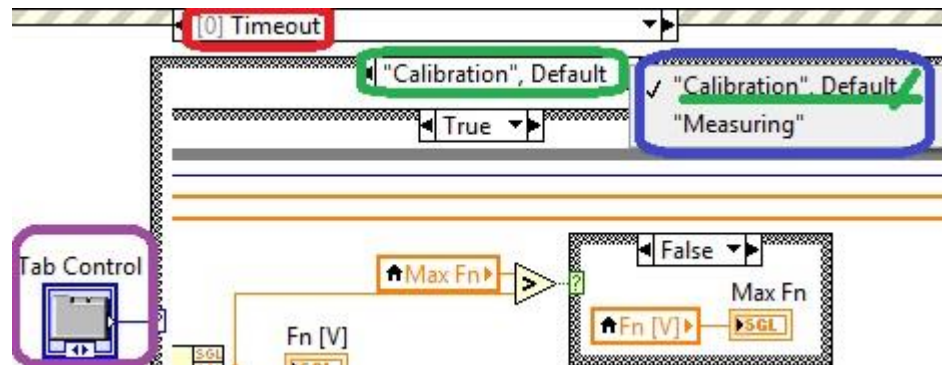


Figure 31: “Timeout” event in red. Tab control in purple and the options to choose for in blue. The default option is marked in green.

4.4.1.4.1 Calibration Tab

In the calibration tab there is a block for getting the data of the sensors as well as the indicators for the distances measured in both axis and the calculation of the forces as well as the blocks to visualize them. There are two small loops at the top right side that are for capturing the maximum values of voltage that both sensors are giving. At the bottom right side there is a small case loop for saving data. The data saved are the tangential and normal forces and the deformation of the cantilever for both axis due to this forces (see Figure 32).

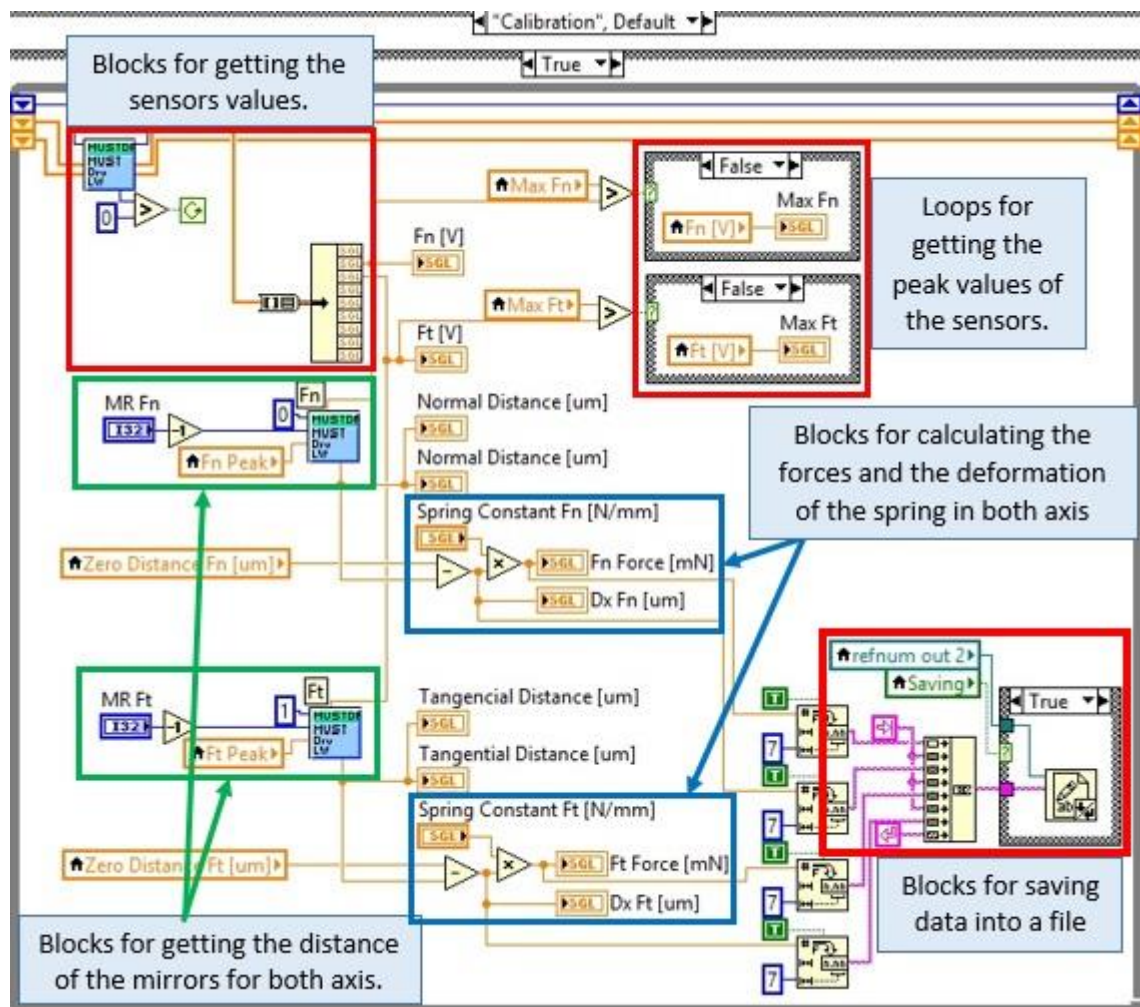


Figure 32: Calibration Tab description

The blocks used to obtain the sensor values is based on the Basalt MUST “Get Stream Data” VI whose parameters were described in the Table 19 and an “Unbundle” block. This specific block was used to split the elements of the “adc” output of the “Get Stream Data” block. Then the elements 1 and 2 of the “unbundle” block were used as according to the description of the MUST block, channel 1 and channel 2 are the ones connected to the Fn sensor and Ft sensor respectively (see Figure 33). The “Fn [V]” and “Ft [V]” indicators are used to show the raw data of the sensors in volt in the GUI.

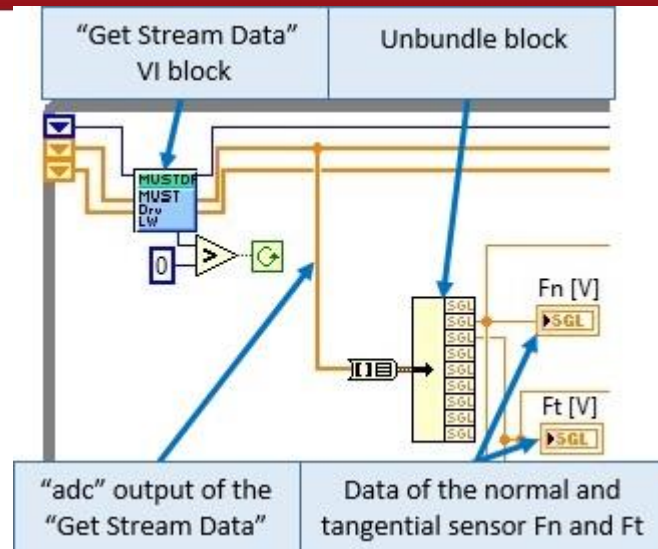


Figure 33: Blocks for getting the raw data of the sensors

The loops for getting the peak values of the sensors consists in a comparison of the actual value obtained by the sensor, with the maximum value obtained before and stored in the variables “Max Fn” and “Max Ft” respectively. These variables have an initial value of zero at the beginning of the execution of the program. Every time there is a read of a value which is higher than the one stored in the variables, this new value will be stored and the previous one discarded (see Figure 34). This part will help to find the voltage peak values for each sensor in order to do a proper calibration.

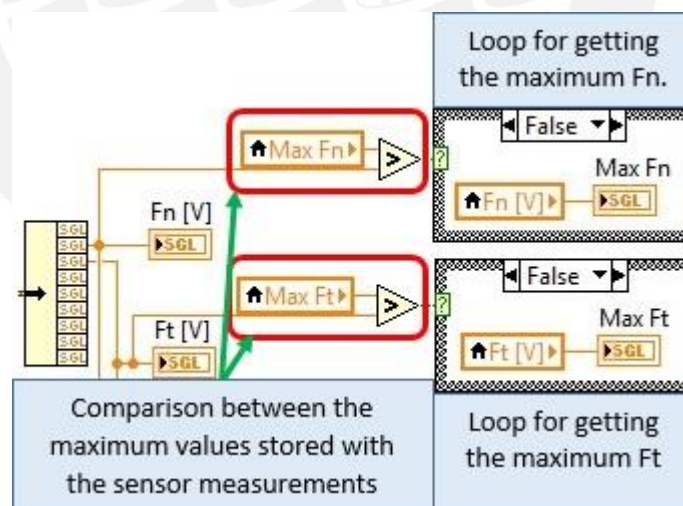


Figure 34: Blocks for finding the maximum values for Fn and Ft

The blocks for getting the distance of the mirrors is including the Basalt MUST block “FOS Get Dist” VI whose parameters are described in Table 22. In order to work with this block, it is needed to connect the data of the sensor obtained by the “Get Stream Data” VI Block after the “Unbundle” to its “adc” input (Figure 35). The “FOS Get Dist” VI block can do the calculation of the distance by entering the parameters “nbSens” and “MR” and with the help of the

adequate "Look-up table". How to load this table will be discussed later. This block parameters are listed in Table 23.

Table 23: "FOS Get Dist" values set

Parameter	Values	Comment
adc	-	
nbSens	0 and 1	As there are two sensors, both values were used. The value of "0" was used for getting the normal distance while the value "1" was used for getting the tangential distance.
MR	0 and 1	As it was explained before, the characteristic curve of the sensors is not linear but instead it has a shape shown in Figure 16. So in order to know in which region the sensor is working, the user can select in which measuring range it is operating (MR1 or MR2)
peakValue	-	This is the peak value obtained after doing the calibration
pWeg out	-	Is the distance obtained

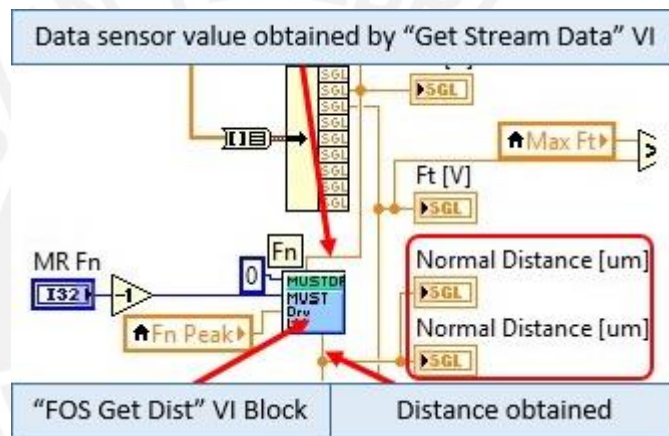


Figure 35: Distance obtained with the block "FOS Get Dist". This figure is for obtaining the normal distance. The configuration for obtaining the tangential distance is the same but the value of "nbSens" equal to 1 instead of 0 as it is shown and also the data of the sensor must be the Ft [V].

For calculating the normal and tangential forces from the distances obtained, the spring deformation is required. As the previous block gives only the relative distance, a reference distance is required where the force is defined as zero. Every time a new distance is measured, it is subtracted of the zero distance. This difference is the deformation of the spring (see Figure 36). Finally, the value of the stiffness constant of the spring is needed. How to obtain this constant will be discussed in **5 Calibration**.

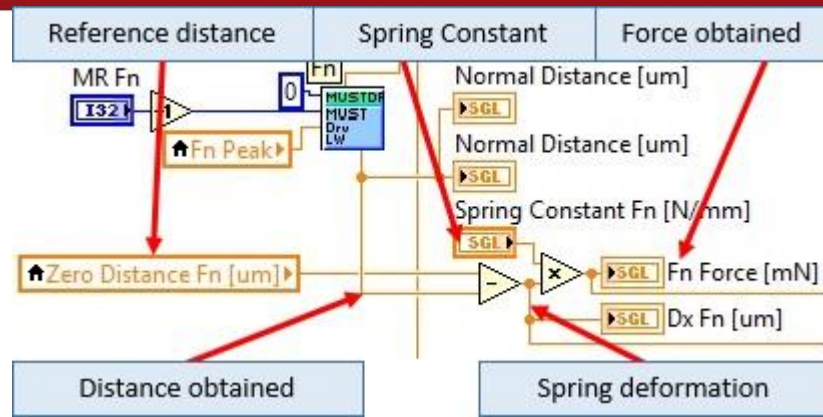


Figure 36: Force calculation. The scheme for obtaining the force is the same for both normal and tangential.

Finally, for saving the data, it is recorded into a file. As the file only accepts string data type, the first step is to change all the numeric values that are obtained into strings. This is done using the block “Number to Fractional String”. For this block, its parameter “Use System Decimal Point” is set “true” so it uses the localized decimal separator. The number of digits for precision is set to 7 (see Figure 37).

Once the recorded data is converted into strings, it must be connected so that a single string can be written into the file. This is done using the block “Concatenate Strings”.

In order to work properly, the file must have a defined path. The correct form of the path implementation will be described in **4.4.1.9 Start_calib event**.

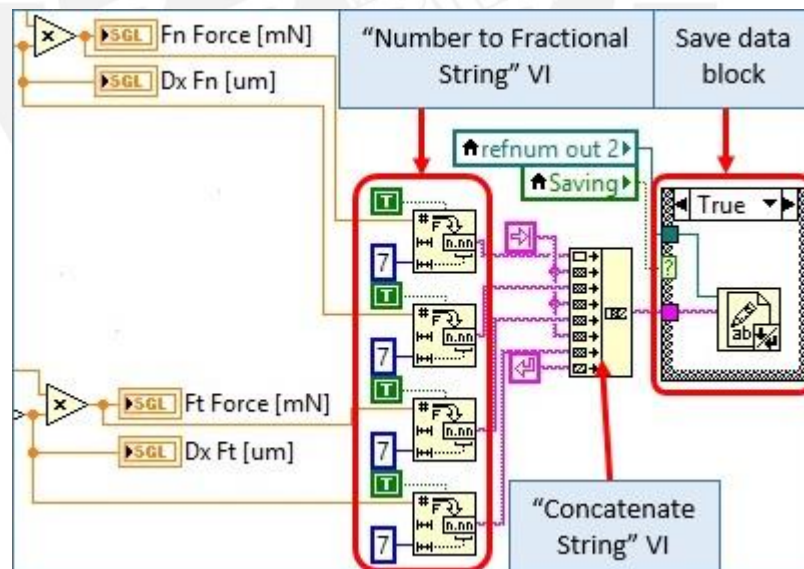


Figure 37: Blocks used to save the raw data into a file.

4.4.1.4.2 Measurement Tab

In the “Measurement” tab, there are two main loops being executed once the “Testing” indicator is activated (see Figure 38). The upper loop is a case structure where the movement for the Basalt MUST LMS20 is generated. The second loop is a while loop where the data of the sensors is obtained and the tangential and normal forces are calculated.

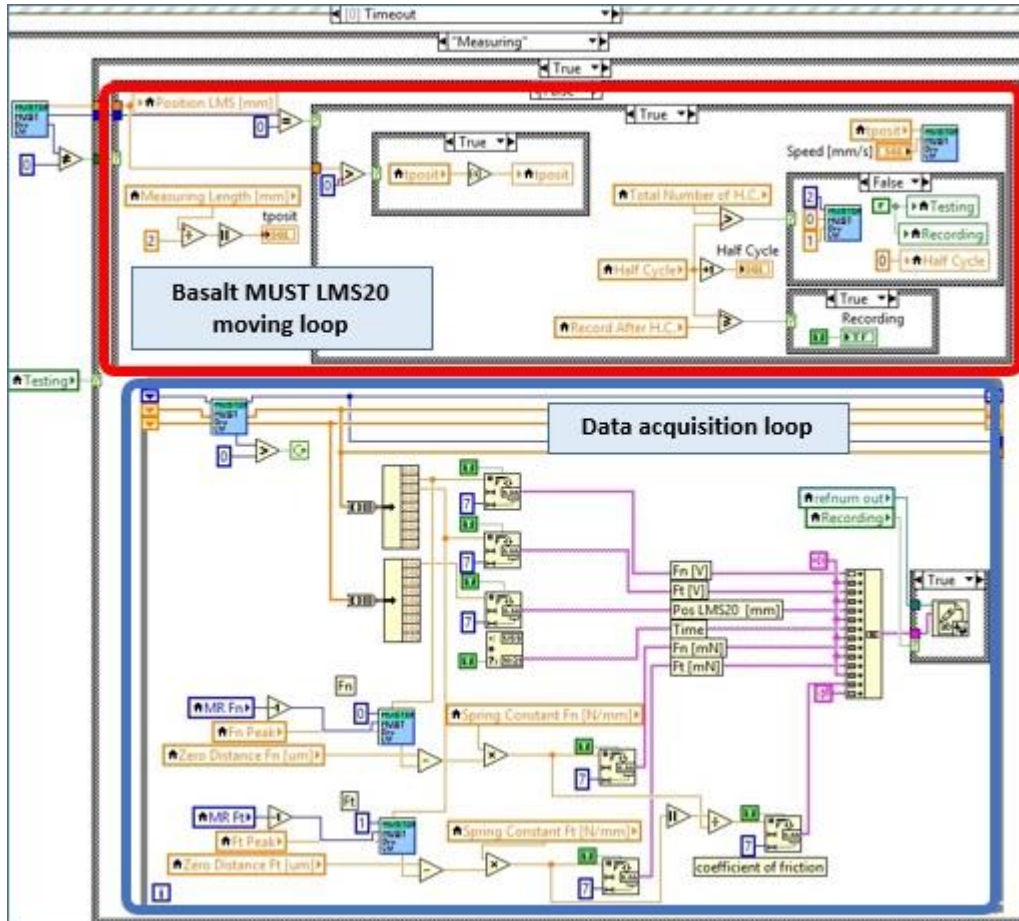


Figure 38: “Testing” tab. The upper part marked in red is where the movement of the LMS20 is generated. The lower part marked in blue, is where the data obtained is calculated and saved in the file.

In the top loop of Figure 38, the block that generates the movement for the Basalt LMS20, is the Basalt MUST “LMS20Move Posit” VI (Figure 39). The parameters that this block needs are the target position in mm and the speed of movement in mm/s. These parameters must be entered by the user. With these parameters set, the tribometer starts moving. The other blocks are for generating the oscillatory movement by inverting the target position and thus making a continuous oscillatory movement. There are also blocks to stop the oscillatory movement once the experiment is done.

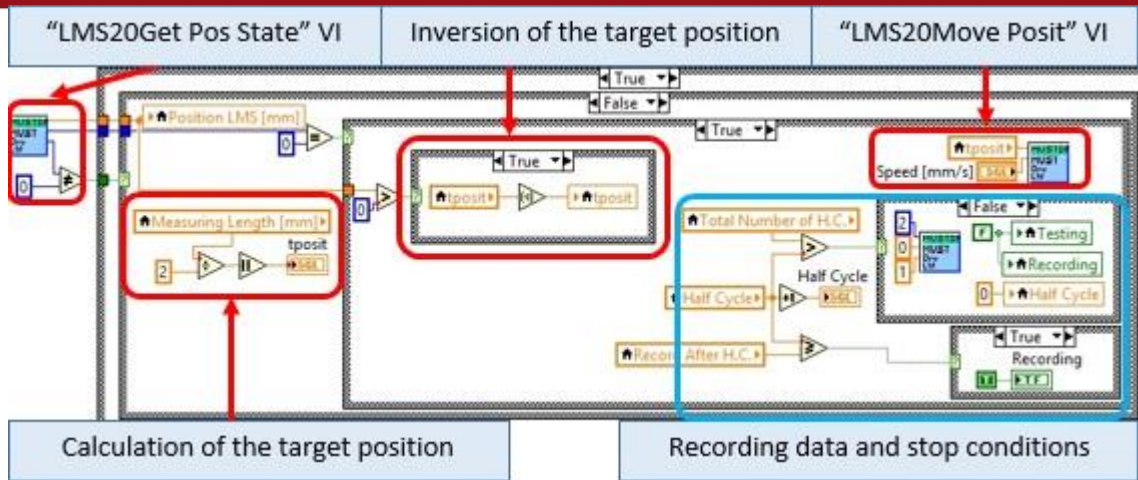


Figure 39: LMS20 Oscillatory movement generation in red and conditions for start saving the tribological data and stop the experiment in blue.

For calculating the target position, the user must enter first the “Measuring Length [mm]”. This value will be divided by two and the absolute value will be stored in the variable “tposit”. This variable will be used as the target position (see Figure 40).

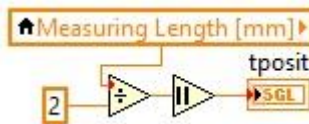


Figure 40: Calculation of the target position

The Basalt MUST “LMS20Get Pos State” VI block gives the actual relative position of the LMS20 (see Figure 41). This value is important because it will help to invert the “tposit” previously calculated so that the LMS20 moves backwards. The inversion occurs in the case loop circled in red in Figure 41. When the “tposit” calculated is positive, it will invert its value for the next half cycle. For the next half cycle this value is recalculated as shown before.

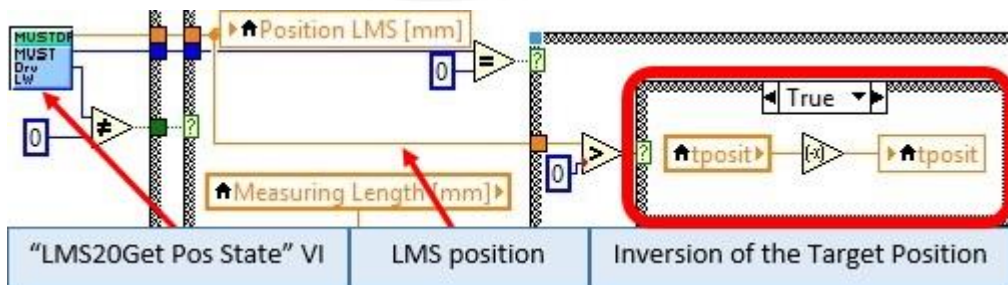


Figure 41: Target Position Inversion. The oscillatory movement is generated by negating the “tposit” value.

For recording the data generated, first the number of half cycles must be calculated. This will be discussed in the **4.4.1.8 Calculate event**. In this part the “Half Cycle” counter is compared to the variable “Record After H.C.”. When the counter is the same or higher, the “Recording” indicator will be activated and this will enable the record of the data (see Figure 42)

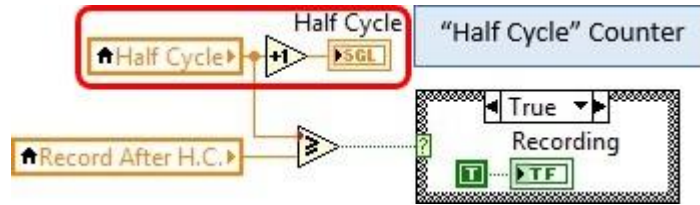


Figure 42: Data recording condition. When the counter “Half Cycle” is higher than “Record After H.C.” the recording condition will be activated.

The experiment will continue while the “Half Cycle” counter is lower than the internal variable “Total Number of H.C.”. Once this condition is false, the program will deactivate the “testing” and “recording” Booleans. The counter “Half Cycle” will be reset and the Basalt MUST “Base Unit Move Axis” VI block will lift up the Basalt MUST 2D-FM 1N to its home position (see Figure 43). Afterwards, there is no contact between the ball and the sample and the sample might be changed safely if required.

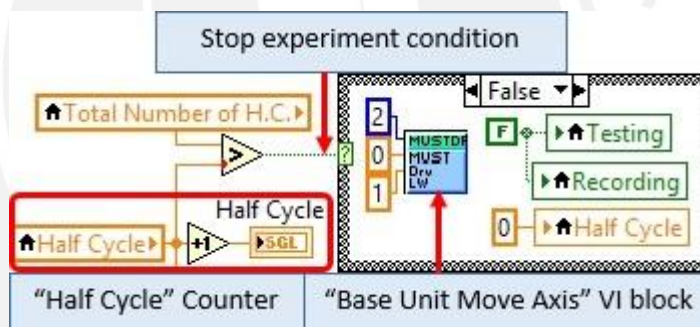


Figure 43: Stop condition. When the counter “Half Cycle” is higher than “Total number of H.C.” the stop case is executed.

In the loop at the bottom shown in Figure 38, the block that collects the data of the sensors is the Basalt MUST “Get Stream Data” VI. The work principle of this part of the program was already discussed on the “Calibration” tab (see Figure 33). The only difference to the “Calibration” tab is the acquisition of the data of the “poslgr” output. This output is including the position of the LMS20 in mm. The way to obtain it is the same as shown for the sensors data before. An “Unbundle” block is required and the channel 0 is the one that corresponds to the data of the position (see Figure 44)

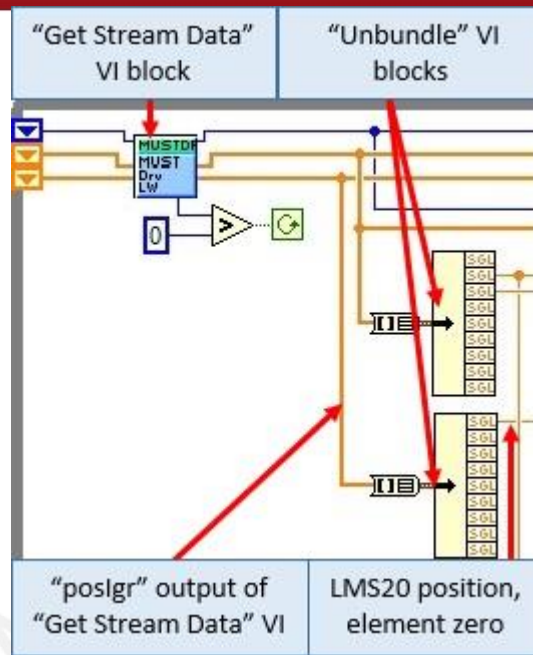


Figure 44: LMS20 Position. The scheme is the same as for the “Calibration” tab but in this case is also used a second Unbundle block to obtain the data of the “poslgr” output.

The calculation of the normal and tangential forces is the same as shown for the “Calibration Tab” (see Figure 35 and Figure 36). The same block “FOS Get Dist” VI is used with the same parameters for choosing the sensor as well as the parameters “nbSens” and “MR” entered by the user. The difference is that here the friction coefficient is calculated (see Figure 45). This is done by dividing the absolute value of the Tangential force \vec{F}_T with the normal force \vec{F}_N (see Equation 2). This value is also stored into the file.

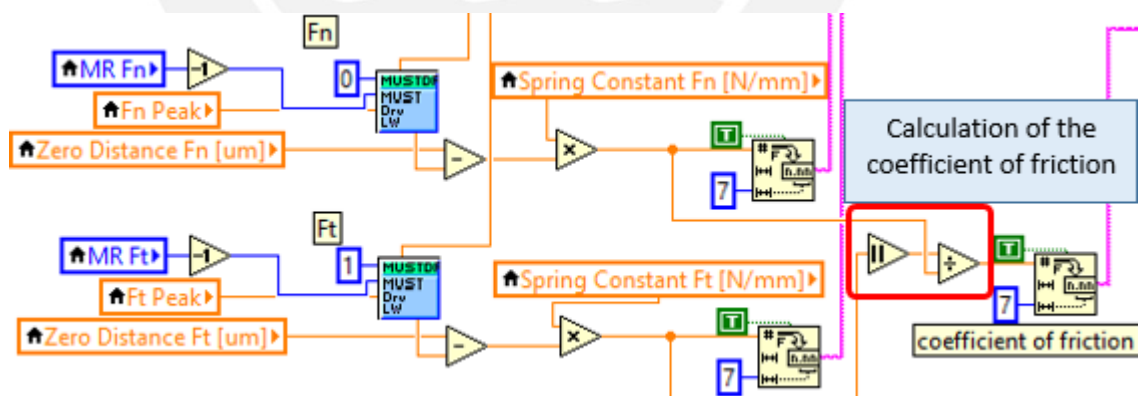


Figure 45: Calculation of the friction coefficient as the absolute value of the tangential force divided by the normal force.

The storage of the data into the file is similar to the one for the “Calibration” Tab. (see Figure 46)

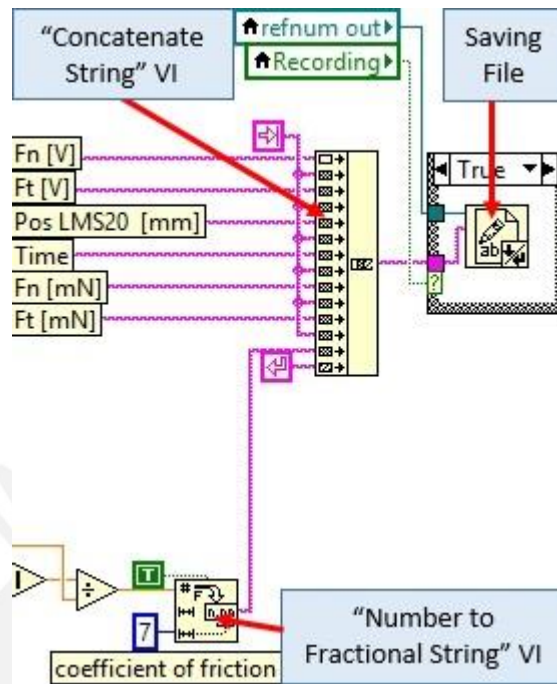


Figure 46: Save tribological data converted to string into the file.

4.4.1.5 Go To PosXYZ event

This event is activated by the button “Goto pos”. This event, labeled as “Go To PosXYZ”, receives as inputs the target position “Target Pos. [mm]”, the velocity of the module “Velocity [mm/s]” and the axis to be moved “Choice Axis Base Unit” (Figure 47). If all the inputs entered are correct (see Table 24), the block “MUST Drw LW Base Unit Move Axis” moves the motion module (Figure 48) in the axis chosen to the desired position with the velocity indicated. The description of its parameters are shown in Table 24. If not, the “true case” is executed and an error message is returned instead.

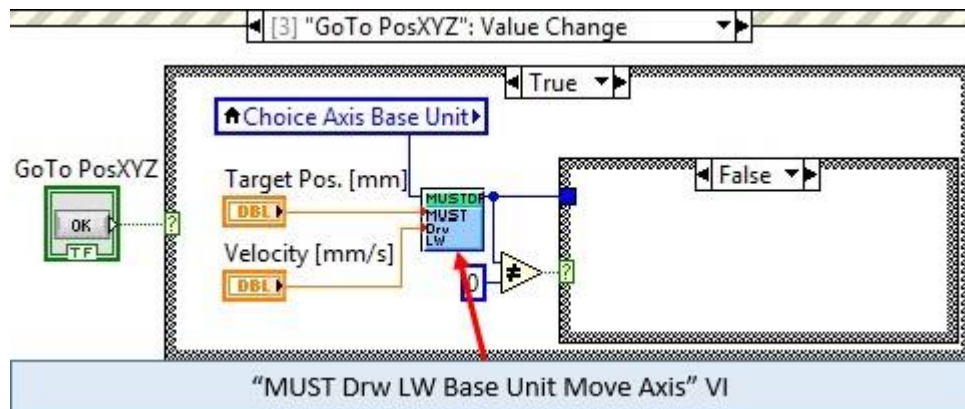


Figure 47: “Go To PosXYZ” event. Moves the selected axis to the target position entered with the speed indicated.

Table 24: "Base Unit Move Axis" parameters

Parameter	Description
axis	It is the axis to be moved. 0 – x axis 1 – y axis 2 – z axis
targetPos	Target position in mm. The values are between -10 to +10 mm.
velocity	Is the velocity of the axis in movement in mm/s. the maximum value for the X-Y positioning unit as well as for the Z positioning axis is 2 mm/s

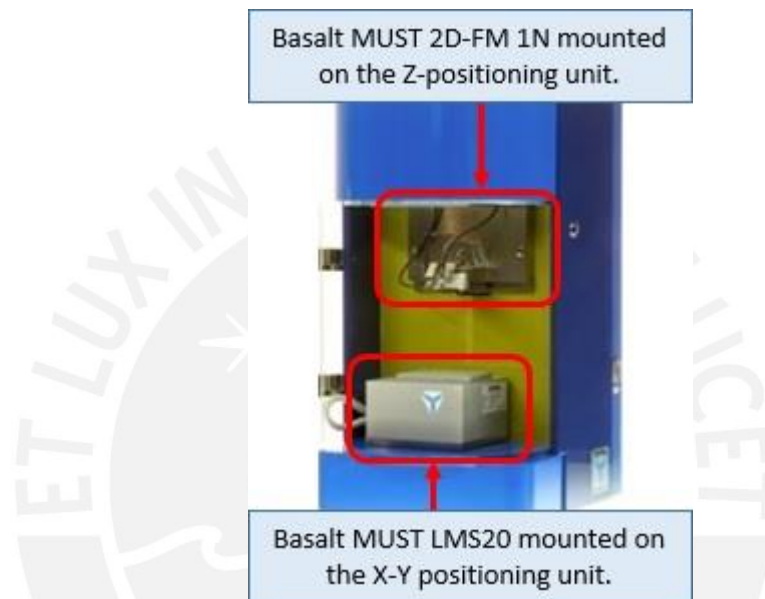


Figure 48: Basalt MUST tribometer. The Basalt modules 2D-FM 1N and LMS20 are mounted on the Z-Positioning axis and the X-Y Positioning unit respectively [28].

4.4.1.6 LMS20 Goto pos event

This event is activated by the button "Goto pos". It performs a similar action as the previous event described but with the difference that in this case, it is been moving only the LMS20 module (Figure 49). This action is performed by the block "MUST Drv LW LMS20Move Posit" and receives as inputs the target position of the LMS20 "LMS Position [mm]" and the velocity of the LMS "LMS Velocity [mm/s]" (see Table 25 and Figure 50). If the inputs entered are correct (Table 25), then the LMS20 module moves to the target position, with the velocity indicated. If not, the "True case" is executed and an error message is returned.



Figure 49: Basalt MUST LMS20

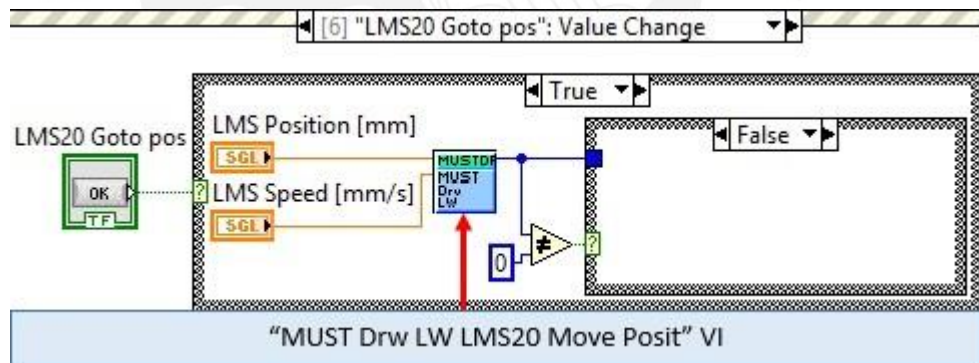


Figure 50: "LMS20 Goto pos" event. The LMS20 module moves to the position entered with the speed indicated.

Table 25: "LMS20 Move Posit" parameters

Parameter	Description
posit	Target position of the LMS20 in mm. the values are between -10 to +10 mm
velocity	Velocity of the LMS20 in mm/s. The maximum speed is 10 mm/s

4.4.1.7 Start Test event

This event is activated by the “Start Test” button. This event creates the file where the tribological data will be stored. The default name of this file is “TriboFile” and the extension is “.txt”. The file created has a format with the headers of all the data that will be obtained (forces, position, and coefficient of friction) and the tribological parameters set before starting the tribological experiment such as the spring constants for both axis, the total length of the experiment, the number of cycles, etc. (see Figure 51). All the values obtained are separated by Tabs. After creating the file with its format, the indicator “Testing” is activated and thus when this event is finished, the tribological experiment will start.

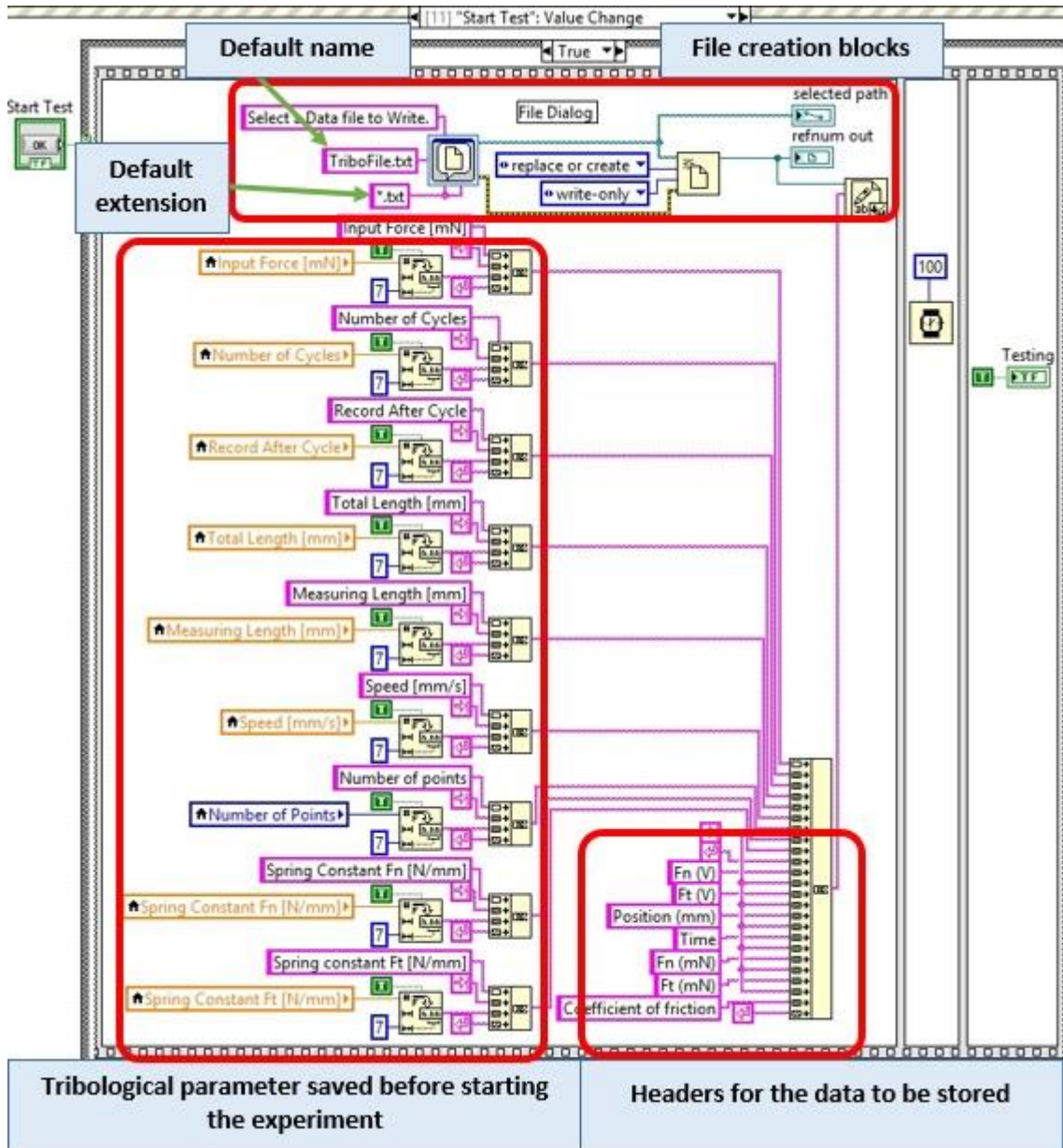


Figure 51: "Start Test" event. The upper part creates the file with default name "TriboFile" and extension ".txt". The lower part, the headers for the tribological parameters as well as the tribological conditions are stored in the file

4.4.1.8 Calculate event

This event is activated by the “Calculate” button. This event calculates the values “Total Number of H.C.” and “Record After H.C.” in terms of half cycles (H.C) because in the “Timeout” event the movement of the LMS20 is done in every Half cycle. When the LMS20 goes from the left to the right side, this is considered as 1 half-cycle. The same goes for the movement from right to left. Therefore, the total movement from the left maximum measuring length position till the right maximum measuring length position and back is one complete cycle. The user must enter the values of the variables “Number of Cycles” and “Record After Cycle” and the event also called “Calculate”, calculates the mentioned internal variables (See Figure 52).

$$Total\ Number\ of\ H.C = \frac{Number\ of\ Cycles}{2} \tag{Equation\ 6}$$

$$Record\ After\ H.C = \frac{Record\ After\ Cycle}{2} \tag{Equation\ 7}$$

Finally, the total length is calculated as the length of every half cycle whose value is entered by the user in the variable “Measuring Length [mm]”, multiplied with the difference of the “Total Number of H.C” variable and the “Record After H.C.” variable. This gives the total length recorded by the ball during the experiment.

$$Total\ Length = (Measuring\ Length) * [(Total\ Number\ of\ H.C) - (Record\ After\ H.C)] \tag{Equation\ 8}$$

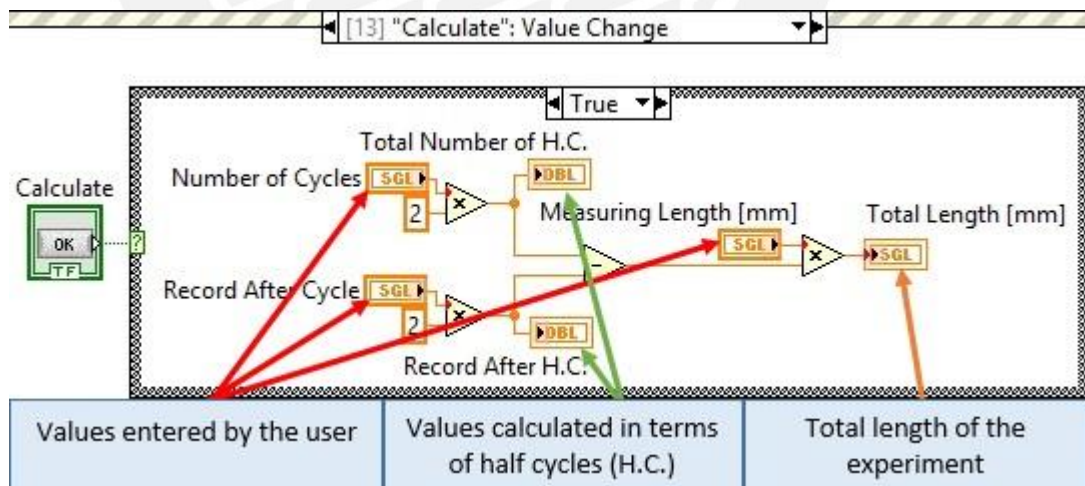


Figure 52: “Calculate” event. The “Total Length” is determined in terms of the “Measuring Length” and the difference of the “Total Number of H.C” and “Record After H.C”.

4.4.1.9 Start_calib event

This event is activated by the “Start Calibration” button. It loads both “look-up tables” for both the sensors (see Figure 53). This is done using the “MUST Drv LW FOS Read Call File” (see Table 26). The paths of the files must be connected to the “pFileNameLTable” input of the Basalt block in order to be loaded. This event also activates the “Calibration” indicator and thus the whole calibration process can start.

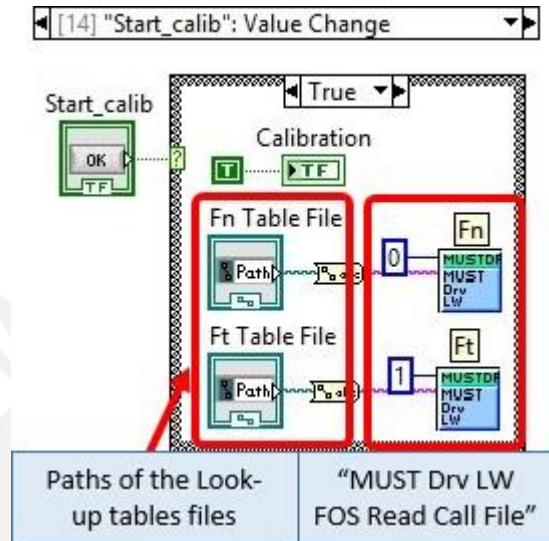


Figure 53: “Start_calib” event. On the left side, the paths of the look-up tables are loaded into the basalt block “FOS Read Call File” on the right side.

Table 26: Description of the “MUST Drv LW FOS Read Call File”

Parameter	Value	Description
nbSens	0 – normal sensor 1 – tangential sensor	Defines the sensor to work with.
pFileNameLTable	Path of the Look up tables	Defines the path of the look up table of the sensor.

4.4.1.10 Sel. as peak event

This event is activated by the “Select Peak” button. In these event labeled as “Sel. as peak”, the maximum values caught by the variables “Max Fn” and “Max Ft” are stored in the variables “Fn Peak” and “Ft Peak” respectively (see Figure 54). These values will be used as the peak voltages in the “peakValue” input of the block “MUST Drv LW FOS Get Dist” to calculate the distance measured by the sensors.

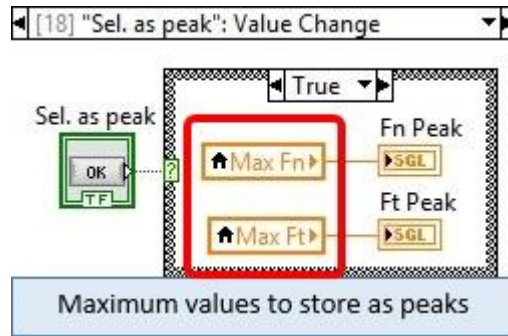


Figure 54: "Sel. as peak" event. The Maximum values obtained are loaded into the variables "Fn Peak" and "Ft Peak"

4.4.1.11 Tarring Fn and Tarring Ft events

These are two events activated by the "Tarring Fn" and "Tarring Ft" buttons. For both cases, the distances obtained by the block "MUST Drv LW FOS Get Dist" in the "Timeout" event, which means without applying any load to the spring, are stored in the variables "Zero Distance Fn [μm]" and "Zero Distance Ft [μm]" (see Figure 55). After the tarring is done, the distance saved is used as a distance reference to measure the deformation of the spring.

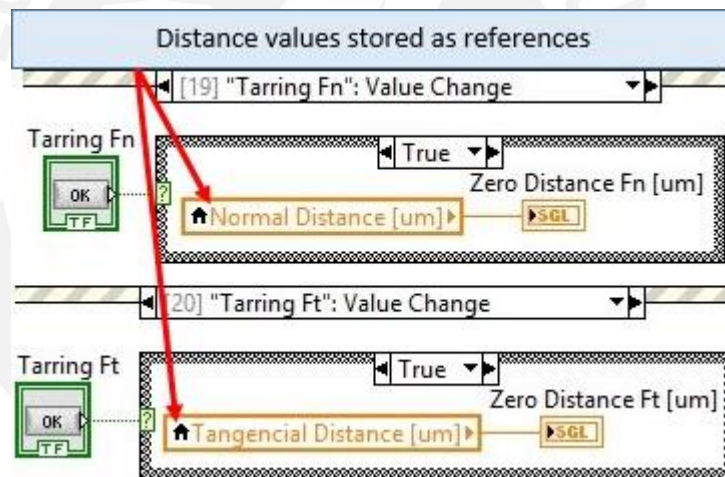


Figure 55: "Tarring Fn" and "Tarring Ft" events. The normal and tangential distances obtained in the "Timeout" event are stored as reference distances named as "Zero Distance Fn" and "Zero distance Ft".

4.4.1.12 Save configurations event

This event is activated by the button "Save Calibration". This event creates a calibration file named by default "Calibration File" and its extension is ".txt". In this event, the user can save the calibration parameters such as the peak values for both sensors that are obtained by moving the sensors in the tribometer manually during the calibration process and the spring constants for both axis (see Figure 56). Once saved, the user is not required to do the calibration every time the program starts. The user only might load this file and can proceed with the experiment.

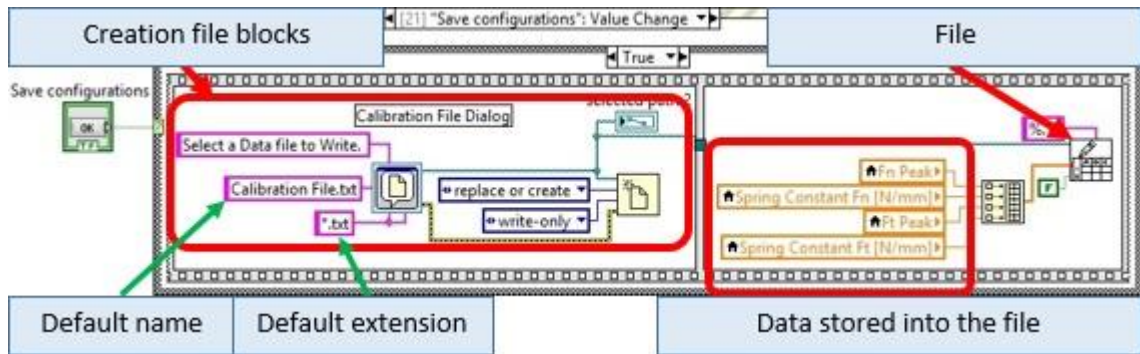


Figure 56: "Save configuration" event. On the left side are the blocks for creating the file with its default name and extension. On the right side are the variables that are saved into this file.

4.4.1.13 Load configuration event

This event is activated by the button "Load Calibration". It reads the calibration file created in the "Save configuration" event and loads to the program the values stored for the voltage peaks and for the spring constants (see Figure 57). This is done with an "unbundle" block to split the data of the "calibration file" into its respective required values.

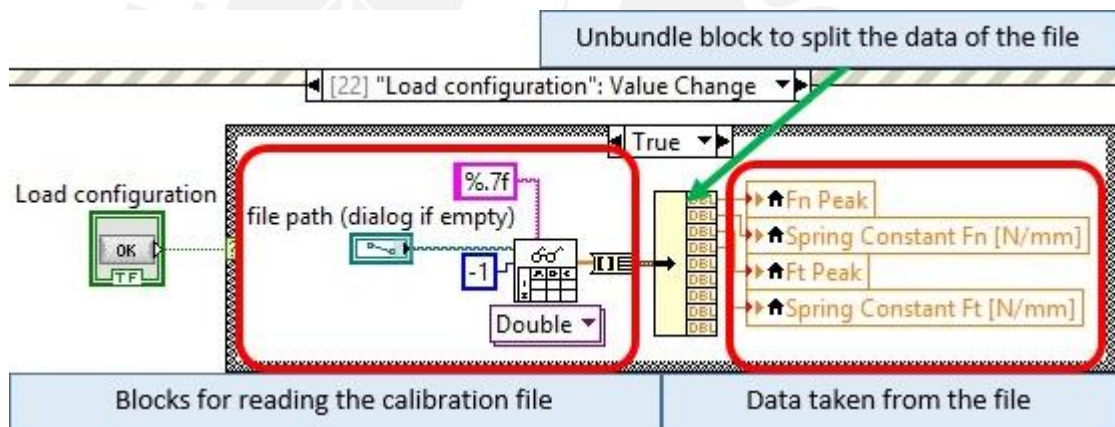


Figure 57: "Load configuration" event. On the left side, the calibration file is read. On the right side, the calibration values are obtained.

4.4.1.14 Z-Positioning event

This event is activated by the "Z-Positioning" button. This event labeled as "Z-Positioning" performs the positioning of the Basalt MUST 2D-FM 1N onto the surface of the sample. In order to accomplish this operation, the user must enter the normal force "Input Force [mN]" that must be applied to the surface of the sample (Figure 58).

It is important to remark that this event must be done after the calibration of the tribometer. So the normal peak value "Fn Peak" the normal spring constant and the normal distance of reference "Zero Distance Fn [μ m]" are known parameters. When this event is activated, the force is calculated using the distance obtained by the Basalt block "MUST Drv LW FOS Get Dist", the "Zero Distance Fn [μ m]" and the spring constant. This force is compared with the force value entered by the user and when the value being measured reaches the input value, the positioning

stops (see Figure 59). While the Basalt MUST 2D-FM 1N is still in movement, the “Moving” indicator is active and is deactivated when the Basalt MUST 2D-FM 1N stops.



Figure 58: The Z-Positioning axis marked in red is moved during the “Z Positioning” event

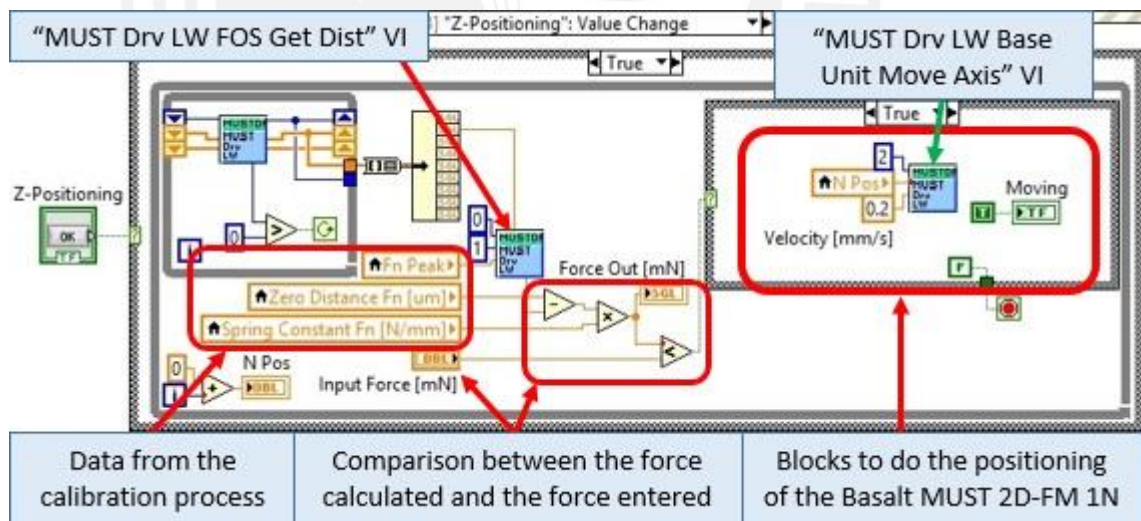


Figure 59: “Z-Positioning” event. This event gets data of the normal sensor and calculates de force that is compared with the force value entered by the user.

4.4.2 Electrical program

This program was developed to control all the Keithley devices used. Like the tribological program developed, this program also consists of an “Event Structure” (Figure 60). In this structure, as for the previous program, is programmed all the events activated by buttons in the GUI (Figure 61).

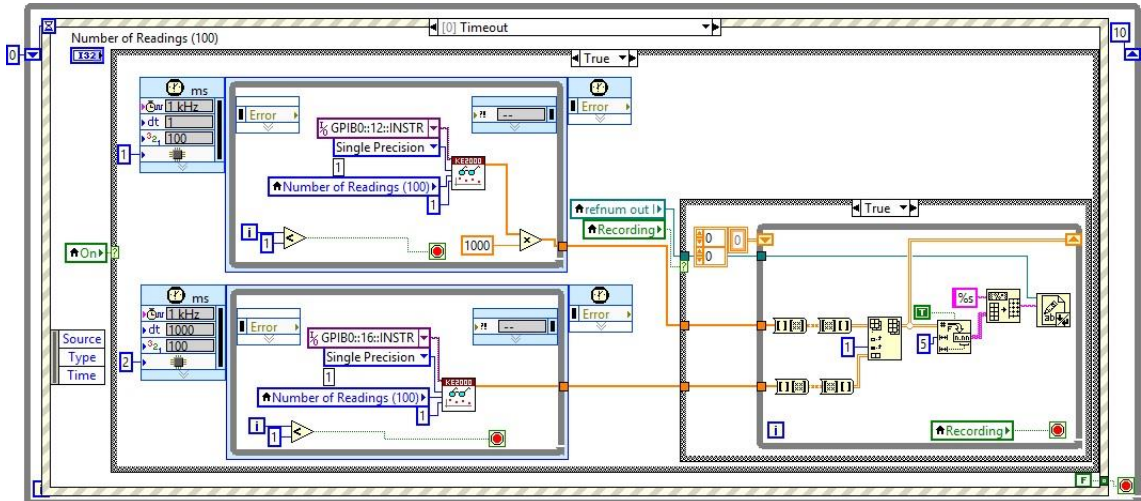


Figure 60: "Timeout" event

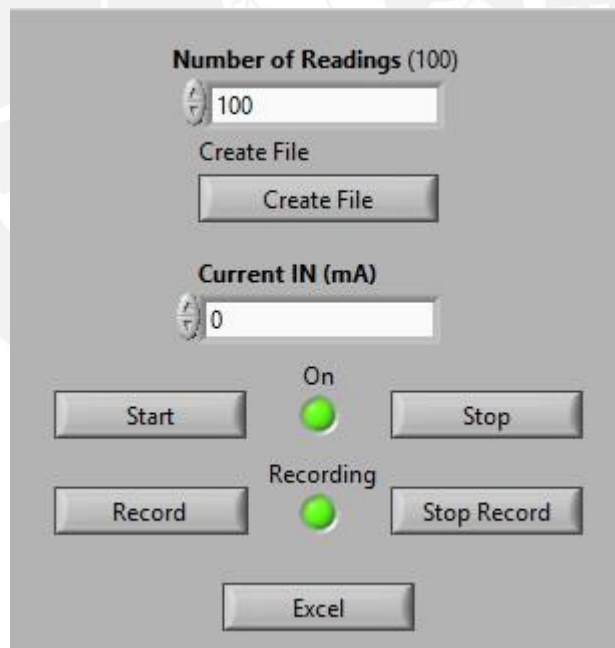


Figure 61: Electrical GUI

4.4.2.1 Timeout event

This event is executed by default as shown for the tribology program. In this event, the electrical parameters such as voltage and current are obtained by the Keithley block “Data Read Multiple” VI (see Figure 62) one for current and the other one for the voltage. The parameters used for this block were discussed previously.

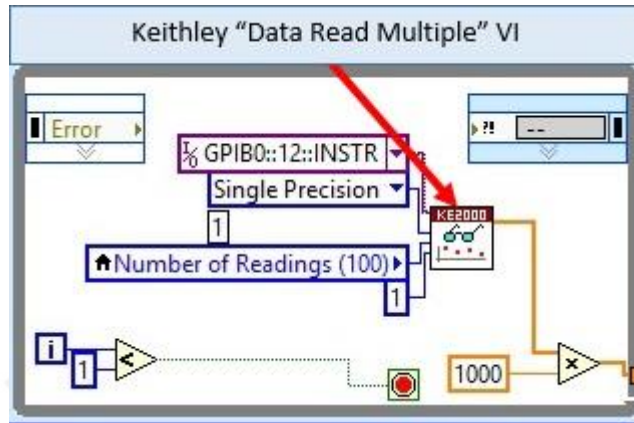


Figure 62: Data Read Multiple VI. This block obtains the electrical data required

Once the data is obtained, it is stored into a file. But unlike for the tribological program, here the data is given in groups according to the value set in the “Number of readings” parameter. So in order to create the two columns one for current and the other for voltage, the 1 dimensional arrays obtained are changed into a 2 dimensional arrays. This is done by using the block “Array to Matrix” in which the input is a 1 dimensional array and as output is obtained a Matrix column vector (Figure 63). The next block is “Matrix to Array” which receives as input a real matrix and gives as output a 2 dimensional array. Then a block named “Insert Into Array” allows to combine both 2 dimensional arrays obtained. Finally this new array is converted into strings and saved into the file.

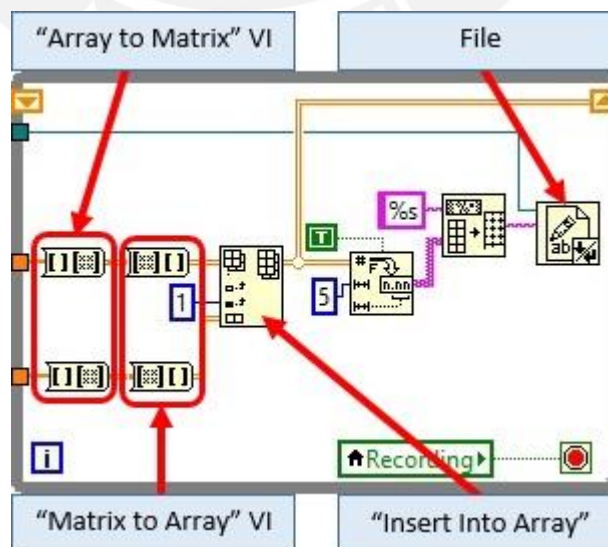


Figure 63: Data saving process. The blocks marked in red are the ones that change the 1D arrays obtained into a 2D arrays. With the help of the block “Insert Into Array”, the two 2D arrays are combined and as a result is obtained one 2D array. This last array is finally written into the file.

4.4.2.2 Start Electrical event

This event is activated by the button “Start” from the GUI. This event first initializes all the Keithley devices and in a next step sends the value of the required current to the Keithley 2400 SourceMeter. The block fulfilling this task is the “Keithley 2400 Configure Output” which was already discussed.

To configure the two Keithley 2000 Multimeters as ampermeter as well as voltmeter, the block “Keithley 2000 Configure Output” was used with the parameters shown in the Table 27. After configuring all the devices and setting the output current, the indicator “On” is activated (Figure 64).

Table 27: Parameters used for the "Configuration Output"

Parameter	Value	Comment
Autorange	False	When deactivated the user can specify the maximum ranges for measurement and therefore, enhancing the speed
Custom range	0.1 A for the ampermeter 20 V for the voltmeter	For limiting the maximum values to read.
Resolution	5 digits	Value recommended in the data sheet of the device to enhance the speed of the data acquisition.
Power line cycles	0.01	Value recommended in the data sheet of the device when the resolution used is 5 digits
VISA resource name	12 for the ampermeter 16 for the voltmeter	Is the address of each device

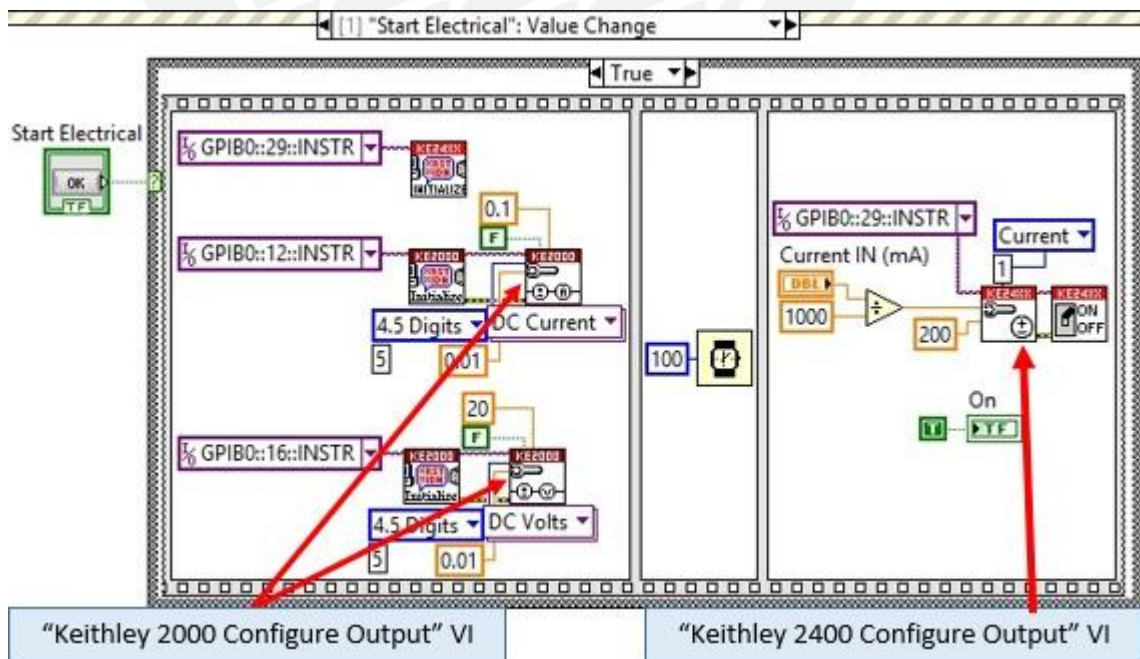


Figure 64: "Start Electrical" event. On the left side, is the configuration of the two 2000 Keithley multimeters as ampermeter and as voltmeter. On the right side is the configuration of the 2400 Keithley SourceMeter

4.4.2.3 Create File event

This event is activated by the button “Create File” from the GUI. This event creates the file where the electrical data will be stored. The default name of the file is “CurrentFile” and the default extension is “.txt” (see Figure 65). This file has a format in which the values of the electrical considered conditions such as the injected current (Current IN [mA]) and the number of samples taken by the “Data Read Multiple” VI block (Number of Readings), are stored before the acquisition starts. Also the headers for the current and the voltage are considered.

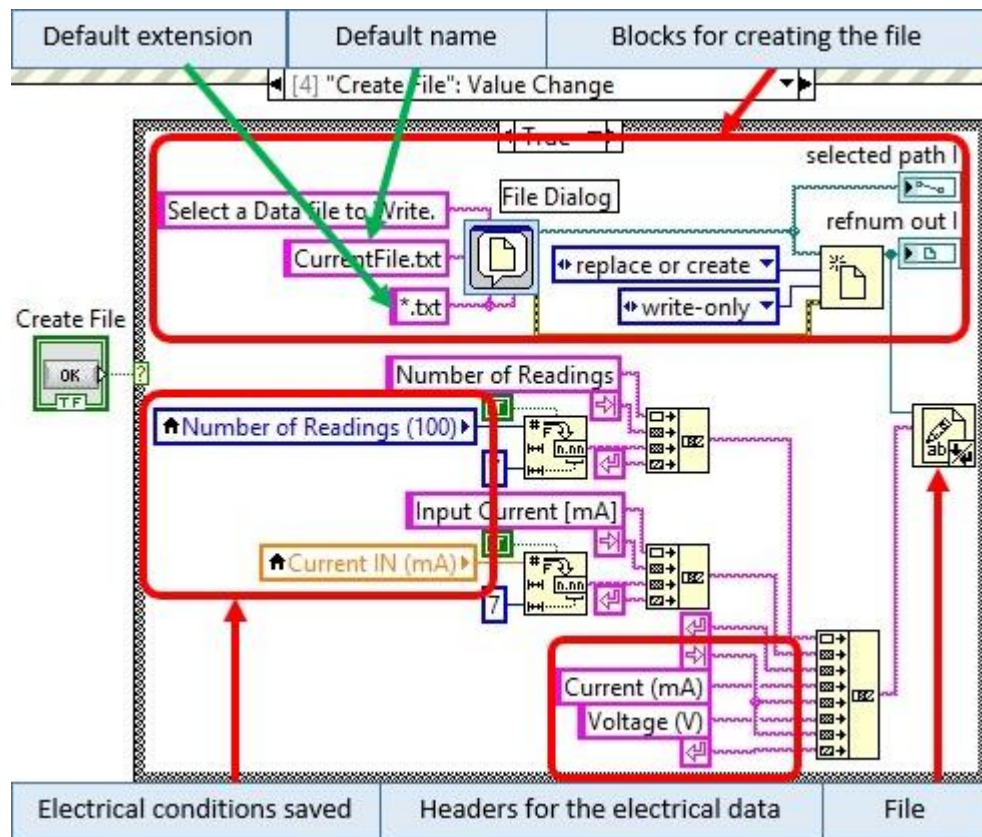


Figure 65: "Create File" event. In the upper part, the blocks creates the file named as default "current file" and an extension ".txt". The lower part the headers for the electrical parameters as well as the electrical conditions are stored in the file.

All the numerical values are converted into strings before saving the data into the file.

4.4.2.4 Start Recording Electrical event

This event is activated by the button “Record” from the GUI. In this event the indicator “Recording” is activated and allows the file previously created starts to be filled with the electrical data (Figure 66). The data acquisition will be stopped when the user clicks the button “Stop Record” at the GUI.

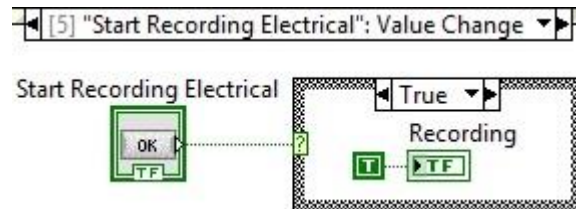


Figure 66: "Start Recording Electrical" event. The "Recording" variable is activated.



5 Calibration

The calibration process is very important because here the parameters of the sensors are configured in order to obtain an appropriate performance of the equipment and thus being able to calculate the forces involved during the tribological experiment. The calibration is done at the very beginning, before any experiment is done with the ball of the Basalt MUST 2D-FM 1N not in contact with the sample or table of the Basalt MUST LMS20 (Figure 67).

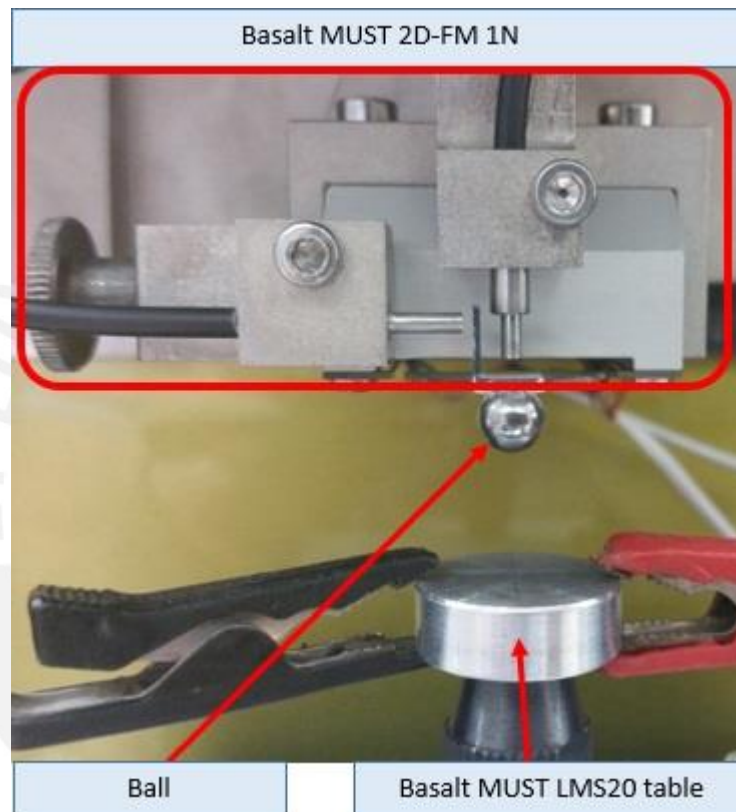


Figure 67: Position for the calibration process. The tool (Ball) of the Basalt MUST 2D-FM 1N has no contact with the table of the Basalt MUST LMS20

5.1 FOS calibration

The first step is the calibration of the fiber optic sensors (FOS). First the user must connect the controlling computer with the Basalt tribometer and then activate the streaming mode. Once these first steps are done, the indicators “Connect” and “Streaming On” must be activated. In a next step, the user must go to the “Calibration” tab (see Figure 68). In this tab, the user must enter the data path of the Look-up tables to the fields “Fn Table File” and “Ft Table File”. These tables contain the normalized characteristic curves of the sensors (Figure 69). This step must be done previously so the program can calculate the distances between the sensor tip and the mirror. After selecting the path of the table files, the user must click the button “Start Calibration” (Figure 68). Once this is done, the indicator “Calibration” is “on” and the fields “Fn [V]” and “Ft [V]” start changing their values in volts according to the readings of the FOS.

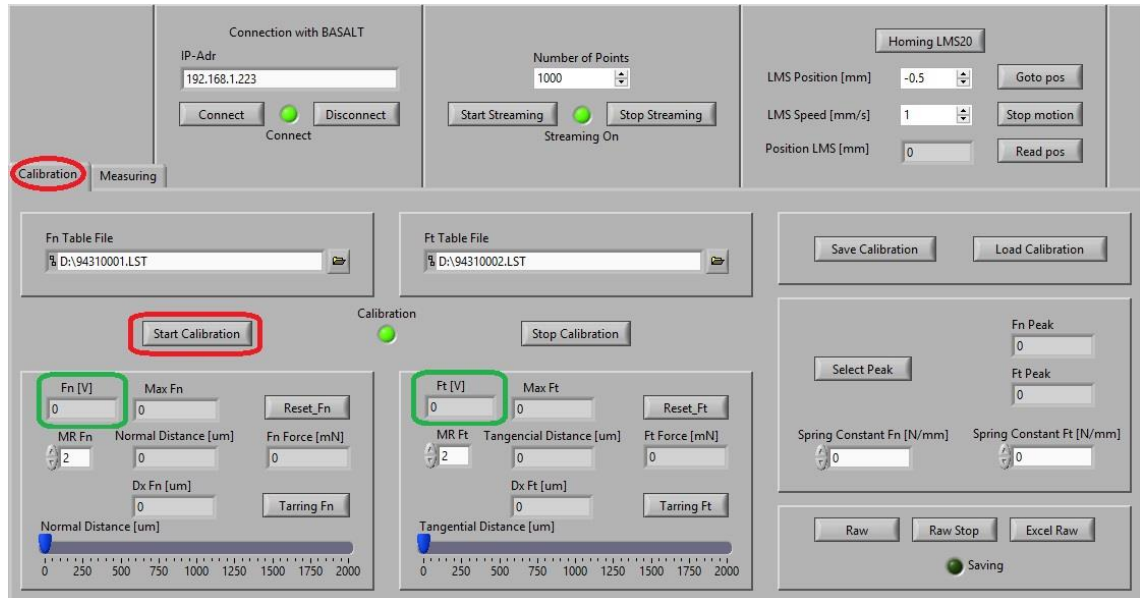


Figure 68: Calibration Tab. The boxes marked in green are where the raw data in volts of the sensors is displayed.

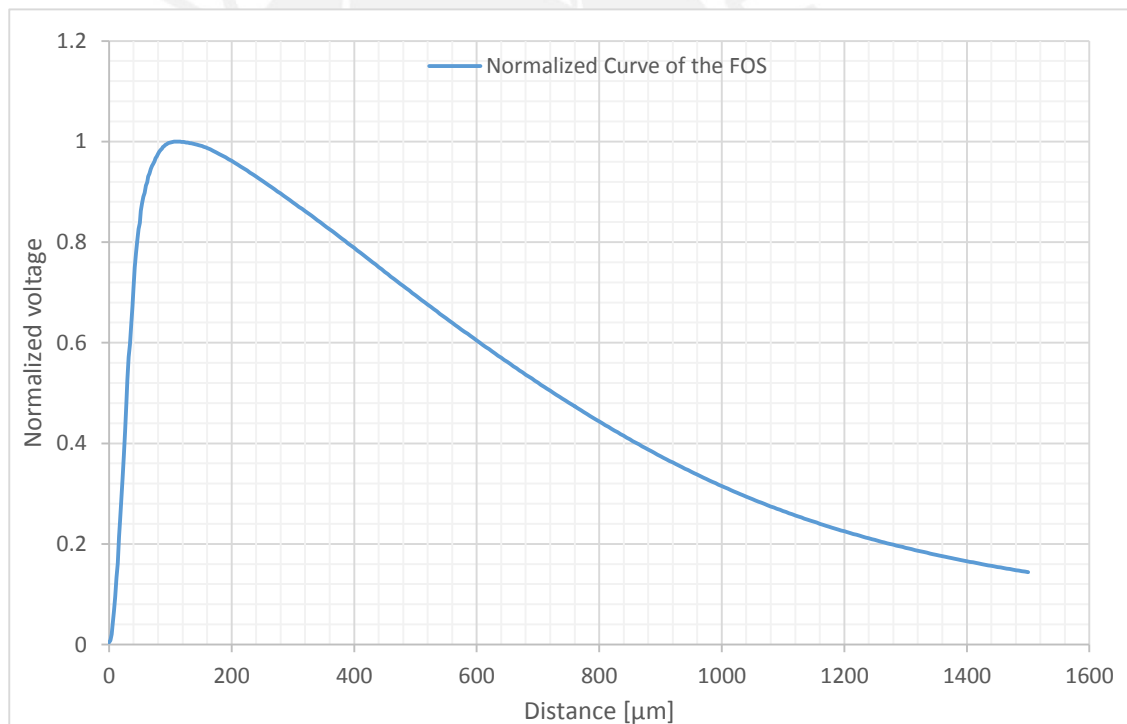


Figure 69: Normalized curve of the FOS. (Look-up table)

The next step is the search of the voltage maximum values for both sensors. This process must be done carefully as it is done manually and the sensors or the mirrors can be damaged during the process. The user must loosen the support of the sensors by using the two tiny screws (see Figure 70). Then, one by one the user must move slowly the sensor towards the mirror as close as possible but without touching it. Afterwards, the sensor must be moved back to its initial position. This will allow the sensor to catch the distance with the highest value for the voltage and this value will be stored automatically in the variable “Max Fn” or “Max Ft” respectively.

There are also two reset buttons (See Figure 71), one for each variable, to clear the obtained values if there was some mistake and thus the user can repeat the process again. After finding the peaks, the user must tight up again the sensors to the blocks that holds them with the tiny screws. Then, the user must click in the button “Select Peak” (see Figure 72) to use these maximum values as the peaks for the Basalt block “MUST Drv LW FOS Get Dist” previously discussed. If the values of the spring constants are known the user must write them in the blocks below (see Figure 72) otherwise these values must be determine experimentally. This will be discuss in **5.2 Determination of the spring constant**.

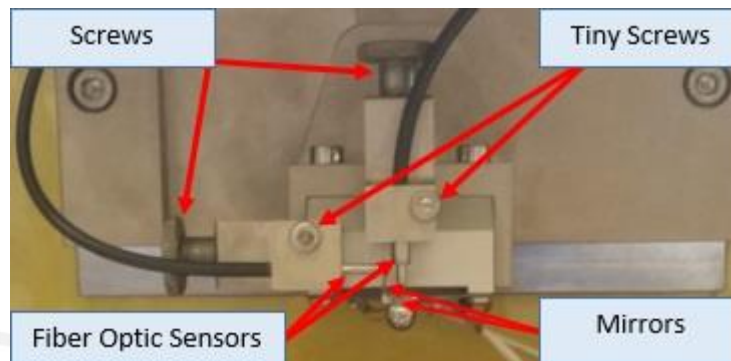


Figure 70: Basalt MUST 2D-FM 1N. The tiny screws are used to loosen the sensors. The FOS are moved towards the mirrors to find the maximum voltage values.



Figure 71: Finding peak values. The buttons “Reset_Fn” and “Reset_Ft” resets the “Max Fn” and “Max Ft” respectively

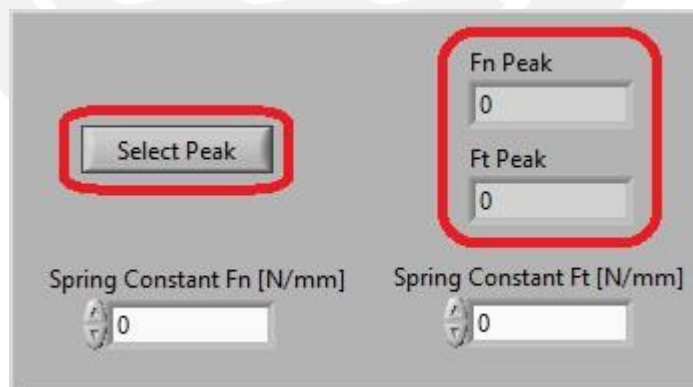


Figure 72: “Select Peak” button stores the maximum values obtained previously into the “Fn Peak” and “Ft Peak” variables.

The next step is to define on which side of the calibration curves the sensors are working. As it was discussed before, these fiber optic sensors have two measuring ranges. In order to indicate in the program the desired measuring range (see Figure 69), the user must choose from the textboxes “MR Fn” and “MR Ft” whether it is working on the first (1), or the second range (2) (see Figure 73). By default, both fields are defined in the second range (2) and the user can change them at any time before the experiment starts. With these parameter sets, the program

is able to determine the distances to the mirrors and give the results in the output windows “Normal distance [μm]” and “Tangential distance [μm]” (Figure 73) and the forces are given in the output fields “Fn Force [mN]” and “Ft Force [mN]”.



Figure 73: Measurement range selection and distances obtained

Once the peak values are found and the measurement ranges are set, the sensors must be located in a position to use as a reference and from which the tangential and normal forces can be measured. This process is done with the help of the two big screws that the machine has for each axis (see Figure 70). To get the maximum normal force value possible with the normal axis sensor, the position must be set when the distance showed in the “Normal distance [μm]” field is close to 1500 μm. The same procedure must be done with the tangential axis sensor, but in this case, in the “Tangential distance [μm]” field, the distance value should be near 1000 μm. The reason for this value is that in the tangential axis, the sample will be oscillating with the ball. This means that frictional force has positive and negative values. So in order to obtain this values, the distance measured by the sensor should be an intermediate value that works as a reference and from it measure positive and negative forces. After setting the position of the sensors, the user must click the “Tarring Fn” and “Tarring Ft” buttons so that these values are selected as the reference distances (see Figure 74). After doing this, the fields “Fn Force [mN]”, “Ft Force [mN]”, “Dx Fn [um]” and “Dx Ft [um]” must be oscillating near zero.



Figure 74: “Tarring” buttons to select the reference distances for both axis.

Finally, in order to avoid doing the whole calibration process every time the program is started, the user has the option to save the main calibration parameters into a file. These main parameters are the peak voltage values “Fn Peak” and “Ft Peak” and the spring constants “Spring Constant Fn [N/mm]” and “Spring Constant Ft [N/mm]”. The saving is done by clicking the button “Save Calibration” the user must indicate where to save the file (see Figure 75). For future use, the user has to load this calibration file and the main parameters will be shown in the program.

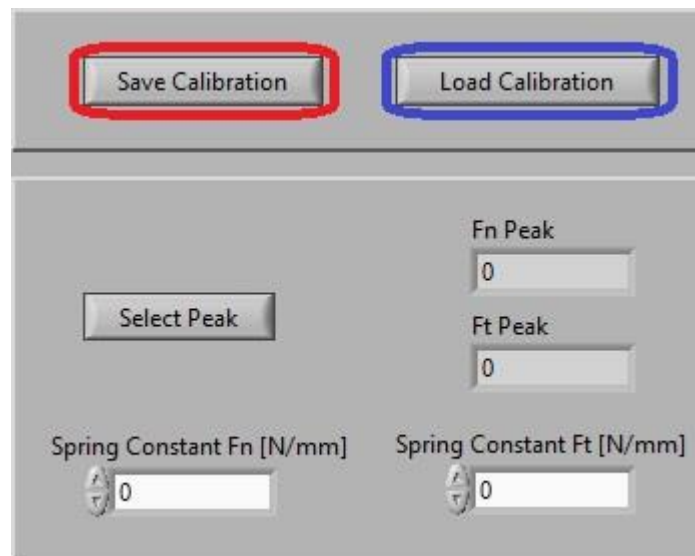


Figure 75: “Save Calibration” in red, “Load Calibration” in blue and the calibration parameters saved into the file.

Finally, after doing the calibration process, the user must click the button “Stop Calibration” and then proceed with the experiment in the “Measurement” tab.

5.2 Determination of the spring constant

This procedure is done if the stiffness constants of the cantilever are unknown. Furthermore, the values of the stiffness constants should be recalculated to see if the values given by the manufacturer of the cantilever are still valid or not. As the cantilever is being used, it wears and the stiffness values might change over time and the aging of the spring. In order to have reliable measurements of the forces during the experiments, the stiffness constants for both axes must be verified and determined if there are early mentioned changes. To achieve this, it is important to have different reference weights. The appearance of the weights used are shown in Table 28.

Table 28: Characteristics of masses used. Not all the masses were used because some of them could not be mounted on the upper part of the ball

Number	Color	Mass [mg]	Weight [mN]
4	Silver – blue	45.1	0.442
6	Silver – red/green	163	1.6
8	Copper – red	521	5.11
9	Copper – blue	756	7.42
10	Copper – green	1011	9.92

First, the user should make sure that the Basalt MUST 2D-FM 1N module is at its home position. This means that there is no contact between the tool ball and the table of the Basalt MUST LMS20. The Basalt MUST LMS20 must be moved away so the vertical axis is free (see Figure 76).

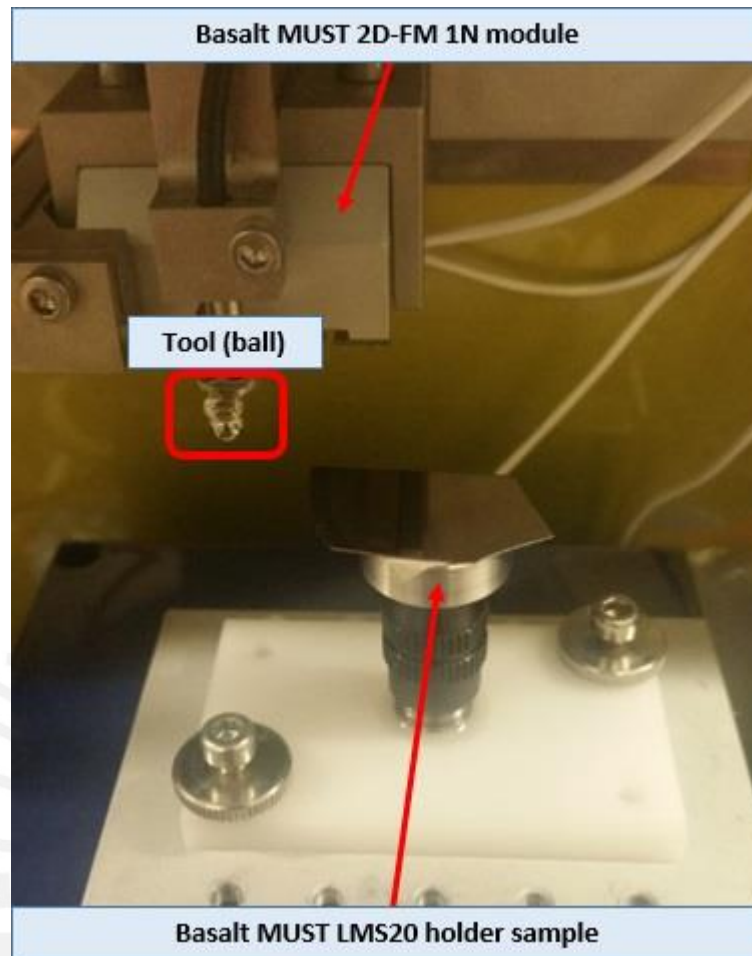


Figure 76: Initial position previous to hang the weights. The Basalt MUST LMS20 must be moved out of the axis of the ball so the mass could be located.

With the configuration shown in Figure 76 the user is able to determine the Stiffness constant in the normal axis hanging the mass onto the cantilever. This procedure is done manually and the user must be very careful otherwise the cantilever and the mirrors can be damaged in the process. The mass must be located at the edge above the ball (see Figure 77). Once the mass is located, the user should wait some seconds so the cantilever reaches a steady state. Then in the “Calibration” tab in the program, the button “Raw” (See Figure 78) should be used in order to collect this data and the indicator “Saving” will be activated. The data collected are the normal and tangential forces “Fn Force [mN]” and “Ft Force [mN]” and also the deformations in both axis “Dx Fn [μm]” and “Dx Ft [μm]”. Once the user has collected data for about three to five seconds, the user should click the button “Raw Stop” to stop data saving and the indicator “Saving” will be deactivated. Finally the user can export this data into an excel file by clicking the “Excel Raw” button (see Figure 78).



Figure 77: Location of the mass above the ball.



Figure 78: Buttons for saving data of the sensor with the weight hanging free.

The procedure previously described must be repeated for each weight used in order to obtain different deformations and thus being able to obtain the behavior of the stiffness constant. For the present thesis were used 5 weights in total (Table 28).

To obtain the tangential stiffness constant, the user must first turn the Basalt MUST 2D-FM 1N ninety degrees to the left into a vertical position (see Figure 79). This is done with the help of main screw that connects the module to the frame. Then, the user must proceed as indicated for the normal axis hanging carefully the weights one by one (see Figure 80).

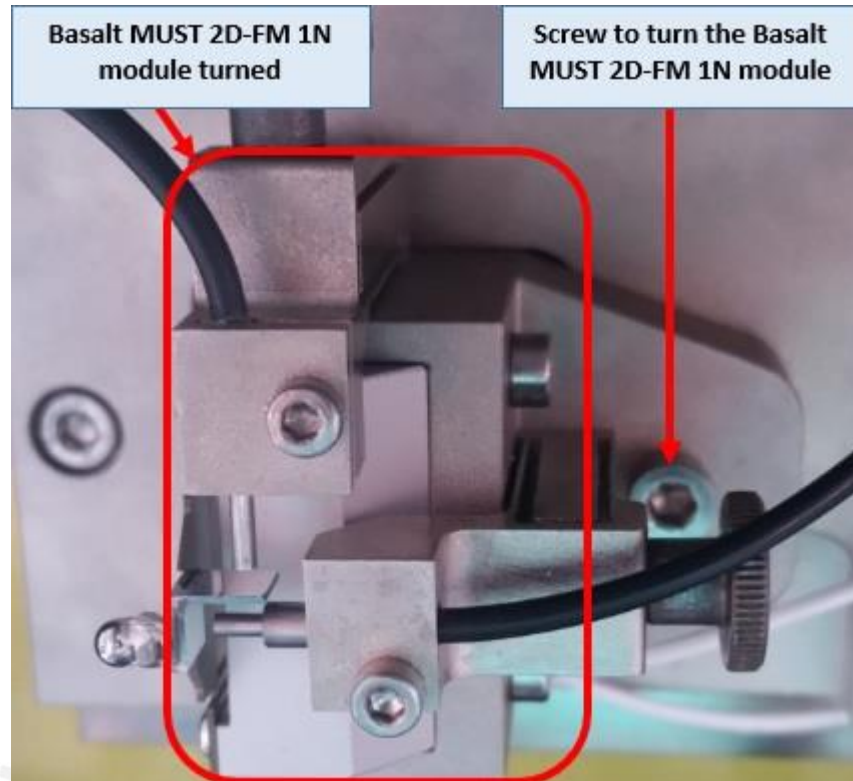


Figure 79: Cantilever turned to the left ninety degrees

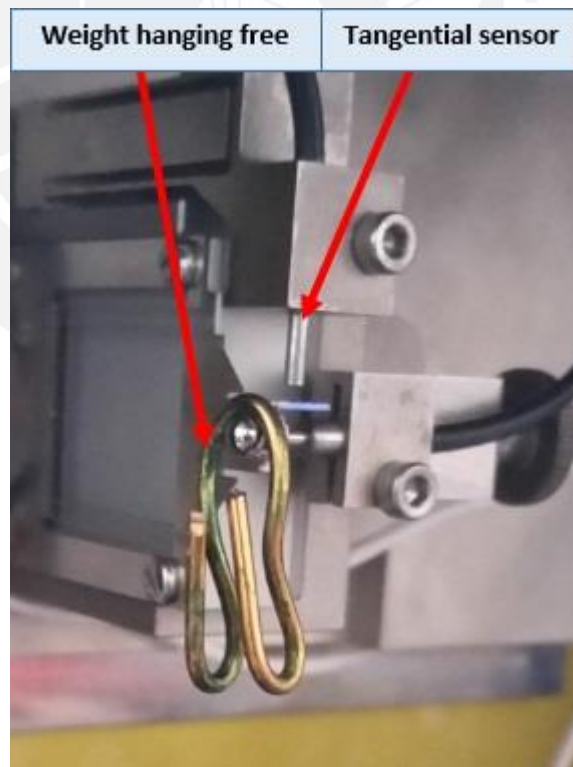


Figure 80: Weight hanging free for the tangential axis

After obtaining the average deformation for both axis, the weight force applied with its correspondent average deformation were tabulated. The data taken from the technical calibration sheet was also tabulated (See Table 29 and Table 30) to compare results. Then, it was plotted both forces with their correspondent deformations and the curves obtained are shown in Figure 81 and Figure 82. The slope of these curves is the stiffness constant.

Table 29: Tabulated values for the normal axis. On the left side top in blue, are the values obtained by hanging weights on the cantilever. On the right side top in orange, are the values shown in the calibration sheet of the cantilever.

Obtained experimentally		Taken from the technical calibration sheet	
Weight force applied [mN]	Average Deformation determined [μm]	Force [mN]	Deformation [μm]
0.00	0.00	0	0
0.442	11.0099873	0.0937	2.5
1.6	35.5934413	0.46	11.3
5.11	117.540414	5.295	121.6
7.42	172.746563	7.709	177.3
9.92	228.982416	10.326	234.8

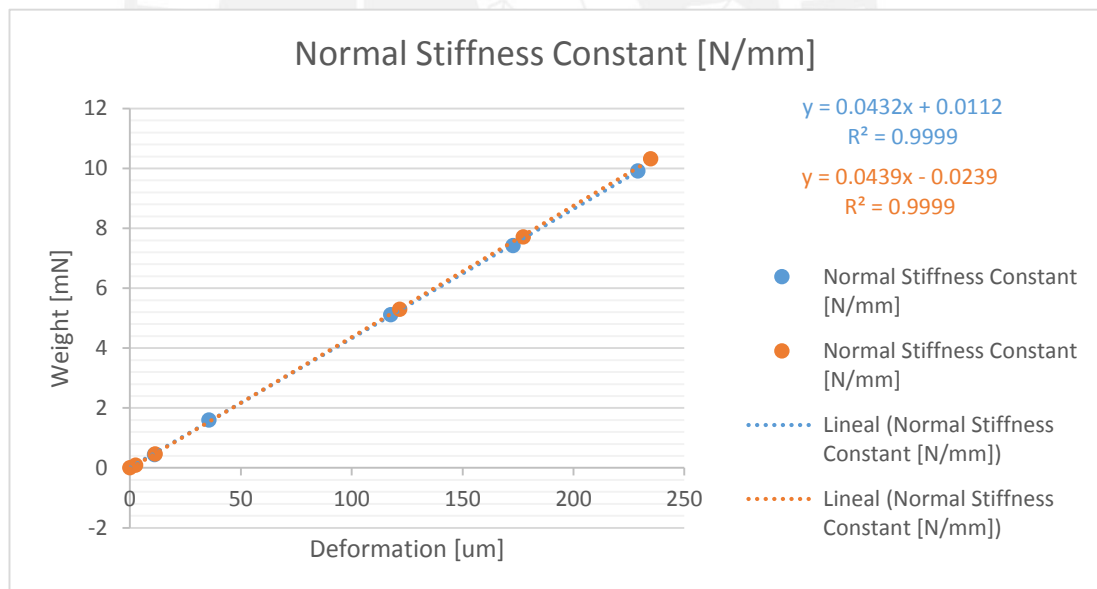


Figure 81: Graphic of the Normal stiffness constant. The blue line is the line obtained. The orange line is the one shown in the calibration sheet of the cantilever.

Table 30: Tabulated values for the tangential axis. On the left side top in blue, are the values obtained by hanging weights on the cantilever. On the right side top in orange, are the values shown in the calibration sheet of the cantilever.

Obtained experimentally		Taken from the technical calibration sheet	
Weight force applied [mN]	Average Deformation determined [μm]	Force [mN]	Deformation [μm]
0.00	0.00	0	0
0.442	7.84892437	0.0937	1.6
1.6	26.0452135	0.46	7.7
5.11	85.2127518	5.295	86.2
7.42	122.12195	7.709	123.7
9.92	163.583018	10.326	166.5

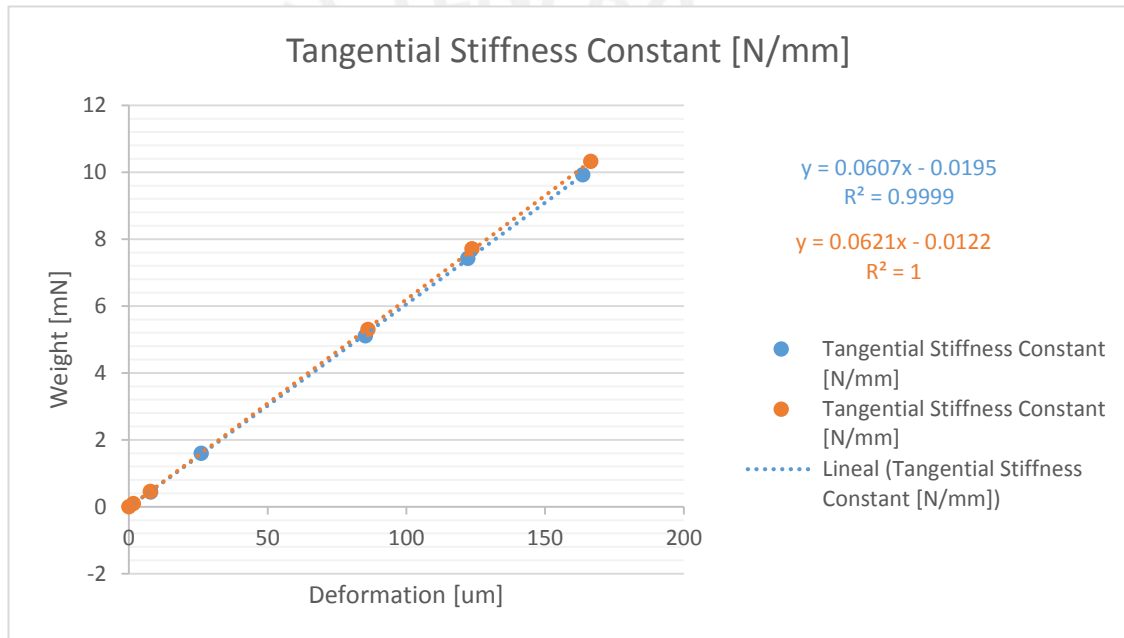


Figure 82: Graphic of the tangential stiffness constant. The blue line is the line obtained. The orange line is the one shown in the calibration sheet of the cantilever.

For both cases, it is observed that the curves are almost overlapping and therefore the spring constants, are quite similar (Table 31 and Table 32). For the present thesis, the parameters given by the calibration sheet were used for further calculations.

Table 31: Normal stiffness coefficient comparison

Normal Stiffness Coefficient	
Experimental stiffness [N/mm]	0.0432
Given stiffness [N/mm]	0.0439
Error [%]	1.6

Table 32: Tangential stiffness coefficient comparison

Tangential Stiffness Coefficient	
Experimental stiffness [N/mm]	0.0607
Given stiffness [N/mm]	0.0621
Error [%]	2.25



6 Measurement tab and error handling

6.1 Measurement tab

In this section the focus will be on the “Measurement” tab.

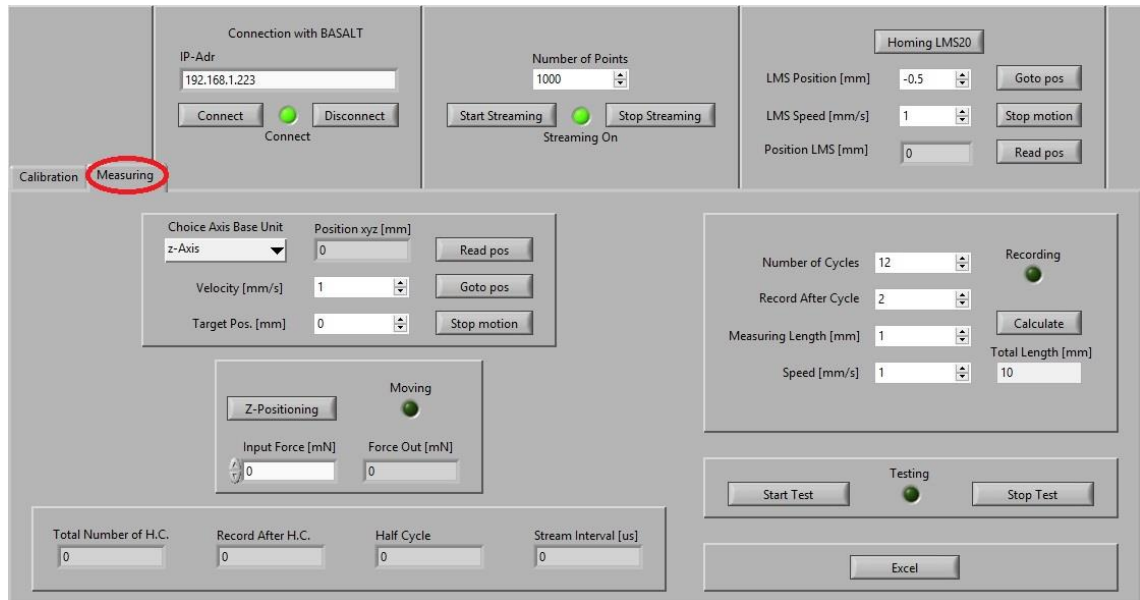


Figure 83: "Measurement" tab.

In this tab, the user can perform the tribological experiment. In order to do this, first the user must enter values such as “number of cycles”, “record after cycle”, “measuring length”, “speed” and “input force”, so that the program can perform the experience. Most of these parameters are located on the block at the right side of the window (see Figure 84).

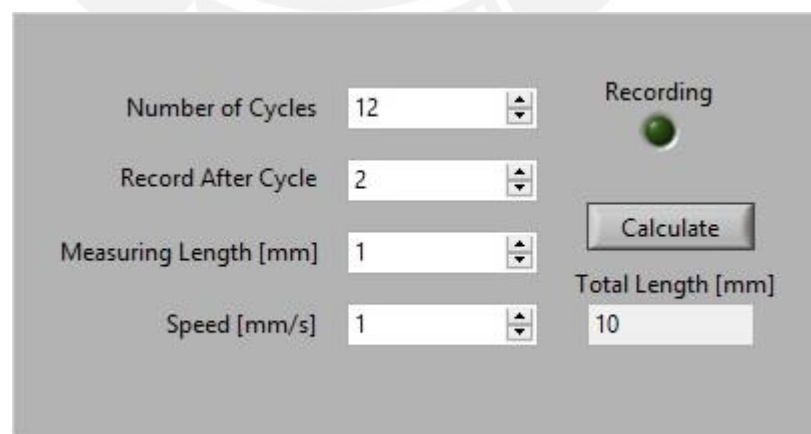


Figure 84: Parameters entered by the user before the experiment and the total length calculated.

These parameters are importance because they determine how long the experiment will take to finish.

The “Number of Cycles” is a parameter that the user enters and defines the maximum number of cycles the experiment will perform. The default value is 12 cycles

The “Record After Cycle” is a parameter the user enters if it is desired to start saving the data not from the first cycle but after a certain number of cycles. The user specifies this value so there is time to start the recording of the electrical parameters. The default value is 2 cycles.

The “measuring Length [mm]” is a parameter for defining the length of one half cycle. The default value is 1 mm.

The “Speed [mm/s]” is a parameter that specifies the velocity of the Basalt Must LMS20 oscillation during the experiment. The minimum value is 0.02 mm/s and the maximum is 10 mm/s [28].

The button “calculate” calculates the total length of the experiment as it was explained in the “Calculate” event. The value calculated is shown in the “Total Length [mm]” indicator.

Finally, the “Recording” indicator is activated after the number of cycles specified in the “Record After Cycle” variable are completed. So it shows the user when the data is being saved.

After entering this values, the user must do the positioning of the ball on the surface of the sample. This is done by the blocks shown in Figure 85.

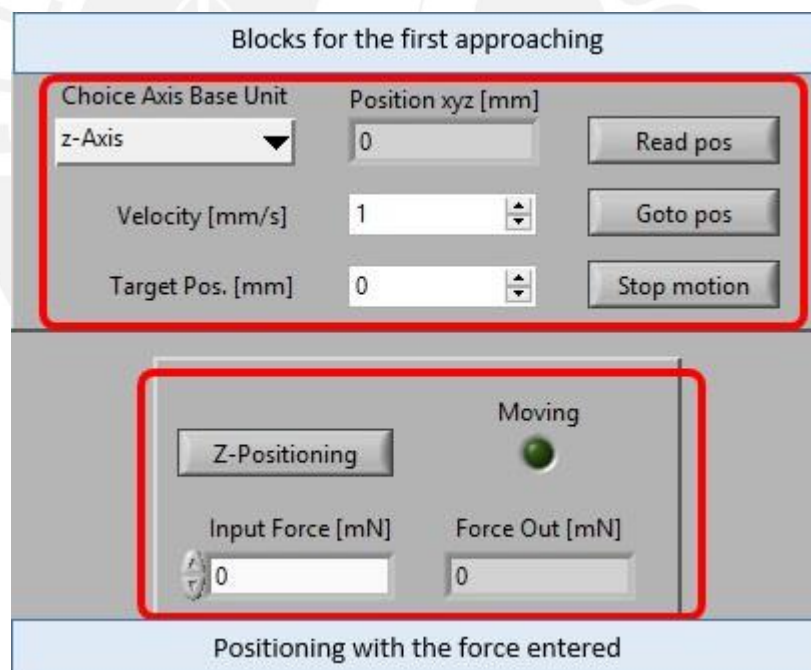


Figure 85: Blocks for positioning the ball. The upper part is used for the first approaching with high velocity. The lower part is for the positioning with the force entered by the user.

The positioning of the ball must be done in two steps. The first one is to do an approaching near to the surface with a high speed but without touching it (see Figure 85). This is done by choosing in the “Choice Axis Base Unit” the “Z-Axis” value which is also the default value used in this work. Then the user must indicate the target position to achieve in the “Target Pos. [mm]” block the default value here is 0 mm which means that the Basalt MUST 2D-FM 1N module is in its home position or will be moved to its home position. Finally, the block “Velocity [mm/s]” specifies the

speed of the approaching. The default value for this block is 1 mm/s. For this first approach the user must be very careful. It is important to know that the separation between the ball and the surface of the table of the Basalt MUST 2D-FM 1N is approximately 10 mm and that the thickness of the sample was less than a 1 mm. So for this work, the first approach was done with a target position of 8.5 mm.

The second step is positioning the ball on the surface of the sample by entering the normal force to apply during the experiment (see Figure 85). This is done by entering the Force in the box "Input Force [mN]" and then clicking the "Z-Positioning" button. This second approach is executed with a speed of 0.2 mm/s set in the program and not changeable by the user (see **4.4.1.14 Z-Positioning event**). While the ball is moving towards the sample, the "Moving" indicator is active. And once the force measured ("Force Out [mN]") reaches the force entered, the Basalt MUST 2D-FM 1N stops moving and the "Moving" indicator is deactivated.

After the positioning of the ball on the surface with the desired force, and before starting the experiment, the user must go to the "Calibration" tab again to correct an offset on the tangential force. This is because when the positioning is done, and the ball is pressed against the sample, a slight offset is generated in the tangential force. This Offset must be corrected otherwise, when the experiment is done, and the data analyzed, the tangential force will not be around Zero (it will not be symmetrical) and this will affect the friction coefficient which will not have a constant tendency but will have different values for each half cycle. So in order to avoid this, in the "Calibration" tab the user must click "Start Calibration". Then in the "Ft Force [mN]" the user can see the offset of the tangential force. This offset is around 0.1 to 0.5 mN and in the "Dx Ft [um]" indicator, the user can see the deformation due to this offset. By clicking the button "Tarring Ft", the user is taking a new reference for the tangential force and the values for the "Ft Force [mN]" and "Dx Ft [um]" will now be around zero.

After correcting the offset in the tangential force, the user can start the experiment. This is done by clicking the button "Start Test" in the "Testing" tab. After that, a window will open where the user can choose the path to save the file of the tribological data that will be recorded.



Figure 86: Buttons for starting/stopping the experiment and exporting the data into an excel file.

After leaving that window, the "Testing" indicator will be activated meaning that the experiment started. In order to have an idea of how much it will take for the experiment to finish, at the bottom part of this tab, there are the indicators "Total Number of H.C", "Record After H.C", "Half Cycle" and "Stream Interval [us]". From the first three, the user can have an idea of the experiment. When the value of the counter "Half Cycle" equals the value of "Total Number of H.C", the experiment will finish.

If the user want to stop the experiment before it finishes, the button “Stop Test” must be pressed. The indicators “Testing”, “Recording” and “Streaming On” will be deactivated and the counter “Half Cycle” will be set to zero.

Finally, when the experiment has finished, the user can open the data in Excel by clicking the button “excel” (see Figure 86).

6.2 Error handling

In order to evaluate how much noise is generated in the system, an evaluation was performed with the Basalt MUST 2D-FM 1N in its home position and with the ball hanging free (Figure 87). For this evaluation, the work space of the tribometer was cleaned from all tools and electrical wires as it is shown in the Figure 88.

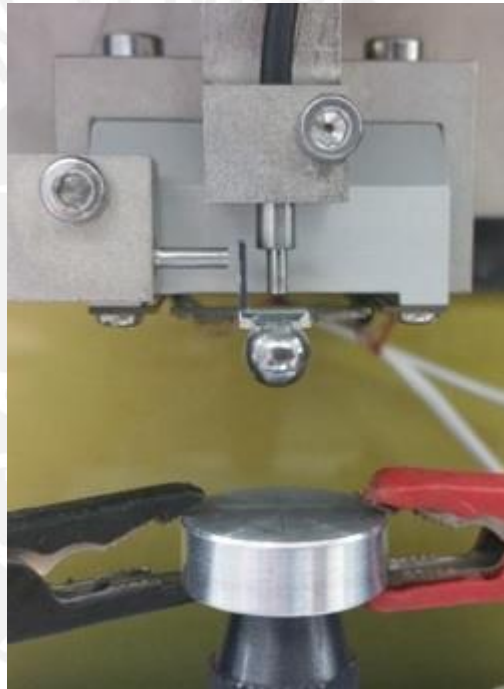


Figure 87: Ball hanging free before doing the analysis of the error.



Figure 88: Work space of the tribometer free from electrical wires and objects.

Once the table was free from objects, in the “Calibration” tab the user must click the “Start Calibration” button and then in the bottom part of the window there is a group of three buttons for getting the raw data (see Figure 89). These buttons were already described in **5.2 Determination of the spring constant**.

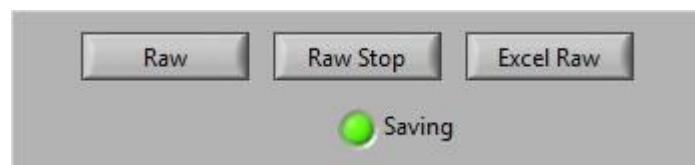


Figure 89: buttons to obtain the raw data.

From the data obtained, it is possible to calculate the average, the standard deviation and the maximum noise amplitude for the tangential and normal force and the deformation for both axis as shown in the Table 33.

Table 33: error parameters obtained

	Normal force [mN]	Normal deformation [μm]	Tangential force [mN]	Tangential deformation [μm]
Average	-0.000240233	-0.005560806	0.010541154	0.169744861
Standard deviation (σ)	0.00652088	0.15094618	0.01201264	0.25734995
Maximum noise amplitude	0.0378185	0.8754273	0.0746231	1.2016601

Although the tangential force is an important tribological parameter, the input that is controlled is the normal force. And because the cantilever used for the present work was not changed, the maximum force possible to apply is around 42 mN. This value was determined experimentally by increasing slowly the input force and observing the deformation generated. It was found that for approximately 42 mN, the observed distance in the “Normal Distance [μm]” in the “Calibration” tab was close to 500 μm which is the minimum distance that the system can read in the MR2. This means that the spring has deformed almost 1000 μm starting from the other edge of the measuring range.

From these two values obtained experimentally, it is possible to calculate the noise and the signal ratio.

$$SNR_{dB} = 20 * \log_{10} \left(\frac{A_{signal}}{A_{noise}} \right) \tag{Equation 9}$$

So replacing the values for the normal force obtained before in Equation 9, it is obtained.

$$SNR^{Normal Force}_{dB} = 20 * \log_{10} \left(\frac{42}{0.0378185} \right) \tag{Equation 10}$$

Doing the same for the normal deformation, it is obtained:

$$SNR^{Normal Deformation}_{dB} = 20 * \log_{10} \left(\frac{1000}{0.8754273} \right) \tag{Equation 11}$$

6.2.1 Errors in the program

The program developed, when used incorrectly, shows error messages. The text indicates the nature of the error. One of the most common errors is the connection between controlling computer with the basalt tribometer (Figure 90). Commonly it occurs when the user forgot to click the button “Connect”. This message can also be displayed when the IP address of the tribometer is wrong.

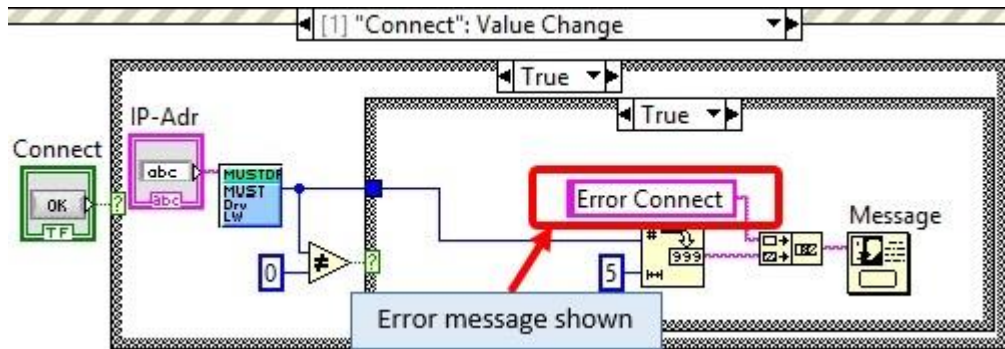


Figure 90: Error message in the connection

In the Table 34, is shown the error codes for the connection.

Table 34: Connection error codes [30]

Error Code	Meaning	Comment
20481	ERR_CONNECT	Error connecting Connection already exists
160	ERR_PROTOCOL_STX	Received no STX
161	ERR_PROTOCOL_CRC	Checksum failed
162	ERR_PROTOCOL_BLK	Reception block failed
163	ERR_PROTOCOL_ID	Incorrect ID
164	ERR_TESTER_UNKNOWN_COMMAND	Incorrect command

Other error message might be shown due to the streaming (Figure 91). The error codes that could be generated are shown in Table 35.

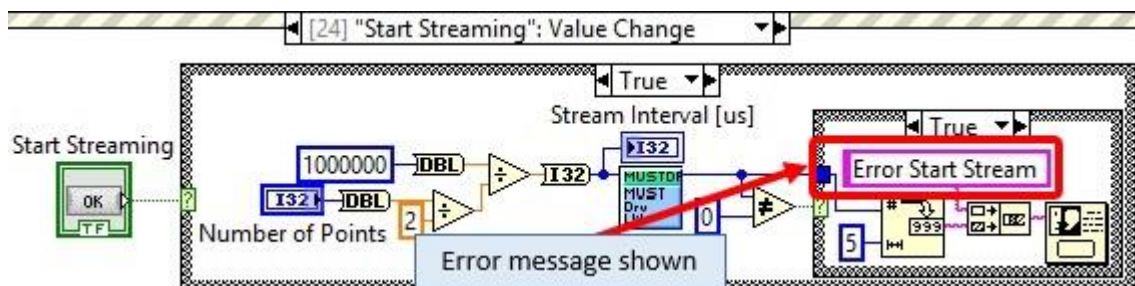


Figure 91: Error message in the streaming

Table 35: Streaming error codes [30]

Error Code	Meaning	Comment
81	ERR_EXT_WRONG_CMD	Wrong answer on command
82	ERR_EXT_NAK	ACK not received
83	ERR_WRONG_NBR_DATA	Wrong number of bytes received
85	ERR_BUFFER_OVERFLOW	Ring Buffer Overflow

To see more error codes that the software can have, see the reference [30] at page 15. There, the company shows all the tables with all the possible error codes that can occur in the tribometer.



7 Experiments

To prove the functionality of the developed system, it should be determine the friction coefficient as well as the current and voltage during the measuring.

In order to avoid disturbances during the experiments, first the user must clean the work table where the tribological machine is locate as it was discussed in chapter 6. So the electrical wires of all types, tools, and other objects must be remove from the table (Figure 92). The table where the tribometer is located, is a granite block that works as a vibration attenuator.

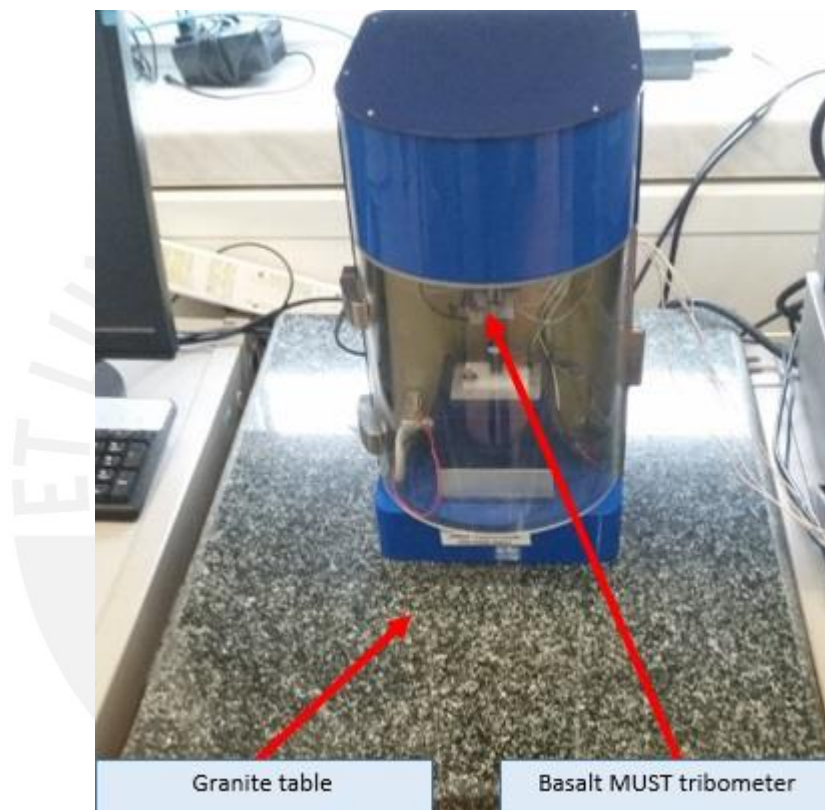


Figure 92: Work space for the Basalt MUST tribometer free from any wire, tool or object.

Second, the user must stick the sample to the table of the Basalt MUST 2D-FM 1N and connect the hooks for injecting the current (see Figure 93). After setting the sample, the user must go to the GUI of the program developed. Here, the user must press the button “Connect” to start communication with the Basalt tribometer, and then the button “Start Streaming” to enable the data acquisition. Finally, the user must click the button “Homing LMS20” to move it to the center position.

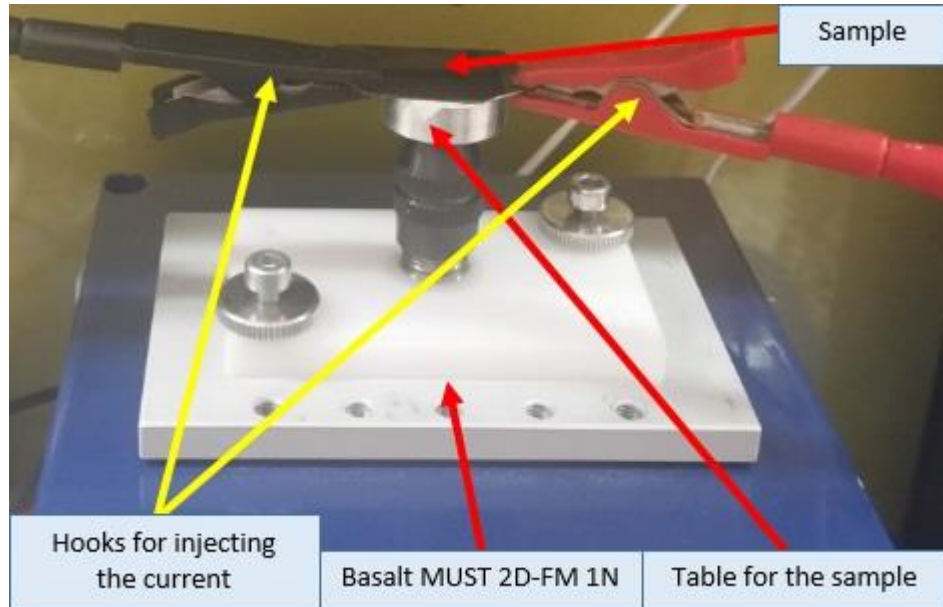


Figure 93: Sample setup and connection. The hooks indicated with the yellow arrows are for injecting the current into the sample.

After doing the previous steps, the user must do the calibration process or import the “Calibration file” if the user has one as stated in chapter 5. Then click on the “Testing Tab” and follow the steps discussed in **6 Measurement tab and error handling**.

For the present thesis work, the experiments were taken with different parameters (see Table 36). The material used as sample was Ti_3SiC_2 and the ball was of 100Cr6 steel.

Table 36: Parameters considered for the experiments.

Number of cycles	Current injected [mA]	Force applied [mN]
100	10	5
100	10	40
1000	0	40
1000	10	15
1000	10	40
1000	100	40
10000	10	15
10000	10	40

For the experiment with 1000 Cycles, 10 mA and 40 mN, the tribological parameters are shown in Figure 94.

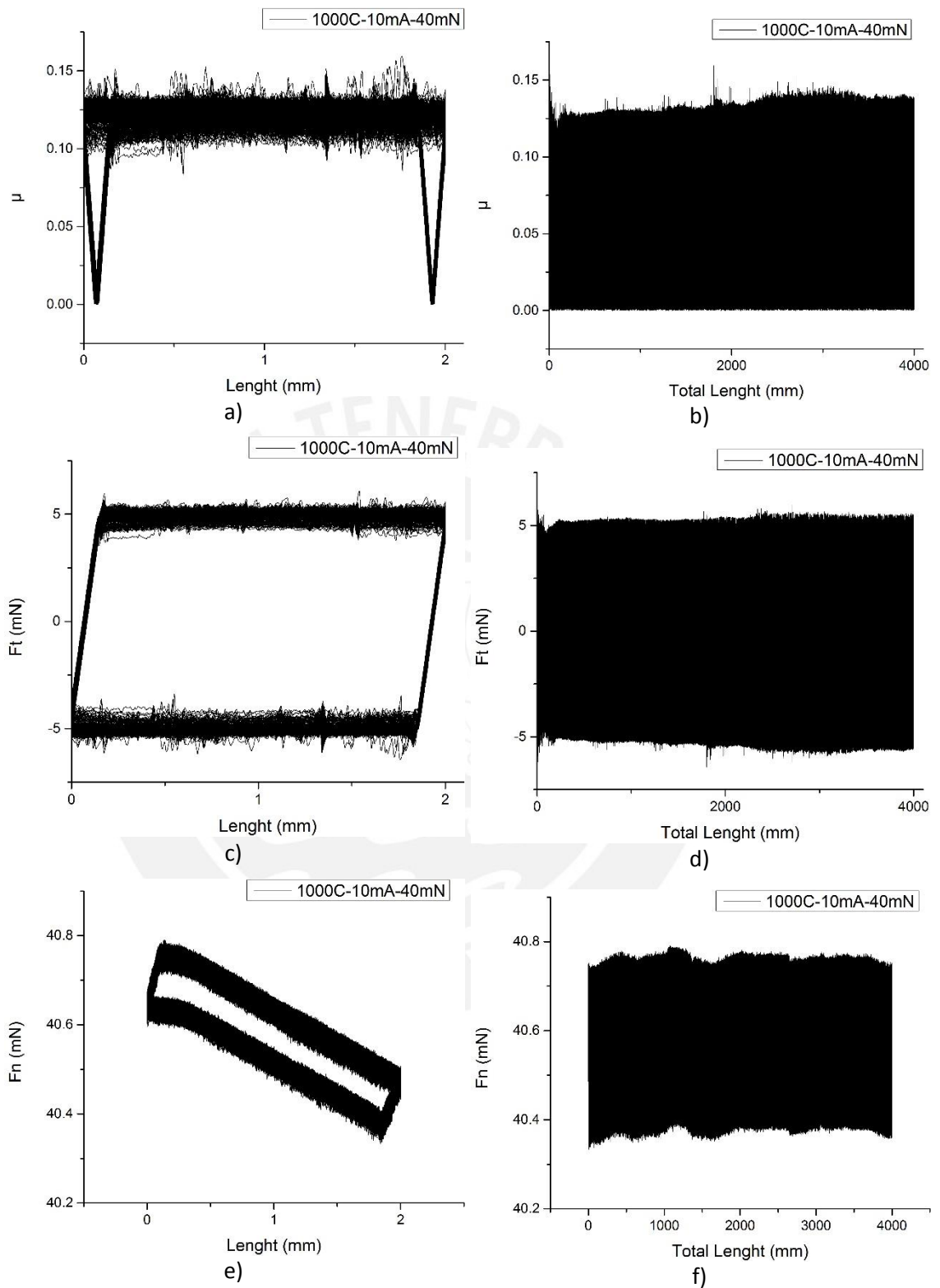


Figure 94: Tribological data plotted. On the top side is plotted the coefficient of friction vs. a) length and b) total length. On the middle, is plotted the frictional force vs. c) length and d) total length. On the bottom, is plotted the normal force vs. e) length and f) total length.

The electrical parameter obtained for the experiment with 1000 Cycles, 10 mA and 40 mN are shown in Figure 95.

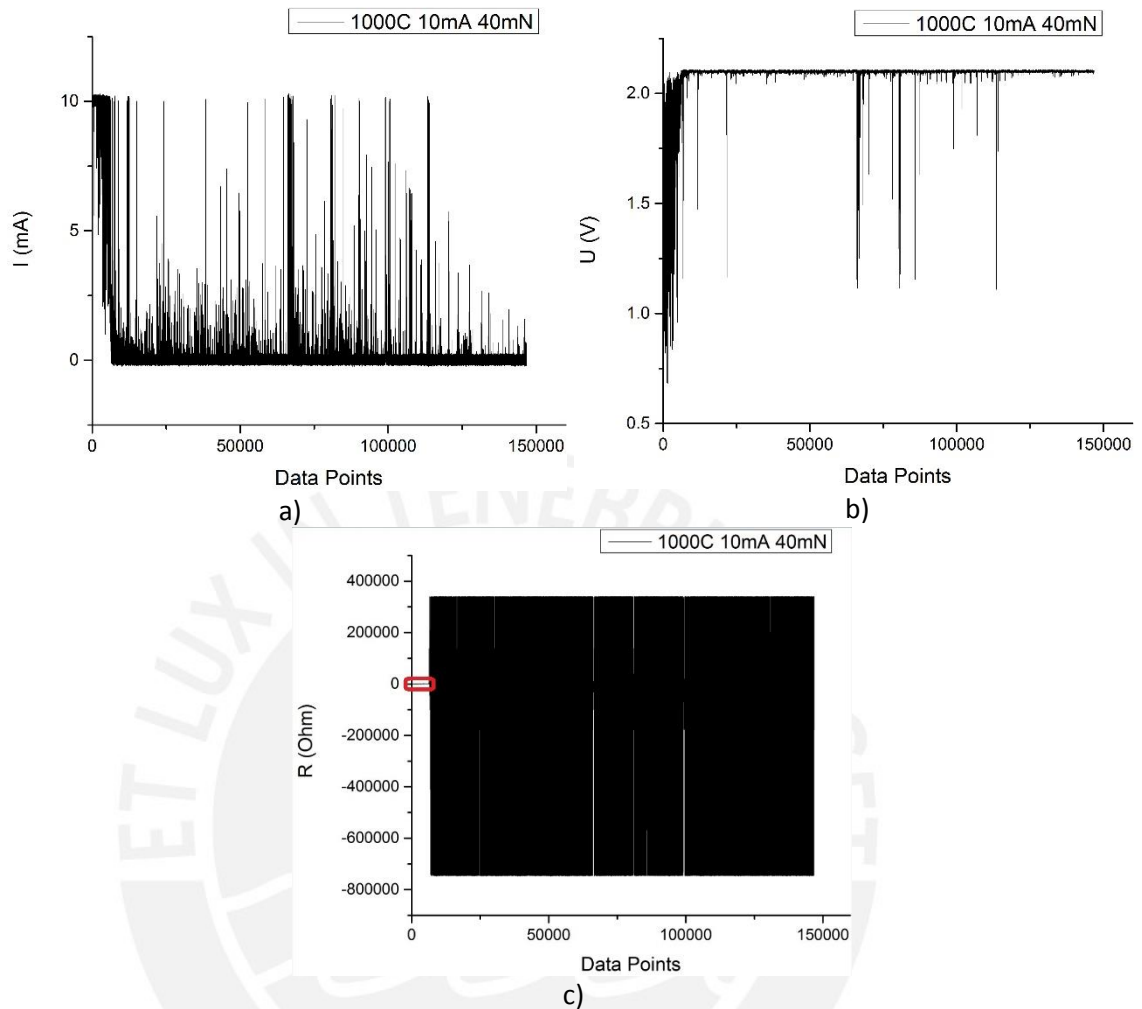


Figure 95: Electrical parameters obtained. a) current, b) voltage and c) resistance.

From Figure 94a, it is possible to observe that the coefficient of friction has a linear behavior. This behavior should be seen in the Figure 94b, but instead is seen a shadow. Also, in the electrical parameters especially in the resistance (Figure 95c) where the behavior of this parameter should be seen, it is seen instead a black square in most of the graphic. Only in the red square marked, it is seen the behavior in the resistance during the firsts cycles of the experiment. Doing an expansion of the coefficient of friction graphic and resistance, it is possible to see the behavior of the friction and what happens in the graphic (Figure 96).

From Figure 96b it is possible to observe peaks going down to zero for the friction coefficient. These peaks are generated when the ball of the tribometer reaches the end of the position and changes direction during the reciprocating movement. At this points, the tangential force also changes direction and at some point its value is zero (Figure 96c and d). From Figure 97, is seen the resistance in the linear zone during the experiment. This linear behavior is obtained before the current goes down to zero.

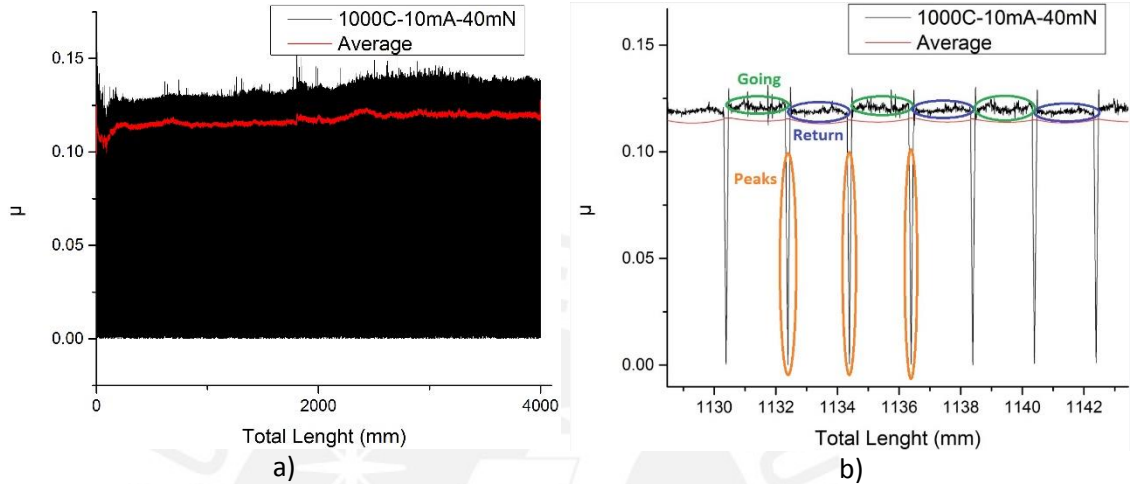


Figure 96: a) shows the average curve for the coefficient of friction in red. This curve was obtained in Origin, using the smooth option and then using the Adjacent Averaging method with 5000 points. B) Shows a cutout of the coefficient of friction vs. distance. Marked in green is the going path. Marked in blue is the return path. Marked in orange are the peaks due to the change of direction of the ball.

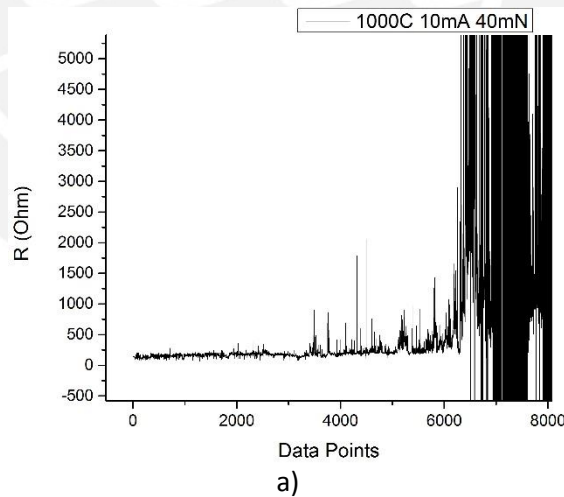


Figure 97: Linear zone of the resistance during the experiment. The black shadow on the right occurs when the current goes down to zero.

In Figure 98, is shown the comparison between the resistance obtained with the electrical parameters with the coefficient of friction, the tangential force and the normal force. It was expected in the tribological parameters to find some sort of disturbance that could explain the behavior of the resistance after approximately 30 cycles. But as it is shown in Figure 98, the behavior of the tribological parameters do not show any abnormalities. So the behavior of the resistance may be because by the accumulation of particles between the ball and the sample and that would be affecting the flow of the current.

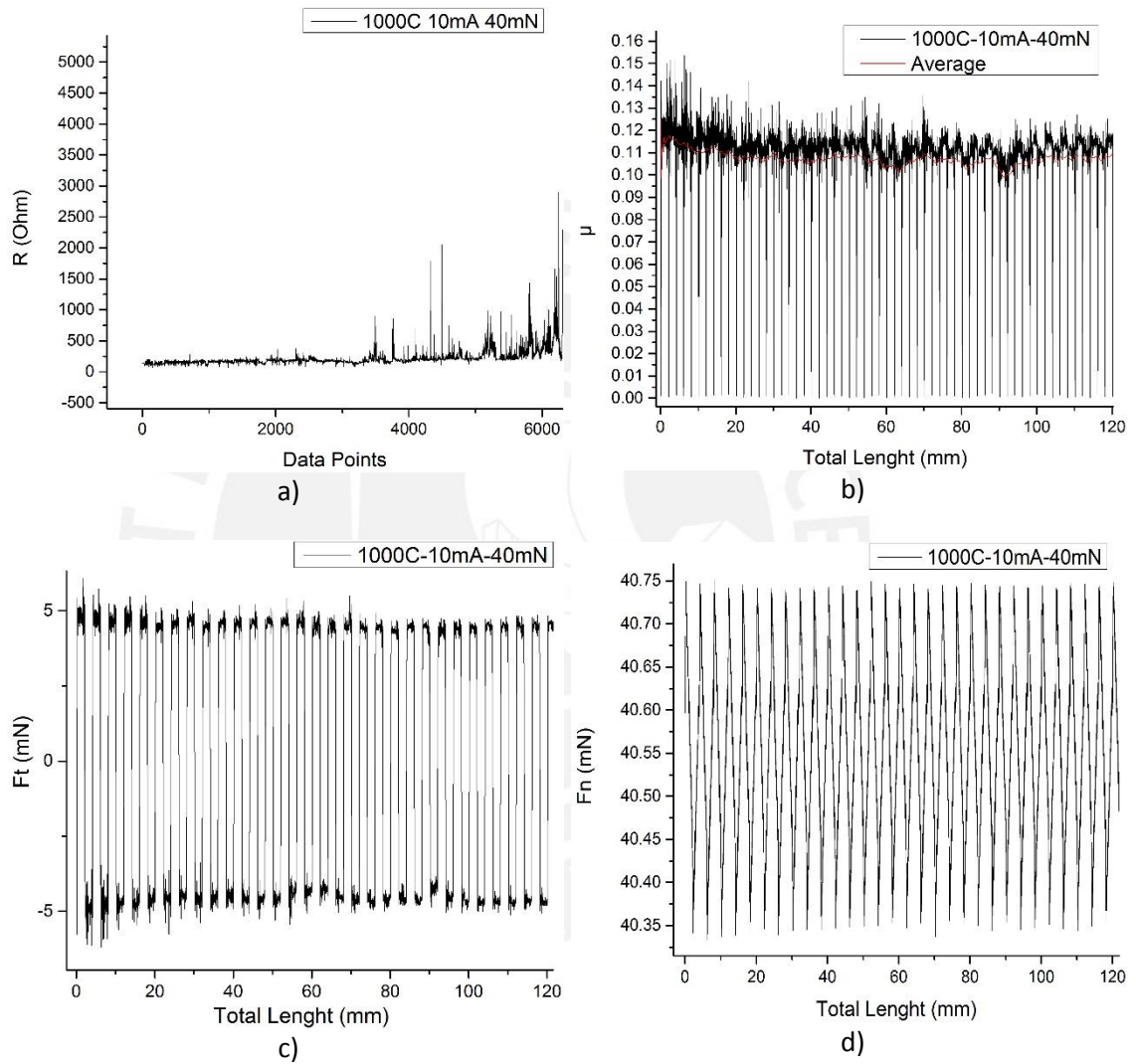


Figure 98: comparison between the linear zone of the resistance with the tribological parameters such as coefficient of friction, tangential force and normal force for the first 30 cycles approximately

In Figure 99, it was obtained the average curve for the coefficient of friction of 6 experiments

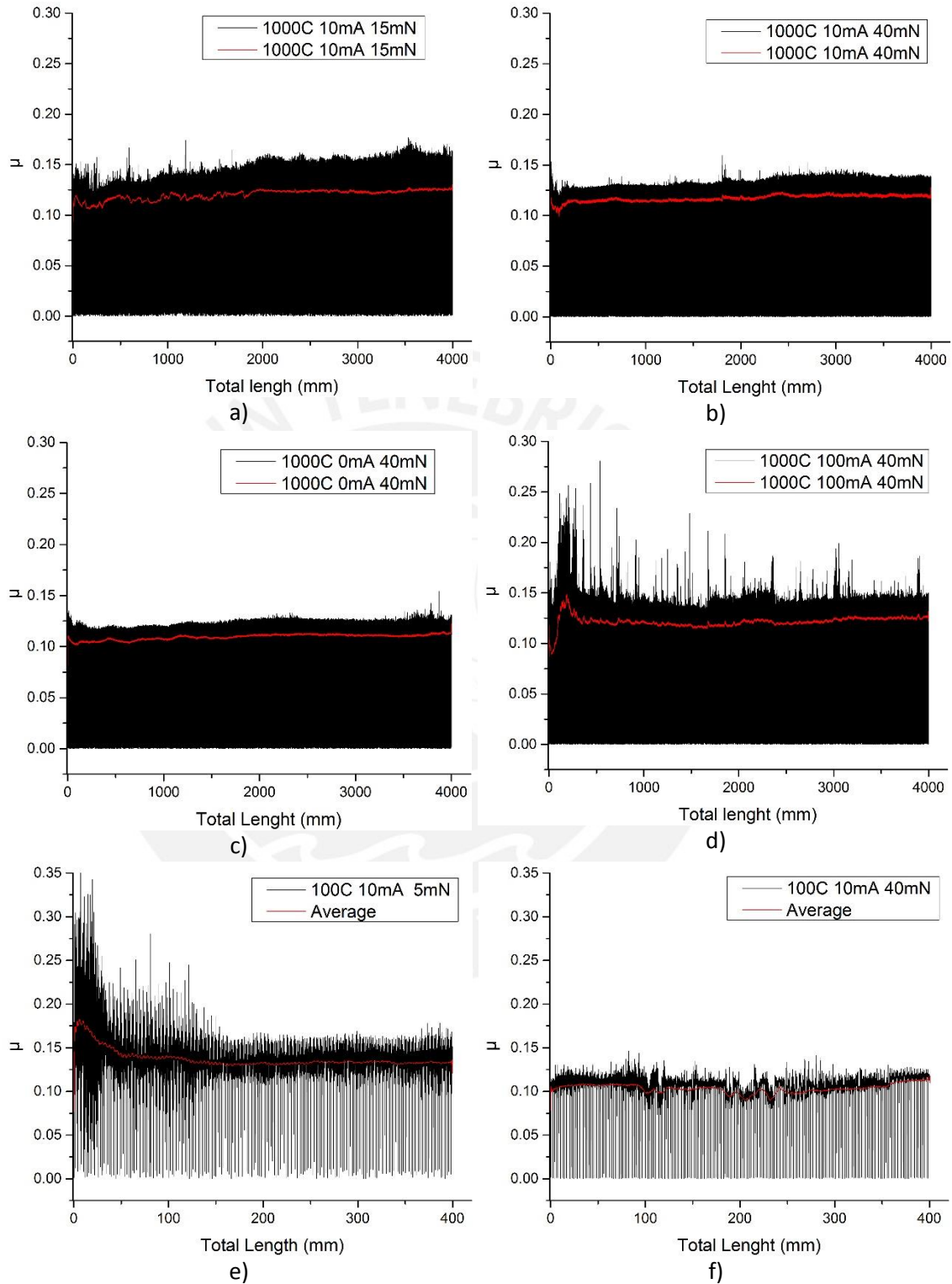


Figure 99: Friction average curves in red for each experiment

From Figure 99, the average curves were obtained using the smooth option of the origin with the method of Adjacent Averaging with 5000 points. With the help of these curves, it is possible to see the behavior of the coefficient of friction and its tendency. From Figure 100 is possible to see that the coefficient of friction at the beginning presents some sort of distortions. These distortions could be caused by particles when the ball starts scratching the surface of the sample. Then as the experiment continues, the coefficient of friction starts showing a linear tendency. This might be because as the experiment continues, the surface is polished by the ball and the particles are no longer disturbing the movement of the ball so the friction is constant.

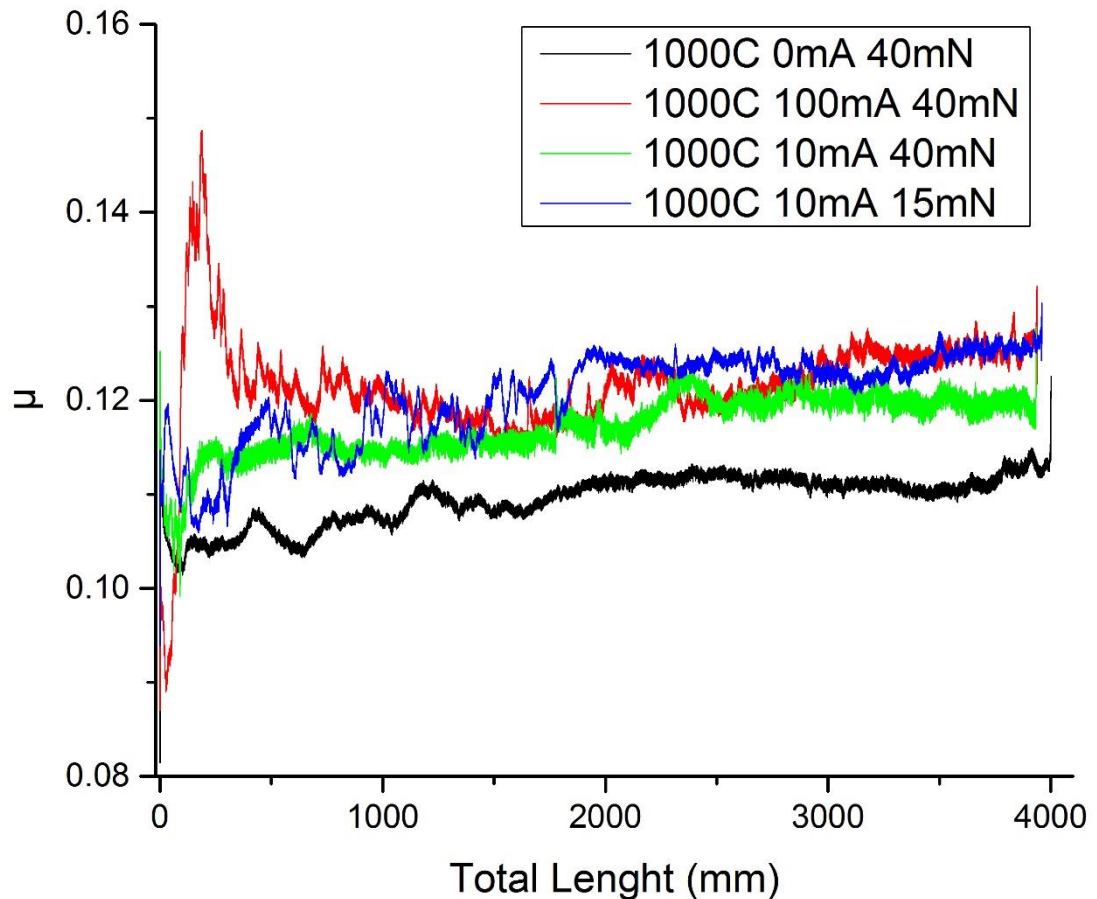


Figure 100: Average friction curves for the experiments with 1000 cycles

Another explanation for the behavior of the coefficient of friction is that at the beginning, the ball is scratching the surface of the sample. As the experiment continues, the sample wears so that the ball is scratching the silicon.

8 Conclusions and future work

8.1 Conclusions

Triboelectrical properties are an interesting area of investigation, especially when it comes to electrical contact materials. The knowledge of friction and wear of electrical plugs and switches are crucial for their proper application. If the switching process takes place under electrical power load, the wear effect is even stronger pronounced.

In order to study this behavior, it was implemented a LabVIEW base solution for operating the Basalt MUST Tribometer and also for the Keithley devices used for the present work.

It was implemented also the calibration process for the program developed and the error ranges for the measurements were presented.

Finally it was presented a solution for the electrical measurements via 4-wire sensing using two crocodile hooks to inject the current into the sample and measure the voltage generated.

For the present work it was used as sample a sheet of Ti_3SiC_2 from which it was determined its triboelectrical properties such as coefficient of friction and the current and voltage.

Finally, a synchronization mechanism between the tribological and electrical measurements could not be implemented successfully. This was because the LabVIEW block that get the tribological data was faster than the block for getting the electrical parameters. This difference in speed could not be compensated in the same program so it was decided to do two programs separate. One only for the tribological parameters and the other one for the electrical parameters. But by doing this, it has to be very precise to activate the acquisition of the electrical parameters as soon as the tribological data is being saved. To help with this, it was implemented one sort of window where the tribometer is already moving but the tribological data is not saved yet. So the user has time to switch to the electrical program to start the recording of the data. This process is not 100% synchronous. Also, as it was shown in the results, the current goes down to zero after some cycles of operation. This makes difficult to analyze the behavior of the electrical resistance during all the experiment because it has absurd values. In Table 37, is shown a summary of the results obtained for the different experiments performed. For the experiments is shown the tribological results as well as the electrical parameters.

Table 37: Results obtained for the sample Ti_3SiC_2

Number of cycles	Current injected [mA]	Force applied [mN]	Coefficient of friction μ		Electrical resistance		
			Mean	Standard deviation	Mean [Ω]	Standard deviation	Number of cycles before losing electrical contact
100	10	5	0.14	0.022	181	281	7
100	10	40	0.10	0.018	181	155	82
1000	0	40	0.11	0.017	-	-	-
1000	10	15	0.12	0.014	165	99	260
1000	10	40	0.11	0.019	204	93	40
1000	100	40	0.12	0.024	11.5	4.6	40

8.2 Future work

Two of the main challenges during the experimentation were the injection of the current to the sample and the fact that there are two programs instead of one to control all the devices.

The injection of the current was done using crocodile hooks. But this hooks tend to break the samples every time the connection was done. Furthermore, sometimes these hooks loose contact with the surface of the sample and in the process of reattach them, they break the sample.

So for the future is needed a better way of subjection of the wires to the sample so they do not loose contact and thus avoid breaking the sample.

The use of two programs instead of one was not planned since the beginning, this was a solution for the challenge that represented acquiring electrical and tribological data from the same program. Here, the faster acquisition of the tribological parameters compared to the slower acquisition of the electrical parameters, means that most of the data obtained by the tribometer was lost. So in order to avoid this, the program was split in two and the electrical parameters could be acquired at its own rate and the tribological parameter at its own rate too. But by doing this, the synchronism was lost.

So for a future, is expected to work with faster devices for the electrical parameters in order to put them in a same program and acquire the data synchronously.

9 Figures

Figure 1: Basalt MUST LMS20 Ball on disk tribometer with reciprocating motion. The black and red clamps connected to the sample holder are used for injecting the current into the system. 2

Figure 2: Four point probe measurement [7] 3

Figure 3: four wire sensing..... 4

Figure 4: Frictional force FT used to cause motion by (a) rolling and (b) sliding..... 4

Figure 5: Microdisplacements δ , F_s maximum static friction, F_{int} intermediate static friction and F_k kinetic friction [4]..... 5

Figure 6: First law of friction 5

Figure 7: Second law of friction 6

Figure 8: Schematic of representative wear modes [9]..... 9

Figure 9: Sliding wear tests [10]..... 10

Figure 10: Stribeck curve and lubrication regimes [12] 12

Figure 11: Generic electronic connector designs used in different electronic systems and devices (taken from [14]–[24])..... 13

Figure 12: Schematic interconnection diagram. The communication of all the devices with the PC is represented with the green arrows. The voltage measured by the voltmeter is represented by the blue arrow. The current injected by the source to the tribometer is represented by a red arrow as well as the current being measured by the ampermeter 19

Figure 13: Image of the connection setup indicating all the used devices to measure the electrical as well as the tribological parameters. 20

Figure 14: Basalt MUST main parts [28], [29]. On the upper part the square in red shows the Basalt MUST 2D-FM 1N module. The arrows in yellow show the main parts of this module which are the Cantilever and the fiber optic sensors. On the lower part the big red square shows the Basalt MUST LMS20 module and just above it, in a small red square is the sample holder. On the right side of the lower part is shown the Ethernet connector used for the tribometer..... 21

Figure 15: On the left side is shown the Basalt MUST 2D-FM 1N and the position of the cantilever, the tool, the mirrors and the FOS. On the right side is shown the cantilever itself and the bending elements (spring). [28] 23

Figure 16: FOS characteristic curve [28]. d is the distance being measured by the sensor. MR1 and MR2 are the measurement ranges 1 and 2 respectively where the curve is considered linear. U_a is the voltage measured where “Peak” is the highest value. 24

Figure 17: Basalt MUST LMS20	25
Figure 18: Configure Output library.....	26
Figure 19: Data Read Multiple library	28
Figure 20: "Connect" library	30
Figure 21: "Start Stream" library.....	30
Figure 22: "Get Stream Data" library	31
Figure 23: "Base Unit Move Axis" library.....	31
Figure 24: "Base Unit Get State" library	32
Figure 25: "FOS Get Dist" library.....	32
Figure 26: Main loop.....	33
Figure 27: Graphical User Interface	34
Figure 28: "Connect" event. Starts the communication between the controlling computer and the tribometer	34
Figure 29: "Start Streaming" event. Starts the streaming mode of the tribometer.....	35
Figure 30: "Homing LMS20" event. Puts the LMS20 module to the center of the X and Y axis.	35
Figure 31: "Timeout" event in red. Tab control in purple and the options to choose for in blue. The default option is marked in green.....	36
Figure 32: Calibration Tab description.....	37
Figure 33: Blocks for getting the raw data of the sensors	38
Figure 34: Blocks for finding the maximum values for Fn and Ft	38
Figure 35: Distance obtained with the block "FOS Get Dist". This figure is for obtaining the normal distance. The configuration for obtaining the tangential distance is the same but the value of "nbSens" equal to 1 instead of 0 as it is shown and also the data of the sensor must be the Ft [V].l	39
Figure 36: Force calculation. The scheme for obtaining the force is the same for both normal and tangential	40
Figure 37: Blocks used to save the raw data into a file.	40
Figure 38: "Testing" tab. The upper part marked in red is where the movement of the LMS20 is generated. The lower part marked in blue, is where the data obtained is calculated and saved in the file.	41

Figure 39: LMS20 Oscillatory movement generation in red and conditions for start saving the tribological data and stop the experiment in blue.	42
Figure 40: Calculation of the target position	42
Figure 41: Target Position Inversion. The oscillatory movement is generated by negating the “tposit” value.	42
Figure 42: Data recording condition. When the counter “Half Cycle” is higher than “Record After H.C” the recording condition will be activated.....	43
Figure 43: Stop condition. When the counter “Half Cycle” is higher than “Total number of H.C” the stop case is executed.....	43
Figure 44: LMS20 Position. The scheme is the same as for the “Calibration” tab but in this case is also used a second Unbundle block to obtain the data of the “poslgr” output.	44
Figure 45: Calculation of the friction coefficient as the absolute value of the tangential force divided by the normal force.....	44
Figure 46: Save tribological data converted to string into the file.	45
Figure 47: “Go To PosXYZ” event. Moves the selected axis to the target position entered with the speed indicated.	45
Figure 48: Basalt MUST tribometer. The Basalt modules 2D-FM 1N and LMS20 are mounted on the Z-Positioning axis and the X-Y Positioning unit respectively [28].....	46
Figure 49: Basalt MUST LMS20	47
Figure 50: “LMS20 Goto pos” event. The LMS20 module moves to the position entered with the speed indicated.	47
Figure 51: "Start Test" event. The upper part creates the file with default name “TriboFile” and extension “.txt”. The lower part, the headers for the tribological parameters as well as the tribological conditions are stored in the file.....	48
Figure 52: "Calculate" event. The “Total Length” is determined in terms of the “Measuring Length” and the difference of the “Total Number of H.C” and “Record After H.C”	49
Figure 53: "Start_calib" event. On the left side, the paths of the look-up tables are loaded into the basalt block “FOS Read Call File” on the right side.....	50
Figure 54: "Sel. as peak" event. The Maximum values obtained are loaded into the variables “Fn Peak” and “Ft Peak”	51
Figure 55: "Tarring Fn" and "Tarring Ft" events. The normal and tangential distances obtained in the “Timeout” event are stored as reference distances named as “Zero Distance Fn” and “Zero distance Ft”	51

Figure 56: "Save configuration" event. On the left side are the blocks for creating the file with its default name and extension. On the right side are the variables that are saved into this file. 52

Figure 57: "Load configuration" event. On the left side, the calibration file is read. On the right side, the calibration values are obtained..... 52

Figure 58: The Z-Positioning axis marked in red is moved during the "Z Positioning" event..... 53

Figure 59: "Z-Positioning" event. This event gets data of the normal sensor and calculates de force that is compared with the force value entered by the user..... 53

Figure 60: "Timeout" event..... 54

Figure 61: Electrical GUI..... 54

Figure 62: Data Read Multiple VI. This block obtains the electrical data required 55

Figure 63: Data saving process. The blocks marked in red are the ones that changes the 1D arrays obtained into a 2D arrays. With the help of the block "Insert Into Array", the two 2D arrays are combined and as a result is obtained one 2D array. This last array is finally written into the file..... 55

Figure 64: "Start Electrical" event. On the left side, is the configuration of the two 2000 Keithley multimeters as ampermeter and as voltmeter. On the right side is the configuration of the 2400 Keithley SourceMeter 56

Figure 65: "Create File" event. In the upper part, the blocks creates the file named as default "current file" and an extension ".txt". The lower part the headers for the electrical parameters as well as the electrical conditions are stored in the file..... 57

Figure 66:"Start Recording Electrical" event. The "Recording" variable is activated. 58

Figure 67: Position for the calibration process. The tool (Ball) of the Basalt MUST 2D-FM 1N has no contact with the table of the Basalt MUST LMS20 59

Figure 68: Calibration Tab. The boxes marked in green are were the raw data in volts of the sensors is displayed..... 60

Figure 69: Normalized curve of the FOS. (Look-up table)..... 60

Figure 70: Basalt MUST 2D-FM 1N. The tiny screws are used to loosen the sensors. The FOS are moved towards the mirrors to find the maximum voltage values. 61

Figure 71: Finding peak values. The buttons "Reset_Fn" and "Reset_Ft" resets the" Max Fn" and "Max Ft" respectively..... 61

Figure 72: "Select Peak" button stores the maximum values obtained previously into the "Fn Peak" and "Ft Peak" variables..... 61

Figure 73: Measurement range selection and distances obtained 62

Figure 74: "Tarring" buttons to select the reference distances for both axis. 62

Figure 75: "Save Calibration" in red, "Load Calibration" in blue and the calibration parameters saved into the file. 63

Figure 76: Initial position previous to hang the weights. The Basalt MUST LMS20 must be moved out of the axis of the ball so the mass could be located. 64

Figure 77: Location of the mass above the ball. 65

Figure 78: Buttons for saving data of the sensor with the weight hanging free. 65

Figure 79: Cantilever turned to the left ninety degrees 66

Figure 80: Weight hanging free for the tangential axis 66

Figure 81: Graphic of the Normal stiffness constant. The blue line is the line obtained. The orange line is the one shown in the calibration sheet of the cantilever. 67

Figure 82: Graphic of the tangential stiffness constant. The blue line is the line obtained. The orange line is the one shown in the calibration sheet of the cantilever. 68

Figure 83: "Measuring" tab..... 70

Figure 84: Parameters entered by the user before the experiment and the total length calculated..... 70

Figure 85: Blocks for positioning the ball. The upper part is used for the first approaching with high velocity. The lower part is for the positioning with the force entered by the user..... 71

Figure 86: Buttons for starting/stopping the experiment and exporting the data into an excel file. 72

Figure 87: Ball hanging free before doing the analysis of the error. 73

Figure 88: Work space of the tribometer free from electrical wires and objects. 74

Figure 89: buttons to obtain the raw data..... 74

Figure 90: Error message in the connection 76

Figure 91: Error message in the streaming..... 76

Figure 92: work space for the Basalt MUST tribometer free from any wire, tool or object. 78

Figure 93: Sample setup and connection. The hooks indicated with the yellow arrows are for injecting the current into the sample. 79

Figure 94: Tribological data plotted. On the top side is plotted the coefficient of friction vs. a) length and b) total length. On the middle, is plotted the frictional force vs. c) length and d) total length. On the bottom, is plotted the normal force vs. e) length and f) total length. 80

Figure 95: Electrical parameters obtained. a) current, b) voltage and c) resistance..... 81

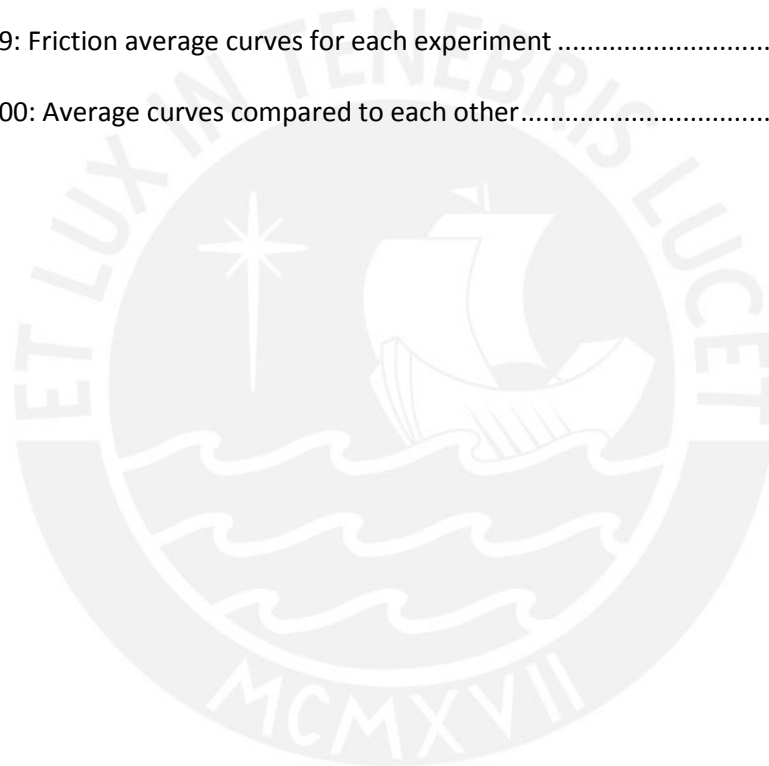
Figure 96: a) shows the average curve for the coefficient of friction in red. This curve was obtained in Origin, using the smooth option and then using the Adjacent Averaging method with 5000 points. B) Shows a cutout of the coefficient of friction vs. distance. Marked in green is the going path. Marked in blue is the return path. Marked in orange are the peaks due to the change of direction of the ball..... 82

Figure 97: Linear zone of the resistance during the experiment. The black shadow on the right occurs when the current goes down to zero. 82

Figure 98: comparison between the linear zone of the resistance with the tribological parameters such as coefficient of friction, tangential force and normal force for the first 30 cycles approximately..... 83

Figure 99: Friction average curves for each experiment 84

Figure 100: Average curves compared to each other..... 85



10 Tables

Table 1: Advantages and disadvantages of some wear test configurations [11]	10
Table 2: Lubrication regimes [1], [2], [12], [13]	11
Table 3: conductor materials used for electrical contacts [4]	15
Table 4: Properties of some Pseudo alloy contact materials [4]	15
Table 5: Compositions and characteristics of Silver-Based contact materials [4]	15
Table 6: Some properties of Silver-Graphite materials [4]	16
Table 7: Some properties of MAX phases compounds	16
Table 8: device description	20
Table 9: BASALT technical parameters [28]	22
Table 10: Technical parameters of the Basalt MUST 2D-FM 1N [28]	23
Table 11: Technical parameters of LMS20	25
Table 12: Keithley 2400 series	26
Table 13: "Configure Output" library description	27
Table 14: Keithley 2000 series	28
Table 15: "Data Read Multiple" library description	29
Table 16: BASALT-MUST Modules	30
Table 17: "Connect" library description	30
Table 18: "Start Stream" library description	30
Table 19: "Get Stream Data" library description	31
Table 20: "Base Unit Move Axis" library description	31
Table 21: "Base Unit Get State" library description	32
Table 22: "FOS Get Dist" library description	32
Table 23: "FOS Get Dist" values set	39
Table 24: "Base Unit Move Axis" parameters	46
Table 25: "LMS20 Move Posit" parameters	47

Table 26: Description of the "MUST Drv LW FOS Read Call File"	50
Table 27: Parameters used for the "Configuration Output"	56
Table 28: Characteristics of masses used. Not all the masses were used because some of them could not be mounted on the upper part of the ball	63
Table 29: Tabulated values for the normal axis. On the left side top in blue, are the values obtained by hanging weights on the cantilever. On the right side top in orange, are the values shown in the calibration sheet of the cantilever.	67
Table 30: Tabulated values for the tangential axis. On the left side top in blue, are the values obtained by hanging weights on the cantilever. On the right side top in orange, are the values shown in the calibration sheet of the cantilever.	68
Table 31: Normal stiffness coefficient comparison	69
Table 32: Tangential stiffness coefficient comparison	69
Table 33: error parameters obtained	75
Table 34: Connection error codes [30]	76
Table 35: Streaming error codes [30]	77
Table 36: Parameters considered for the experiments.	79
Table 37: Results obtained for the sample Ti_3SiC_2	87

11 References

- [1] c. M. Mate, *Tribology on the Small Scale: A bottom up approach to friction, lubrication, and wear*. Oxford: Oxford University Press, 2008.
- [2] I. M. Hutchings, *Tribology: Friction and Wear of Engineering Materials*. London: Edward Arnold, 1992.
- [3] G. W. Stachowiak, *Wear: Materials, Mechanisms and Practice*. Chichester: John Wiley & Sons, Ltd, 2005.
- [4] M. Braunovic, V. V. Konchits, and N. K. Myshkin, *Electrical Contacts: Fundamentals, Applications and Technology*. Boca Raton, Fla.: CRC Press, 2007.
- [5] H. Pan, J. Ding, X. Wang, and B. Li, "Design, implementation, and assessment of a high-precision and automation measurement system for thin film resistivity," *2010 Int. Conf. Mech. Autom. Control Eng. MACE2010*, pp. 2235–2238, 2010.
- [6] L. B. Valdes, "Resistivity Measurements on Germanium for Transistor," *proceeding of the I.R.E.*, vol. 42, no. 2, pp. 420–427, 1954.
- [7] F. Smits, "Measurement of Sheet Resistivities With the 4-Point Probe," *Bell Syst. Tech. J.*, pp. 711–718, 1958.
- [8] N. P. Suh and N. Saka, "2.800 tribology, Fall 2004," *Massachusetts Institute of technology: MIT OpenCourseWare*, 2004. [Online]. Available: <http://ocw.mit.edu/courses/mechanical-engineering/2-800-tribology-fall-2004/#>.
- [9] K. Kato and K. Adachi, "Wear Mechanisms," in *Modern Tribology Handbook. Vol 1*, 2001, p. 28.
- [10] N. Axén, S. Hogmark, and S. Jacobson, "Friction and Wear Measurement Techniques," in *Modern Tribology Handbook*, no. 1987, 2000, pp. 493–510.
- [11] M. Hussein, A. Mohammed, and N. Al-Aqeeli, "Wear Characteristics of Metallic Biomaterials: A Review," *Materials (Basel)*, vol. 8, no. 5, pp. 2749–2768, 2015.
- [12] L. Fernández Ruiz-Morón, "Desarrollo De Un Procedimiento Para El Cálculo De La Fuerza De Fricción En Un Contacto Ehd. Validación Experimental Del Procedimiento," Universidad Politécnica de Madrid, 2012.
- [13] H. Rachlin, "The Science of Self lubrication," p. 3, 2000.
- [14] Molex LLC, "0731375003." [Online]. Available: <http://www.digikey.com/product-detail/es/0731375003/WM5514-ND/1465136>. [Accessed: 13-Jan-2016].
- [15] Amphenol-RF Division, "31-315-RFX." [Online]. Available: <http://www.digikey.com/product-detail/es/31-315-RFX/ARFX1049-ND/100584>. [Accessed: 13-Jan-2016].

- [16] J. Probert, "RJ45 Ethernet Connector." [Online]. Available: <http://www.stl-illustrator.com/artwork/jean-probert/rj45-ethernet-connector>. [Accessed: 13-Jan-2016].
- [17] WIZnet, "RB1-125BAG1A." [Online]. Available: <http://www.digikey.com/product-detail/es/RB1-125BAG1A/1278-1011-ND/3829637>. [Accessed: 13-Jan-2016].
- [18] On Shore Technology Inc., "ED281DT." [Online]. Available: <http://www.digikey.com/product-detail/es/ED281DT/ED3050-5-ND/4147600>. [Accessed: 13-Jan-2016].
- [19] Sullins Connector Solutions, "PPPC102LFBN-RC." [Online]. Available: <http://www.digikey.com/product-detail/es/PPPC102LFBN-RC/S6106-ND/807245>. [Accessed: 13-Jan-2016].
- [20] FCI, "67996-420HLF." [Online]. Available: <http://www.digikey.com/product-detail/es/67996-420HLF/609-3221-ND/1878553>. [Accessed: 13-Jan-2016].
- [21] Assmann WSW Components, "A-CCS-032-Z-SM." [Online]. Available: <http://media.digikey.com/Photos/Assmann Photos/A-CCS-032-Z-SM.jpg>. [Accessed: 13-Jan-2016].
- [22] DHgate.com, "Precision Electronic SATA Plug R/A SMT Type Connectors." [Online]. Available: <http://de.dhgate.com/product/productdisplay.do?seoproname=precision-electronic-sata-plug-r-a-smt-type&itemcode=236453562#s1-5-1;onsh|2719267987>. [Accessed: 13-Jan-2016].
- [23] Cirrus Logic Inc., "EP9315-IBZ." [Online]. Available: <http://www.digikey.com/product-detail/es/EP9315-IBZ/598-1263-ND/1245713>. [Accessed: 13-Jan-2016].
- [24] ELNEC, "BGA-Top-202 ZIF." [Online]. Available: http://www.elnec.com/en/products/programming-adapters/BGA-Top-202_ZIF/. [Accessed: 13-Jan-2016].
- [25] Z. M. Sun, "Progress in research and development on MAX phases: a family of layered ternary compounds," *Int. Mater. Rev.*, vol. 56, no. APRIL 2011, pp. 143–166, 2011.
- [26] M. Hopfeld, R. Grieseler, A. Vogel, H. Romanus, and P. Schaaf, "Tribological behavior of selected Mn+1AX_n phase thin films on silicon substrates," *Surf. Coatings Technol.*, vol. 257, pp. 286–294, 2014.
- [27] M. Camargo, I. Diaz, U. Schmidt, and A. Bund, "Synthesis, characterization and corrosion resistance of electroless Ni-P and Ni-P-SiC coatings: A comparative study," *Galvanotechnik*, vol. 103, no. 1, pp. 48–56, 2012.
- [28] TETRA GmbH, "User Manual BASALT MUST." p. 67, 2004.
- [29] TETRA GmbH, "BASALT -MUST Modular Universal Surface Tester." Ilmenau.
- [30] TETRA GmbH, "Beschreibung MUST - LabView Interface." p. 18, 2009.